R. & M. No. 3753

PROCUREMENT EXECUTIVE, MINISTRY OF DEFENCE

AERONAUTICAL RESEARCH COUNCIL

REPORTS AND MEMORANDA

Longitudinal Motions of Aircraft Involving High Angles of Attack

By H. H. B. M. THOMAS and JOAN COLLINGBOURNE

Aerodynamics Dept., R.A.E., Farnborough

LONDON: HER MAJESTY'S STATIONERY OFFICE

1974

PRICE £4·85 NET

Longitudinal Motions of Aircraft Involving High Angles of Attack

By H. H. B. M. THOMAS and JOAN COLLINGBOURNE†

Aerodynamics Dept., R.A.E., Farnborough

Reports and Memoranda No. 3753*
January, 1973

Summary

After a general introduction to the longitudinal motion of aircraft over an extended range of angle of attack there follows a wide-ranging investigation of various aspects of the low-speed-deceleration manoeuvre with excursion to very high angles of attack in the case of failure to recover. The entry into such flight conditions of two distinct types of aircraft—one with a wing of moderately large aspect-ratio and having a high tailplane, the other a tailless slender aircraft—is considered in some detail by examining the effect of various inputs on the motion.

In Part I some attention is paid to the factors influencing the ease with which control of the aircraft may be regained, particularly in cases in which normal recovery has only been achieved by forceful recovery action and those in which the aircraft only recovers after an excursion to extreme angles of attack. The possibility of recovery depends on the general nature of the motion under the action of markedly non-linear aerodynamic forces and moments. For aircraft having pitching-moment characteristics like those of the subject aircraft three types of motion can follow an attempt at recovery. There can be a reduction to two or even one as outlined in Appendix A. The problem of the stability of these motions in the broad sense is investigated. Examination of the allied single degree-of-freedom motion in pitch provides much insight into the more general problem, whilst phase-plane and similar three-dimensional plots prove useful means of displaying and interpreting results.

The effect of varying the aircraft characteristics is examined. Various forms and levels of damping are considered as well as the more evident effects of the centre-of-gravity position and the inertia-in-pitch of the aircraft.

* Replaces R.A.E. Technical Report 73011—A.R.C. 34 703.

† The second author was involved in the investigations which formed the basis for Part I of the report. Part II and the Appendices result from later work undertaken by the first author.

LIST OF CONTENTS

1. Introduction

During any motion which involves excursion to large angles of attack the flow around an aircraft (in the most general sense of the word) undergoes changes in its character. Associated with these are marked changes in the nature of the forces and moments that arise during the motion. In particular those quantities which are due to the angle of attack and the angle of sideslip may become much more non-linear with respect to these two motion variables. The underlying causes of the breakdown of the low angle-of-attack flow pattern depend on a number of factors principally the wing geometry, the disposition of the tail surfaces and the flight condition as specified by Mach number and Reynolds number. However regardless of the root causes, there exist a whole range of problems which relate to aircraft motions in which the aerodynamic forces are strongly non-linear and in certain circumstances may be sufficiently time-dependent to call for a formulation of the aerodynamic terms different from that usually used in studies of aircraft dynamics.

In this report we are concerned with a particular group of problems of this nature, namely those in which the motion of the aircraft is confined to the longitudinal plane. Typical of the problems encountered are 'pitch-up', wherein difficulty is experienced in controlling a pull-up manoeuvre during which the angle of attack reaches and exceeds that for which the pitching moment curves show a destabilising tendency, and the 'super-stall', which refers to motion in which the aircraft can easily enter into high angle-of-attack conditions (post-stall in the conventional case) from which recovery becomes increasingly difficult and finally impossible. Clearly the two forms of trouble have a good deal in common, but the distinction is perhaps worth making, since in the former case the pitching moment non-linearities can occur below the maximum lift coefficient condition (or the breakdown of the low angle-of-attack flow pattern, in general). There may be some loss of longitudinal control effectiveness with increase of the angle of attack, but this is not usually marked and the loss of speed during the manoeuvre is small.

In the superstall case the intention is to reach the limiting angle of attack at which breakdown of the flow occurs, so that in the ensuing motion this angle of attack is exceeded. The attendant loss in lift and more rapid increase in drag that may occur with further increase of angle of attack play an important part in this subsequent motion. Loss of lift results in increase of the angle of attack, whilst the accompanying changes in drag slow down the aircraft resulting in further loss of lift and an increasing rate of descent. The ability to recover depends strongly on the pitching moment characteristics and the inertia of the aircraft. It also depends critically on the extent to which the longitudinal control effectiveness falls off as angle of attack is increased and whether or not the pitching moment characteristics exhibit a 'pitch-up' tendency. These latter features reduce the capability of the restoring moment due to the longitudinal control to overcome the angular acceleration in pitch, whilst loss of speed aggravates the situation further. When the 'pitch-up' trend is sufficiently severe that even for maximum-down elevator* a nose-up pitching moment results over a certain range in the angle of attack the aircraft tends to settle into the second (very high angle of attack) statically-stable trim condition.

Furthermore the manoeuvre intended in the essentially low speed case is a much more restrained one than that which gives rise to the 'pitch-up' troubles. The requirements (in this country) call for an approach to limiting conditions during which the speed is reduced at about 1 knot per second and also in circumstances during which a mild pull-up to these conditions takes place resulting in a more rapid loss of speed. There exists the possibility that during such manoeuvres the attitude in pitch changes only slowly as compared with the changes in angle of attack. This feature can lead to a lack of appreciation on the part of the pilot that the aircraft is in a high angle-of-attack condition (unless this is indicated by other aerodynamic effects, special instrumentation or by suitable devices) and so delay his recovery action until too late.

Conventional 'static' wind-tunnel tests provide clear indications of possible sources of trouble assuming that the angle-of-attack range covered goes well beyond the limiting angle of attack. Nevertheless it is necessary to examine in greater detail the dynamics of the manoeuvre. It is important to assess the height losses that occur in a recovery and the dynamic conditions below the limiting angle of attack which constitute critical recovery conditions for a range of centre-of-gravity location. This is not merely essential in order to predict the acceptability or otherwise of particular aerodynamic characteristics, but also to indicate the degree to which protection must be sought by a stick-pusher or other automatic system against such dynamic conditions.

It is not intended to discuss in detail the separate influences of the wing geometry, tail location and fuselage and nacelles on the longitudinal forces and moment. We shall content ourselves by noting that a pitch-up tendency can be due to a loss of lift on the outboard portions of sweptback wings, increased downwash and

---

* Although the form of longitudinal control may differ from aircraft to aircraft the term 'elevator' is used in the text to imply any of these forms.

loss of kinetic pressure at the tail or a combination of these effects. Further information on the subject can be found in the existing literature.[1-7]

Problems of this kind were recently highlighted by a series of deep-stall accidents and incidents. In the investigation of these accidents a number of calculated aircraft responses in approaches to large angle-of-attack conditions had indicated the potential dangers. During the earliest of this work doubts had been expressed about the adequacy of the formulation of the aerodynamics. These doubts remain and further work is needed to resolve the matter. However in the case considered in Ref. 8 there were records available of a number of the motion variables, but unfortunately not of the pilot's input. A reconstruction of the aircraft's motion was undertaken on the basis of using the non-linear $C_D(\alpha)$, $C_L(\alpha)$ and $C_m(\alpha)$ data, based on static wind-tunnel tests. The results, reproduced here as Figs. 5 and 6, seem to indicate that in this particular circumstance there is no strong time-dependent element involved in the aerodynamics.

The investigations just mentioned were sufficient to explain the causes of the incidents, but it was considered that a more general study of the dynamics was desirable. It is the purpose of the present report to describe the methods and findings of this more generalized study, which used as specific examples the aircraft of Ref. 8, whose aerodynamic and other characteristics are given in Figs. 1, 2, 3a, b and c and Table 1, and a slender-wing tailless aircraft the data for which are given in Figs. 47, 48 and 49 and Table 2.

In the first of the two example aircraft we have the following features present;

(1) Marked drop-off in lift with change of angle of attack as the flapped wing stalls.

(2) The favourable mild nose-down pitching trend in the pitching moment at the onset of stalling.

(3) The rapid loss of kinetic pressure in the flow over the tail post-stall.

(4) Much increased downwash at the tail location over a wide range of the angle of attack in the post-stall régime.

(5) The much reduced moments from the tailplane consequent on (3) and (4) and hence the reversal in slope of the curve of pitching moment coefficient against angle of attack.

(3) and (4) arise from the high tail (T tail) configuration, the choice of which was dictated by the substantial performance and economic benefits to be derived from such an aircraft layout.

In the second aircraft we have different characteristics. In this case there is,

(1) No abrupt break in the lift curve against angle of attack as the type of wing used does not stall in the conventional sense and is unflapped.

(2) The longitudinal control effectiveness decreases much more slowly with increase in the angle of attack.

(3) There is an adverse pitching moment arising from the engine thrust, the effect of which depends on the extent to which the speed of the aircraft drops during the manoeuvre and the thrust falls with increase of angle of attack. These different aerodynamic characteristics are reflected in the aircraft responses as mentioned earlier and discussed more fully later. Solutions to the three degree-of-freedom equations of motion, which are rendered strongly non-linear by virtue of the form assumed for the aerodynamic forces and moments, were obtained for varying longitudinal control inputs by numerical integration of the equations using a digital computer. As a certain vagueness had crept into what rates of approach to the stall it is reasonable to specify in a requirement and whether, in fact, this should be specified in terms other than a speed decay, there seemed every reason to broaden the type of response from which recovery would be attempted. It is, in fact, important to attempt to define the dynamic situations from which recovery is possible or not, as these not only prescribe the limits to which the unprotected aircraft can be flown, but also give information relevant to the design of a 'stick-pusher' system or other protective systems.

PART I—AIRCRAFT WITH HIGH TAILPLANE

2. The Dynamics of the Decelerating Manoeuvre

The manoeuvres studied herein consist of a reduction in speed brought about by the combined use of thrust adjustment and an elevator input.* To initiate the deceleration the thrust is instantaneously reduced to give an initial deceleration of a prescribed amount. Thereafter the elevator is applied in an upward sense from the static trim position to sustain the manoeuvre. The exact amount of elevator applied at each stage of the manoeuvre governs the rate of rotation of the aircraft in pitch and hence the growth of the inclination or pitch

* This procedure differs somewhat from that prescribed in some Airworthiness Requirements, but was chosen as the most convenient means of generating a more or less constant deceleration up to the stall. The results show that the differences have little significance.

attitude and is used in the present study as the means of generating different dynamic conditions, in particular, values of $\dot{\alpha}$, from which recovery was attempted.

As mentioned earlier this part of the present investigation arose directly from the calculations made in Ref. 8 and for which Figs. 5, 6 and 7 give some of the results. In that investigation a further change in thrust was made after an interval of 6 seconds from the start of the manoeuvre. Because a number of solutions had been obtained with these assumptions it was decided to retain them for the present more general study. In any case it has already been noted[8] that this additional input would have but a slight effect on the speed changes and even less on other variables.

The equations of motion used in the analysis are of the same form as those used in previous investigations,[5,8] namely those resulting from resolving the forces along and normal to the flight path together with a moment equation referred to a body axis. In the usual notation they are,

$$m\dot{V} = F\cos\alpha - \tfrac{1}{2}\rho V^2 S C_D(\alpha, \eta) - mg\sin\gamma,$$

$$mV\dot{\gamma} = F\sin\alpha + \tfrac{1}{2}\rho V^2 S C_L(\alpha, \eta) - mg\cos\gamma$$

and

$$I_y\dot{q} = \tfrac{1}{2}\rho V^2 S l \left\{C_m(\alpha, \eta) + C_{mq}(\alpha)\frac{ql}{V} + C_{m\dot{\alpha}}(\alpha)\frac{\dot{\alpha}l}{V}\right\} + Fd$$

with the kinematic relationships

$$q = \frac{d\Theta}{dt},$$

$$\Theta = \alpha + \gamma$$

and

$$\frac{dh}{dt} = V\sin\gamma.$$

These equations together with the relationship for the air density

$$\rho = \rho(h)$$

determine the motion of the aircraft. In the present instance η represents the 'elevator' angle applied and d, the moment arm of the thrust, is assumed zero. Furthermore it is implicit in the form taken by the force equations that any inclination of the thrust line to the angle-of-attack datum is ignored.

The effect of the elevator deflection on the drag coefficient is neglected, but the effects on the lift and pitching moment coefficients is represented as in the expressions given below.

$$C_L(\alpha, \eta) = C_L(\alpha) + Q(\alpha)\left(\frac{\partial C_L}{\partial \eta}\right)\eta$$

and

$$C_m(\alpha, \eta) = C_m(\alpha) + Q(\alpha)\left(\frac{\partial C_m}{\partial \eta}\right)\eta,$$

where $Q(\alpha)$ is the factor (a function of angle of attack) which represents the change in kinetic pressure in the tail region.

Notwithstanding some doubts as to the validity of the assumption[5] the functions $C_D(\alpha, \eta)$, $C_L(\alpha, \eta)$ and $C_m(\alpha, \eta)$ are assumed to be as given by static wind-tunnel tests. The contributions due to rate of pitch, q, and the rate of change in the angle of attack, $\dot{\alpha}$ are taken to be those estimated on a quasi-steady basis with due

allowance for the changes in the kinetic pressure of the flow over the tail and in its direction as indicated by wind-tunnel tests, where such allowances are applicable. Finally the quantities so estimated, are modified to give reduced damping in the neighbourhood of the stalling angle of attack ($16° \leqslant \alpha \leqslant 19°$) to conform with the very limited experimental data available, at present,[7] *see* Fig. 3c.

The basic aerodynamic data as obtained from the best available wind-tunnel test data and the form used in the calculations are displayed in Figs. 1 to 3.

The nature of the decelerating motion depends on the extent to which the elevator is used to control the changes in speed and angle of attack. It was anticipated that for a small steady loss in speed little more elevator deflection would be required than that which corresponds to 'static' trim conditions at the current value of the angle of attack, and to a large extent this dictated the approach to angles of attack in the neighbourhood of the stall. Fig. 4a illustrates a typical manoeuvre of this type. In response to the reduced engine thrust the aircraft decelerates and, under the particular elevator input shown, does so at a nearly constant rate. We may note, from the history of the motion variables shown, that the rotation of the aircraft as indicated by its inclination, Θ, is small until, of course, a recovery is effected by the downward application of elevator. The angle of attack, on the other hand, increases steadily towards and just beyond the stalling value. These variations are reflected in the history of the excess normal acceleration factor which exhibits a slight break as the lift developed by the wing drops during passage through the stall. By way of contrast with this rather innocuous and well controlled manoeuvre we now consider the motion which gave rise to the incident mentioned earlier. In this as can be seen from Fig. 4b (the main variables are displayed together in Fig. 4b to ease the task of comparing with Fig. 4a, whereas the calculated results for the same motion are compared with data recorded during flight in Figs. 5, 6 and 7) the rotation of the aircraft although greater than in the case previously discussed is, nevertheless, small during the approach to the high angle-of-attack condition. Since, however, the angle of attack (*see* Fig. 4b) passes through its stalling value fairly rapidly there is a marked loss of lift due to the combined effect of the decrease in the lift coefficient and in the speed. In addition the fact, that, for angles of attack in excess of about 19 degrees, the pitching moment variation with angle of attack exhibits a 'pitch-up' tendency and the elevator effectiveness begins to fall off, results in a condition being reached in which even the application of fully-down elevator fails to arrest the growth in the angle of attack by generating a sustained and adequate nose-down rotation of the aircraft. The reduction in the nose-down rate of pitch around 16 seconds in Fig. 4b is the first indication of this. These particular calculations were terminated at about 20 seconds on the chosen time scale and the subsequent development of motion with fully-down elevator is not detailed.

The nature of the motion during this last phase is of interest and as the result of the more comprehensive study reported herein we can now discuss the classification of the types of motion that can asise. These are three in number and are*

(1) the normal or 'preventative' recovery—that is, a motion in which the growth in the angle of attack is successfully arrested and reversed thus preventing the aircraft attaining potentially hazardous conditions.

(2) the 'superstalled' motion—in which high angles of attack are reached and from which the aircraft enters an oscillatory motion around a near steady-state descending path (in a non-uniform atmosphere there is strictly speaking no steady state of this type, *see* Appendix C),

(3) the 'bounce' recovery—in which again large angles of attack are experienced, but from which, in these cases, the aircraft eventially recovers.

In this context recovery is used to indicate that there is a return to a condition of low angle of attack, since without furthes action by the pilot the aircraft would tend towards a negative angle-of-attack trim condition. We shall consider the ease or otherwise with which the pilot can return to some prescribed steady state at modest positive angle of attack in greater detail later. The three classes of motion under fixed control are illustrated in Figs. 8, 9 and 10.

It is convenient here for us to consider these cases in greater detail. In Fig. 8 the elevator is applied in the nose-up sense and produces some nose-up rotation of the aircraft as shown by the variation in the inclination, Θ. As the speed falls and the nose-up rotation occurs the angle of attack increases. Around 8 seconds the stall is reached and the normal acceleration curve exhibits the expected break. During a short interval following the attainment of an angle of attack of about 17·5 degrees, the aircraft, with the fixed position of the elevator (*see* curve of η), experiences a slight nose-down trend in the pitching moment (*see* Fig. 2) which, however, is insufficient to have much effect on the angle of attack. When finally the elevator is moved to the fully-down position at 10 seconds and held there a sluggish recovery of the aircraft ensues. The sluggishness of the recovery

* *See* 'Note on nomenclature'.

demonstrates that in this case the dynamic conditions pertaining at the instant when the elevator first reaches the 5 degrees, fully-down, position are near the limit.

To obtain the results shown in Fig. 9 we merely delay the instant at which the elevator is moved to the fully-down position. In the present calculations this was made to correspond with the attainment of a specified angle of attack and for the case illustrated the value chosen is 27 degrees. The retention of the elevator angle of -5 degrees for 2 seconds reduces the nose-down rate of rotation at the stall sufficiently to ensure that the aircraft's angle of attack passes through 27 degrees at such a rate that the elevator, which at the large angles of attack becomes much less effective, fails to arrest the further growth in the angle of attack, because the nose-down rotation soon gives way to a nose-up rotation trend. Finally the aircraft oscillates about the near steady state corresponding to the high angle-of-attack trim condition, which is 'statically' stable. This near steady state is defined by the values of the motion variables corresponding to the arrows on Fig. 9. The glide angle becomes nearly constant and height is lost quite rapidly in this particular type of motion.

If now instead of maintaining a constant up-elevator position beyond 6 seconds some additional up-elevator is applied as shown in the input curve on Fig. 10, the character of the motion can again change. Here almost total suppression of the small nose-down tendency at the stall is achieved and in consequence the aircraft's inclination (Θ) increases further beyond 10 seconds. When eventually the recovery action is taken it is so ineffective that the inclination and the angle of attack continue to increase, but from a maximum value of around 60 degrees the angle of attack begins to decrease again and continues to do so. This type of recovery is designated a 'bounce' recovery.

It is interesting to compare the speed changes in these three manoeuvres, as speed features prominently in the formulation of the airworthiness requirements. In all three cases the speed during the approach to the angle of attack chosen for the attempted recovery falls at a slightly increasing rate as the drag builds up and the manoeuvre develops. Beyond some minimum value the speed increases in all three cases and at much the same rate. Eventually, of course, the speed variation is quite different as the aircraft becomes established in the 'superstalled' condition. It is, thus, apparent that speed alone provides little or no guide to the state of the aircraft during the more critical phase of the motion.

For a given final state (*i.e.* fixed configuration including fixed down elevator angle) of the aircraft the separation of the motion into these different types depends on the dynamic condition pertaining at the moment when the elevator becomes fixed in its final recovery position. To illustrate this we can examine the effect of changes in the recovery angle of attack, that is, the angle of attack at which the elevator begins to move towards its fully-down position at a fixed rate of application of 30 degrees per second and also the effect of varying the rate of application for a given value of the recovery angle of attack.

Figs. 11 and 12 illustrate the effect of varying the 'recovery' angle of attack and from the later stages of the motions, there illustrated, we see that, for other conditions fixed, there is a critical value of the so-called recovery angle of attack. The difference in the elevator input prior to the recovery attempt makes the ensuing recovery much more sluggish for a recovery angle of attack of 26 degrees in the case of the manoeuvre of Fig. 11 than for the corresponding manoeuvre of Fig. 12. This indicates that the recovery angle of attack alone is an inadequate description of the dynamic conditions at the start of the recovery attempt as defined above.

For the manoeuvres displayed in Figs. 11 and 12 the rate of application of down-elevator is the same. In the light of what has been said previously we would expect that varying this parameter also provides a means of controlling the initial conditions of the recovery phase of the motion, and hence of generating motions falling into one of the categories outlined above. That this is so is demonstrated by the results shown in Fig. 13. As the rate of application of down-elevator is reduced 'normal' recovery becomes progressively more sluggish and ultimately ceases to take place. Again, if we examine the curves of Fig. 14, which also show the effect of varying the same parameter, but with the recovery attempt initiated later, we see how the subsequent motions separate into 'bounce' recoveries (those corresponding to 2 degrees per second and 3 degrees per second) and 'superstall' (those corresponding to 4 degrees per second and 5 degrees per second). From these examples we may conclude that the rate of change of the angle of attack and the associated rate of change of the inclination (or rate of pitch), at the instant the elevator is fixed for recovery, exert a strong influence on the character of the subsequent motion. For a fixed condition in terms of angle of attack the smaller values of the rate of change of the angle of attack are associated with normal recovery, an intermediate range with 'superstall', whilst high values correspond to 'bounce' recoveries. As is evident from the results just discussed these higher rates of change of the angle of attack, which result from too late or too slow application of recovery elevator, cause the aircraft to attain angles of attack in the range in which these is a strong positive (or nose-up) pitching moment acting even for fully-down elevator (*see* Figs. 2 and 3). This causes the aircraft to rotate nose-up and brings about a further marked increase in the angle of attack. From this flight condition and as the elevator reaches its fully-down position, the motions separate into the two categories we would expect.

Since the extent of the positive portion of the pitching moment curve depends on the amount of down-elevator, we would expect somewhat similar results from varying the amount of down-elevator applied. In this connection the results of Fig. 15 are of some interest. Here the down-elevator is applied at a fixed rate, but the final fixed value is changed. The motion during the recovery phase continues to be a 'bounce' recovery for most of the values of the elevator angle, but for the smallest value of 1 degree it becomes instead a 'super-stall' motion.

In the course of investigating which factors exert the greatest influence on the final phase of the manoeuvre and what decides whether a certain recovery attempt is going to finish as a normal recovery, 'superstall', or a 'bounce' recovery many individual cases were computed. It is not particularly helpful to detail all these results, but among them were a number showing behaviour similar to that displayed in Fig. 16. This particular case shows quite clearly the degree to which the subject aircraft possesses an inherent tendency to recover at the stall. Following a relatively gentle approach to stalling conditions, with but little rotation of the aircraft, we note that a nose-down rotation occurs though the elevator is held at a constant setting in the nose-up sense. Decrease in the amount of up-elevator around this time would have reinforced this trend, whilst application of more up-elevator would have tended to obliterate it. In the case in question the trend is not mantained for long. As the angle of attack falls below a value of 17 degrees the elevator contribution to the pitching moment coefficient has increased sufficiently to overcome that due to the angle of attack. A reversal in the sense of the rate of pitch ensues and in consequence the angle of attack begins to increase. This time the aircraft passes through similar conditions, but with increased momentum. When finally fully-down elevator is applied (at an angle of attack of about 27 degrees and after the lapse of about 40 seconds) it comes too late to arrest the growth in the angle of attack. In this particular case an oscillation about the statically stable high angle-of-attack trim condition occurs before finally the aircraft enters a 'bounce' recovery. During this phase of the motion a considerable loss of height takes place. This is characteristic of all motions during which a 'superstalled' condition occurs. We shall return later to a discussion of the tendency of the aircraft to depart slowly from the 'superstall' oscillation and the underlying causes. At this stage it is worth noting that the oscillation is almost constant in amplitude, if anything increasing in amplitude and non-linear in character. These features of the motion and the question of stability over the whole angle-of-attack range are considered more fully later, because at this stage it is interesting to digress a little and consider the difficulties the pilot may encounter in regaining control of an aircraft after it has effected a recovery of either type.

3. Regaining Control

In connection with near critical normal and 'bounce' recoveries there arises the question of whether the difficulties of regaining control rule out the usefuleness of the 'bounce' recovery as an emergency technique for avoiding 'superstalled' conditions and set some practical limits on certain of the more sluggish normal recoveries. To resolve some of the issues involved we now consider the problem of manoeuvring the aircraft out of these two sorts of recovery towards a steady state of flight at some angle of attack well below that for the stall. In the results presented in Fig. 17 the manoeuvre is attempted as the angle of attack is decreasing after reaching a maximum value of 30 degrees or so. The first action required is a reversal in the elevator input and, as is to be expected, if the elevator is reversed either too much or for too long (as here, in Fig. 17) there is a real danger that a 'superstall' condition will develop. In the case corresponding to the dotted-line input the angle of attack settles very quickly to almost its near-steady-state value (indicated by the arrow on the right-hand side of the figure). The speed, the aircraft's attitude and the incremental normal acceleration oscillate about their near-steady-state values to a greater extent. However, if instead of easing the stick forward at 25 seconds, the elevator deflection of $-3{\cdot}8$ degrees is maintained there is a rapid nose-up rotation of the aircraft accompanied by a rapid loss of speed. These may be sufficient to alert the pilot to the hazardous situation which is developing. In both cases the engine thrust is increased to a level which corresponds to that required for a 2 degree glide at an angle of attack of 5 degrees. If the thrust is not increased to a sufficiently high level, height continues to be lost during the settling-down phase of the motion, *cf.* Figs. 17 and 18. The results of Fig. 18 refer in the one case to the same elevator input as one of the cases of Fig. 17, but without the increase of thrust (*see* Fig. 19). Fig. 18 itself shows that provided the angle of attack has been allowed to decrease sufficiently and the other parameters are not varying too rapidly, adjustments to the flight condition can be made just as we would expect.

From the cases shown in Fig. 20 we see that restoring the thrust to its initial value (*i.e.* that which gave an initial deceleration of $1{\cdot}8$ kn/s) has a relatively small effect on the character of the motion and this is true, although to a lesser degree, of the much larger increase in thrust involved in the corresponding cases of Figs. 17 and 18 as shown in Fig. 19. As can be seen from the curves of elevator angle, the pilot is assumed to aid the

damping of the motion bey adding a rate-of-pitch term in his input. The differences caused by a large, as against a modest, increse in thrust are illustrated in Fig. 21. Here we see clearly the manner in which height is regained with the large thrust level, whilst it continues to be lost with the lower level.

The cases so far examined refer to regain of control from a marginal normal recovery. An allied and more interesting question is to decide whether matters are entirely different for regain of control from a 'bounce' recovery. We now turn our attention to this question.

The manoeuvre illustrated by Fig. 22 is like that of Fig. 16 one in which the aircraft, after making a partial normal recovery by virtue of its inherent recovery tendency, fails to completely recover, because the elevator is held in an up position. The action of the elevator in due time rotates the aircraft nose-up and the aircraft executes a 'bounce' type recovery. The very small effect of returning the thrust to its original value at a late stage in the manoeuvre is again evident.

We see that there are indications that, even though in the final recovery the aircraft pitches nose-down fairly rapidly to an attitude of about -33 degrees, the variables are tending to settle. Fig. 23 shows the same effect more clearly over an extended time. The main difference, in the two motions illustrated there, is in the increased stabilisation of the closing stages (provided by including a term proportional to the rate of pitch in the elevator input). Thrust is raised at 20 seconds to the level required to give a level flight steady state, for the dotted curves. The change in thrust occurs at 28 seconds for the full curves. In Fig. 24 the latter case is compared with a motion in which only the strength of the term proportional to rate of pitch in the elevator input is changed. If we again compare the results shown in Fig. 24 with those of Fig. 23, it is clear that the exact timing of the thrust increase is not important.

That, there is some stage in the 'bounce' recovery at which it may be courting disaster to attempt to take off the down-elevator applied for recovery, seems almost self-evident. The margin between successful regaining of control and failure to do so depends not only on the flight condition in terms of the angle of attack, but also on the dynamics of the situation. This can in the main be represented by the rate of change of the angle of attack. Take, for example, the motion displayed in Fig. 25. It seems that a somewhat slower launch into 'bounce' conditions results in a slower emergence, that is, the rate of change (negative) of the angle of attack is numerically less than for the cases shown in Fig. 24 when the up-elevator is applied. This causes the 'bounce' to change to a 'superstall' motion, which in this case is convergent owing to the increased damping provided by the pilot's input.

Delaying the reversal of control, until the angle of attack has decreased somewhat further. renders the action safe as can be seen from the curves of Fig. 26, in which the previous motion is compared with that resulting from the same type of elevator input but with a remarkably small delay in time for the instant of reversal of control. This action is, in fact, governed by the angle of attack rather than time and the two values are 28·5 and 25 degrees respectively.

The conclusions to be drawn from the study of the mechanics of regaining control after recovery are that

(1) it is comparatively easy to regain control well within the régime for normal recovery,

(2) it is possible, but perhaps more difficult, to regain control after a sluggish normal recovery or a 'bounce' recovery,

(3) to avoid entering 'superstalled' conditions the pilot should guard against too early reversal of recovery action. Up-elevator should only be applied when it is clear that the aircraft has returned to an angle-of-attack condition well below the critical,

(4) it is probably impossible to assess the situation adequately without an accurate indication of the angle of attack.

4. Stability of the Aircraft Motion with Fully-Down Elevator

The problem of recovery of the aircraft from a high angle-of-attack flight condition is related to the stability, over the entire angle-of-attack range, of the strongly non-linear system described by the equations of Section 2 for the condition corresponding to fully-down elevator.

Strictly speaking a full description of the motion topographically demands a multi-dimensional space. However, certain phase-planes do tend to be dominant in the composition of this space. In particular we would expect from the previous discussion that the α, $\dot{\alpha}$ plane falls into this category. Accordingly the computed solutions of the equations for the condition of fixed down elevator ($\eta = +5$ degrees), are analysed on this basis. To obtain different initial conditions it is necessary to make variations in the form of the input so that the aircraft is brought to a given angle of attack with a variety of dynamic conditions, specifically with different rates of change in the angle of attack. The results are shown in Fig. 27, in which to preserve clarity only the normal recovery and the 'bounce' recovery are represented. Motions involving 'superstalled' conditions,

that is, oscillations around the statically stable trim point $\alpha = 50{\cdot}2$ degrees, occupy the unfilled region in the neighbourhood of this point. Attention has already been drawn to the fact that we find that for the assumed characteristics of the aeroplane—these 'superstall' motions are mildly unstable dynamically. This is evident from the various phase-plane plots of Figs. 28, 29 and 30. The very slow divergence away from the steady-state condition being most clear in the α, $\dot{\alpha}$ plot of Fig. 28.

A marked negative slope to the curve of lift coefficient against angle of attack, and decrease of the other damping terms C_{m_q} and $C_{m_{\dot{\alpha}}}$ at large angles of attack, all contribute to this instability. Increase in the damping-in-pitch or a modification to the lift curve to make its slope less negative will tend to stabilize the motion, so that if these effects are sufficiently powerful the motion tends to settle into the high angle-of-attack trimmed state. Fig. 31 through to Fig. 39 illustrate this both for the separate and the combined modifications to the damping. Figs. 31 to 33 refer to an incremental modification to the C_{m_q} value of constant amount throughout the angle-of-attack range. It represents, in fact, a 50 per cent increase in the contribution of the fuselage to the total C_{m_q}. The curves of Figs. 34 to 36 refer to the aircraft with the curve of lift coefficient against angle of attack modified so that its slope near $\alpha = 50$ degrees is zero (*see* Fig. 3c). We see that the latter modification has a stronger influence on the motion and when these two effects are taken in combination the resulting curves exhibit a marked convergence towards the points which define the near-steady-state condition, that is, $\alpha = 50{\cdot}2$ degrees, $\Theta = 0{\cdot}4$ degrees and $V_E = 112$ kn (the corresponding value of V is obtained approximately by using the value of the relative density of air for the last value of the height recorded in the computation). An examination of these results indicates that even on the limited presentation of the α, $\dot{\alpha}$ phase-plane the motion 'trajectories' separate fairly clearly in well-defined regions corresponding to the three types of motion previously discussed. Of these the normal recovery motions are of most interest, and this presentation indicates the extent and manner in which the dynamic conditions must be reflected in an automatic device such as a stick-pusher system, designed to preclude the possibility of entering the region of the 'bounce' recovery or worse still the 'superstall'. It also indicates the way in which a suspected 'superstall' motion could be changed into a 'bounce' recovery, which may offer hope of final return to reasonable angles of attack.

From this discussion we have reason to think that it would be instructive as well as interesting to consider the corresponding single degree-of-freedom pitching motion (*cf.* Ref. 10). Such a motion corresponds to the assumption of constant speed (V = constant) and constant height ($\gamma = 0$) in the equations of motion of Section 2. This disposes of the first two equations, whilst the third (or moment) equation reduces to

$$I_y\ddot{\alpha} = \tfrac{1}{2}\rho V^2 Sl\left\{C_m(\alpha, \eta) + \left(C_{m_q} + C_{m_{\dot{\alpha}}}\right)\frac{\dot{\alpha}l}{V}\right\}$$

where ρ = const., η = const., and the thrust moment term is omitted.

If for convenience we write $\dot{\alpha} = q$ the above equation can be rewritten as

$$\frac{dq}{d\alpha} = F_2(\alpha) + \frac{F_1(\alpha)}{q}$$

in which form it can be analysed using a phase-plane presentation. In this instance the motion is completely defined by the two parameters α and q (or $\dot{\alpha}$). One important consequence of this is the fact that the boundaries between the three regions, which correspond to those of the wider problem, consist of special trajectories, which can be calculated directly. Consideration of the stability of the motion in the neighbourhood of the statically unstable trim point shows the singularity in the α, $\dot{\alpha}$ plane to be a saddle point. The trajectories through this point are the boundaries just referred to and are usually called the 'separatrix' curves. Solutions within each region can be obtained either by working in the time domain or more directly by working in the phase-plane according to the second form of the equation of motion (*see* Appendix A).

We first consider the motion, in which $F_1(\alpha)$ and $F_2(\alpha)$ are based on coefficients which vary with angle of attack in the same way as they did in the three degree-of-freedom motion. The results, some of which were derived from calculations in the time plane, are displayed in Fig. 40. However, since in this case the damping depends solely on the coefficient derivatives C_{m_q} and $C_{m_{\dot{\alpha}}}$ it does not change sign throughout the angle-of-attack range. Consequently the high angle-of-attack equilibrium condition is stable and in its neighbourhood the 'trajectories' spiral into the value of the angle of attack so defined.

The simplifications, that result from restriction of the motion to the single degree of freedom, permit us to distinguish more clearly the three categories of motion—the normal recovery, the 'superstall' and the 'bounce' recovery. To emphasise this further these are coloured green, red and blue respectively with the boundary curves in black in both Figs. 40 and 41. To appreciate the extent to which the fall-off of damping with increase

in the angle of attack affects the motion, we compare these two figures. In the calculations, the results of which are displayed in Fig. 41, it is assumed that the damping remains invariant at its value for small angles of attack. As compared with Fig. 40 we note that in the case of constant damping a much larger portion of the α, $\dot{\alpha}$ plane is now occupied by trajectories which 'superstall' or spiral into the statically stable high angle-of-attack trim condition. Also, since in addition the stiffness function is linear beyond $\alpha = 50$ degrees, the final convergence on to the steady-state condition becomes close to that of the linearised equations in this region. Exceptionally large rates of pitch are required to generate a 'bounce' recovery in this case. On the other hand, the region occupied by normal recovery trajectories is only very slightly affected as might be expected since the damping in the two cases only differs towards the boundaries of this region.

Clearly both the values of the trim angles of attack and separatrix curves depend on the setting of the elevator. This effect is illustrated in Fig. 42. It is seen that the régime for normal recovery contracts as the amount of down-elevator is reduced, whilst the catchment area for the 'superstall' conditions becomes enlarged. This points to the greater danger of superstalling if the recovery action taken is tentative in character. Not only is the régime of normal recovery enlarged by the application of as much down-elevator as possible (as is obvious), but the early application of down-elevator will tend to contain the motion within this region of the α, $\dot{\alpha}$ plane. Furthermore, in cases in which normal recovery does not result, the chances of generating a 'bounce' recovery are greater and could in an emergency offer a possible means of averting disaster (*see* Section 9).

Attention has already been directed to the fact that for the three degree-of-freedom motions those entering the superstalled conditions were just unstable and tend, after some time and a number of oscillations about the high angle-of-attack trim state, to return to low angle-of-attack flight conditions. As already remarked the basic cause of this behaviour is the variation of the damping terms with angle of attack and this becomes clearer in the context of a single degree-of-freedom motion. Accordingly further studies were undertaken as outlined in Appendix A. For these we retain the previous stiffness function and assume a linearly varying damping term such that the damping reverses sign beyond, at and ahead of the trim value of the angle of attack. Separatrix curves for the three types of damping are given in Figs. 43, 44 and 45 together with such trajectories as help to clarify the picture. The broad features of these three cases may be summarised as follows.

The curves of Fig. 43 are similar to those of the single degree-of-freedom motion in which the damping varies as indicated by the estimated values of C_{m_q} and $C_{m_{\dot{\alpha}}}$. The null case of Fig. 44 has broadly the same regions, but 'trajectories' within the 'superstall' region converge on to a limiting cycle, indicated by the thicker line. In this case the high angle-of-attack trim state is a centre and motions within the limiting cycle are constant amplitude oscillations. For the unstable situation of Fig. 45, in which the equilibrium points are a saddle point and an unstable spiral point, all trajectories tend to seek the steady state (if such exists and it is stable) on the negative angle-of-attack axis. Qualitatively we see that the three degree-of-freedom motion for the basic aircraft is closely allied to the motion in Fig. 44, but with a slight shift towards the conditions of Fig. 45.

Further details, and in particular a discussion of the results displayed in Fig. 46, are given in Appendix A.

PART II—SLENDER TAILLESS AIRCRAFT

5. The Longitudinal Motion of a Slender Tailless Aircraft

The previous work on the general topic is extended in what follows to the case of a slender tailless aircraft. Some wind-tunnel test results exist for such an aircraft over a range in angle of attack of -10 degrees to $+36$ degrees. For the purpose of the present investigation, these were extrapolated to an angle of attack of 90 degrees on some plausible aerodynamic assumptions and in consequence the motions at the extreme angles of attack although qualitatively correct may not be so quantitatively. The aerodynamic characteristics so derived are displayed in Figs. 47, 48 and 49 or quoted in the table of data.

Certain features of these data merit comment. It is seen from the curves of Figs. 47, 48 and 49 that abrupt changes must occur in the pressure distribution over the wing at around an angle of attack of 25 degrees. These changes are probably caused by changes in the vortex pattern. Likewise deflection of the elevon may result in modification of the vortex pattern and give rise to the asymmetric nature of the forces and moments due to elevon deflection. This class of aircraft does not stall in the usual sense as there is no significant loss of lift associated with the above changes in the flow pattern. This implies that the break in the normal acceleration curve, which is so characteristic of the larger aspect-ratio wing, is now absent. Consequently rotation of the aircraft plays a greater role in the build-up of the angle of attack in the type of manoeuvre considered here.

In the almost total absence of experimental data the damping derivatives C_{m_q} and $C_{m_{\dot{\alpha}}}$ were assumed to be constant throughout the angle-of-attack range. Additional damping is assumed to be provided by an auto-

stabiliser, whose authority is limited to 4 degrees of elevon, and which in the present calculations is approximated by treating it as a simple gearing of value unity.

5.1. Typical Examples of the Longitudinal Behaviour of the Aircraft

The behaviour of this class of aircraft up to angles of attack of 36 degrees, for a range of conditions, had been examined in an unpublished paper. Here we are more concerned with the broader pattern of behaviour and how it compares with, and differs from, that of the high-tail aircraft. However it is useful to first examine some examples of the longitudinal motion under various conditions.

5.2. Effect of Thrust Moment and Recovery Angle of Attack

The pilot is assumed to initiate the manoeuvre in the manner previously described and to apply thereafter an increasing amount of up-elevon. When the angle of attack for recovery (α_r) is reached, down-elevon is applied at the rate of approximately 30 degrees per second until 15 degrees has been applied, when it is fixed. It would be likely that the thrust passes below the centre of gravity for this type of aircraft, in which case it produces a nose-up pitching moment. At large angles of attack there is almost certainly a fall-off in the engine thrust. No information is available on this effect and so to simplify the calculations the unrealistic and conservative assumption is made that there is no loss of thrust.

If, for a centre of gravity location of $0{\cdot}52c_0$, the recovery angle of attack is taken to be 26 degrees, Fig. 50 shows that, for no thrust moment, a marginal normal recovery occurs. If the thrust line is assumed off-set so that a nose-up pitch moment results, the form of elevon input assumed (*see* Fig. 51) implies that somewhat lower values of up-elevon angles are used. However the rate of application of up-elevon, after an angle of attack of 12·6 degrees has been reached, is the same. Up to the instant when this angle of attack is reached the elevon angle is taken as that required to give static trim conditions. It is clear that the slight differences between the two cases converts the marginal normal recovery of Fig. 50 into the 'superstall' motion of Fig. 51. The near steady-state conditions are indicated by the arrows.

In the motions illustrated in Figs. 52 and 53 the recovery angle of attack is changed to 28 degrees. This delay in recovery causes the motion with no thrust moment to become a 'superstall', and that with the thrust moment included to become a 'bounce' recovery. These trends are in line with those we have noted previously.

In all the above cases the rate of application of elevon was the same during the approach to the selected recovery angle of attack. Variation of the rate of application of elevon has an important bearing on the resulting motion.

5.3. Variation of the Elevon Input

From among the responses computed with the object of generating widely different dynamic conditions at the selected recovery angle of attack, some extreme cases have been selected to illustrate the effect of the rate of application of up-elevator. Fig. 54 shows an even more rapid nose-up rotation, and associated build-up in the angle of attack, than is evident in the motions defined by Figs. 50 to 53. In all these cases the build-up of the angle of attack causes the drag coefficient to increase and the speed to fall off much more rapidly than the initial deceleration determined by the initial value of thrust. On the other hand it is possible to select elevator inputs which produce far less rotation of the aircraft and for which the deceleration remains constant during the approach to high angle-of-attack conditions, *see* Figs. 55 and 56. During such motions the pilot would be less aware of the growth of the angle of attack than in those cases in which appreciable rotation gives a direct motion cue.

It is evident from the few examples displayed that, according to the dynamic conditions prevailing at the instant down-elevon is applied and held, the subsequent motions fall into one or other of the three types we have already encountered for the tailed aircraft. A point of interest is the low values of rate of change in the angle of attack required, at an angle of attack of 26 degrees to 28 degrees, to bring about a 'superstalled' or 'bounce' motion particularly as the statically unstable trim condition for the aircraft corresponds to much higher values of the angle of attack (*see* Figs. 57 and 59). It is also worth noting that since the elevon remains effective to quite large angles of attack, and the range of angle of attack for which the pitching moment is positive for the aft centre of gravity at an elevon angle of $+15$ degrees is small, particularly for zero thrust moment, only a modest increase in maximum down deflection of the elevon is required to eliminate the locked-in 'superstall' motion (*cf.* Appendix A and Fig. 74). Phase-plane and space plots of the motions under attempted recovery give a greater insight into these features.

6. The Motion in the α, $\dot{\alpha}$ Plane

The history of the motion during the recovery phase ($\eta_P = 15$ degrees) from a number of different flight conditions, produced by a range of elevon inputs, is examined in Fig. 57 for a centre-of-gravity location of $0{\cdot}52c_0$ and with a thrust moment (which can alternatively be interpreted as an aircraft with more adverse pitching moment characteristics).

Of the trajectories shown (i), (ii) and (iii) typify the 'bounce' recovery motion, (iv) is a 'superstall' convergence on to the high angle-of-attack trim condition ($\alpha \approx 63$ degrees), whilst (v) is a marginal normal recovery. It is seen that there is not in the case of the tailless aircraft the same degree of separation of these different types of trajectory, as represented on the α, $\dot{\alpha}$ plane alone, especially within the region enclosed by the dotted-line rectangle shown on Fig. 57. As can be seen more clearly on an enlargement of this region, Fig. 58, the various trajectory curves cross each other in a complicated manner. Since the relative effect of the thrust moment, under the assumptions made herein, is appreciable at the larger angles of attack, it is reasonable to consider the effect of omitting this moment. With zero thrust moment the two trim states are closer together and we then have a more compact pattern of trajectories as shown in Fig. 59. It is of interest to note that curves in Figs. 57 and 59 carrying the same number correspond to the same variation of the elevon input and the same value of the recovery angle of attack, although, of course, the instant at which the latter occurs will be different. Again an enlargement of the region enclosed by the dotted-line rectangle on Fig. 59 is shown, *see* Fig. 60. This, together with a similar set of curves related to a further aft centre-of-gravity position of $0{\cdot}53c_0$ and with a thrust moment (Fig. 61) indicate that these differences in the aircraft characteristics do not have a marked effect on the nature of the trajectory curves. Hence, we may conclude that the underlying cause of the confused nature of curves for certain combinations of the angle of attack, and rate of change of the angle of attack, lies outside the parameters considered.

To examine the matter further and enable more detailed analysis of the motion to be undertaken further calculations were made, in which the acceleration along the flight path, the rate of pitch, the rates of change of the angles of climb and attack, as well as the individual terms in the equations of motion were evaluated. These calculations refer to the cases identified by the numbers (i), (ii), (iii) and (iv) on Figs. 59 and 60. Other results for the same cases are shown in Figs. 54, 52, 62 and 50 respectively, whilst the additional data are given in Figs. 63, 64 and 65.

If we consider the sluggish recovery of case (iii), for which the basic motion variables are shown in Fig. 62, we see from Fig. 63 that in the early stages the motion consists of a build-up in the nose-up rate of rotation and an associated growth in the angle of attack. The rate at which the lift and drag coefficients change more than compensates for the rate at which the speed falls. As a consequence the rate of change of the angle of climb increases up to around 10 seconds. Between this time and 13·5 seconds, when the down-elevon is applied, we see that there is a continued growth in the nose-up rate of pitch. During this same period the drag force continues to increase and there is an associated increase in the deceleration. In the main this is due to the rapid increase in the drag coefficient with increase in the angle of attack, but there are small contributions from the slowly increasing component of the weight and the slowly decreasing thrust component. On the other hand, although the lift coefficient increases during this time interval, the increase is insufficient to offset the speed loss and the lift force decreases. The thrust component normal to the flight path increases, whilst the weight component decreases. The nett result is an easing off of the growth of the rate of change of the climb angle as indicated by the curve in Fig. 63. Later, at around 15 seconds and beyond, the combined effect of the lift and thrust no longer overcomes the gravitational force so that the rate of change in the path inclination angle changes sign. With further loss of speed and lift the trend towards more negative values of the rate of change in the path inclination angle continues and becomes sufficient in this case to overcome the effect of the nose-down rotation imparted to the aircraft by the down-elevon. Hence the rate of change of the angle of attack ($\dot{\alpha} = \dot{\Theta} - \dot{\gamma} = q - \dot{\gamma}$) remains small for some time and even becomes slightly positive for a short while around 19 seconds. In this way the angle of attack builds up to a second maximum and there are changes in the moment equation taking place at this time, which result in an easing-off of the nose-down rotation trend. This also contributes to the trends in the rate of change of the angle of attack.

As soon as the speed begins to increase (beyond 21 seconds) the nose-down rate of pitch starts increasing more rapidly and is thereafter the dominant effect, so that the aircraft returns to normal angles of attack.

The history of the motion just described may be compared with that for case (iv), illustrated by dotted curves in Fig. 63 and the curves of Fig. 50. Here the up-elevon is applied at a much slower rate and the nose-up rotation is correspondingly less as is the associated growth of the angle of attack. We need not consider the motion in detail, but some trends may be noted. The easing-off of the rate of pitch in the nose-down sense is less pronounced, also the dip in the curve of the rate of change of the path inclination angle is not so marked.

Consequently the curve for the rate of change of the angle of attack exhibits only a brief hesitation before it increases rapidly in the negative sense. The result is the rather flat topped curve of angle of attack of Fig. 50. It seems from the other results displayed elsewhere that this trend would be expected to continue as the rate of approach to the high angle-of-attack condition is reduced further.

We next consider the effect of an increase in the value of the recovery angle of attack in both the cases just discussed. The comparisons are made in Figs. 64 and 65 respectively.

If we consider the faster approach to the high angle-of-attack condition first, then an increase in the recovery angle of attack from 26 degrees to 28 degrees changes case (iii) to case (i) (*see* Figs. 64 and 54). The initial stages of the motion are naturally the same as for case (*iii*), already discussed, but the delay in taking recovery action implies some increased deceleration, lower speeds and more nose-up rotation, hence higher maxima in both the rate of pitch and the rate of change of the angle of attack. Under the action of the down-elevon the aircraft rotates in the nose-down sense as shown in Figs. 54 and 64. This is insufficient to arrest the growth in the angle of attack, because of the changes which occur in the other variables. It is necessary, therefore, to examine the changes taking place within each equation of motion. At angles of attack just a little in excess of the new recovery value the increase in the drag coefficient following an increment in the angle of attack becomes less, and this in combination with a reducing speed results in a lower drag force. The adverse effect of the weight component also becomes less, but this is partly compensated for by the reduction in the component of the thrust. Consequently the decleration becomes less and at about 21 seconds changes sign to give thereafter a speed increase.

There is a decrease in the lift force from 10 seconds onward. During the interval 10 to 15 seconds approximately, this is mainly a speed effect, since the lift coefficient actually increases during this time, but from 15 to 25 seconds approximately the lift coefficient itself is decreasing as the angle of attack increases towards its maximum, which, together with the low level of the speed, causes the lift force to drop to a low minimum value around 25 seconds. The combined effects of the small, but slightly increasing thrust component, and the lift cannot overcome the weight component. Hence the rate of change of the climb angle becomes negative and in this case reaches a lower minimum than in case (iii). It is sufficient to swamp the weak nose-down rotation, which is in any case being eroded by an increase in the nose-up pitching moment coefficient due to angle of attack and a reducing contribution to the pitching moment coefficient due to the elevons. The resulting positive rates of change of the angle of attack continue its build-up until its contribution to the pitching moment coefficient again changes sign to become nose-down. This now adds to the nose-down contribution from the elevons, which at this stage reaches its lowest level. Nevertheless the combined effect results in an increased negative slope in the rate of pitch.

At this stage the aircraft is following a steep descending flight path (*see* Fig. 54, $\gamma = \Theta - \alpha$). The favourable weight component overcomes the drag, which is still increasing due to both the increase in speed and drag coefficient, to give in time the almost constant acceleration during the interval 25 to 35 seconds. Under the influence of a reducing weight component and a lift force, which starts to increase as the speed increases, the trend in the rate of change of the flight-path-inclination angle is reversed. This together with the nose-down rotation brings about a reduction and in time a change of sign in the rate of change of the angle of attack. The ensuing reduction in the angle of attack brings in its train a reduction of the drag coefficient and an increase in the lift coefficient. In turn the first of these causes the drag to reach a maximum around 32·5 seconds and the second returns the rate of change of the flight-path-inclination angle to a positive value. However as the angle of attack decreases it retraces values for which the pitching moment coefficient due to the angle of attack is once more in the nose-up sense. In spite of the favourable elevon contribution, which at this stage of the motion is increasing under the influence of a decreasing angle of attack and an increasing speed, this nose-up tendency is sufficient to cause the nose-down rotation to decrease between 30 and 35 seconds. These trends in the rate of pitch and the rate of change of the angle of climb are reflected in a slackening of the rate of reduction of the angle of attack.

However as the motion proceeds the dominating influence of the down-elevons ensures an ultimate rapid nose-down rotation and recovery. This type of recovery, which involves an excursion to very large angles of attack prior to the final recovery to small angles of attack, we have previously referred to as a 'bounce' recovery.

We now consider the manner, in which an increase in the angle of attack chosen for the recovery attempt affects the motion that results from a slower approach to high angles of attack (Fig. 65). The motion up to about 19·5 seconds has already been discussed in the context of the comparison of Fig. 63. As in Fig. 64 the delay in taking recovery action again results in further loss of speed and a higher maximum nose-up rate of pitch. The reduction in the rate of pitch at the instant of attempted recovery is such that by 22 seconds the aircraft beings to rotate slowly in the nose-down sense.

From about 20 seconds the drag, which up to this time increases due to the increase in the drag coefficient in spite of the deceleration accompanying the increase in drag, begins to decrease for a while due to much reduced speed. Associated with these changes, the weight component along the flight path decreases, and so the deceleration is reduced and the drop in speed shows signs of being halted. In the case of the lift force, the speed reduction more than offsets the increase in the lift coefficient from about 15 seconds onward. The decreasing lift is insufficient to overcome the weight component, in spite of a small favourable increase in the thrust component, with the result that the flight-path inclination begins to be directed downward ($\dot{\gamma}$ becomes negative beyond 21 seconds). This in turn causes the weight component changes already mentioned.

From 20 to 25 seconds it is seen that the rates of change of the speed and the path inclination are not much different for the two cases (ii) and (iv). The continued increase in the angle of attack is thus mainly the result of the inability to produce sufficient nose-down rate of rotation. Associated with the increase in the angle of attack is an increase in the nose-up moment coefficient due to the angle of attack and a decrease in the nose-down moment coefficient due to the elevon angle. These trends keep the rate of pitch (still nose-down) to a small numerical value. Meanwhile the decrease in the lift force continues and from the instant at which the coefficient reaches its maximum value ($\alpha \approx 35$ degrees and $t = 25$ seconds)—this trend continues a little longer as the decrease in the lift coefficient offsets the tendency for the speed loss to slacken. At the same time the weight component decreases but this only begins to arrest the growth in the negative path inclination beyond 28 seconds or thereabouts. Meanwhile as the drag coefficient is still increasing the drag force too increases and the speed trends change to become an acceleration from around 28 seconds onwards. This accelerating motion persists for some time due to the favourable weight component which together with the thrust component exceeds the drag sufficiently to yield a maximum acceleration of about 1·37 m/s^2 at about 34 seconds. During this period of increasing speed the lift force passes through a minimum and begins to increase. The decreasing weight component and a slightly increasing thrust component associated with this trend cause the rate of change of the downward path inclination to begin to increase. A decrease in the rate of growth of the angle of attack is thus brought about. At the prevailing angle of attack the total pitching-moment coefficient is small, so in the subsequent motion the stable high angle of attack is only slightly exceeded. From then on the motion converges to the near-steady state condition determined by the high angle of attack for which the aircraft is trimmed, as can be seen in the curves of Figs. 52 and 65. This type of motion is called a 'superstall' in this report.

Since the argument has to be consequential to a certain extent the foregoing type of analysis is never entirely satisfactory. It does, however indicate clearly the extent to which variables other than the angle of attack and its rate of change are important to a full interpretation of the motion. This can be further illustrated by considering the nature of the trajectories within the two three-dimensional spaces defined by the two trios of variables α, $\dot{\alpha}$, V and α, $\dot{\alpha}$, Θ.

7. Effect of Airspeed and Inclination Angle

A necessary step in the preparation of diagrams within the chosen three-dimensional space is a plot of the third variable against the angle of attack. The resulting curves are sufficiently interesting in themselves to merit reproduction here and the curves are shown in Figs. 66 and 67 for some of the cases represented within the α, $\dot{\alpha}$ plane alone in Fig. 57.

Fig. 66 shows the manner in which the aircraft speed varies with the angle of attack during the course of the motion, for each of the cases presented. Since, as previously noted, there exist no steady states in the strict sense for motion within a non-uniform atmosphere (*see* Appendix C)—the speed will change slowly during the near-steady state when the angle of attack is virtually constant. On the other hand the equivalent airspeed is nearly constant at around the value given by the approximate solution, which ignores the variation in the air density, hence the equivalent airspeed in case (iv) eventually tends to approach the value of 47·36 m/s (*cf.* Fig. 51). For the near-steady-state associated with the trim angle of attack of around 43 degrees the corresponding equivalent airspeed according to the same approximation is 46·68 m/s and, at a height of 4000 m, this yields a true airspeed of 57·05 m/s, which is within the region that each of the trajectory curves circumvents. However the introduction of the additional parameter speed (V) does little to separate the trends in the trajectories in the neighbourhood of an angle of attack of 30 degrees, so we are naturally led to consider the influence of the inclination angle, Θ.

With the same approximation of an invariant air density the values of the angles of attack and inclination for the near-steady states can be determined. The two points so defined are marked on Fig. 67, which shows the variation of the inclination angle, Θ, with the angle of attack, α, for the same three cases as previously. Here the individual curves are well separated over most of their length and in particular during the early stages of the attempted recovery. Again all three curves veer away from the point defined by the near-steady values of Θ

and α associated with the lower of the two high angles of attack, whilst the curve for case (iv) converges towards the point associated with the higher of the two angles of attack.

We may combine these plots with the plot in the α, $\dot{\alpha}$ plane to yield the three-dimensional plots of Figs. 68 to 70. For clarity Fig. 68 shows the curve for a 'bounce' recovery (case (iii) of Figs. 57 and 66), whilst Fig. 69 refers to a 'superstall' motion (case (iv) of Figs. 57 and 66). For the three-dimensional space defined by Θ, α, $\dot{\alpha}$ the two cases are shown together in Fig. 70. These can, of course, be interpreted in terms of the flight path since the path inclination angle, γ, is given by $\Theta - \alpha$. Thus, in both motions in the very early stages after the attempted recovery, the aircraft follows a climbing path which soon levels out and becomes a glide which steepens rapidly as the angle of attack increases, whilst the attitude angle remains more or less constant. At corresponding points, defined by equal values of the angle of attack, the path is steeper in the case of the 'superstall'. These features ensure that the curves of Fig. 70, like those of Fig. 67, are easily distinguishable unlike the representation of the motion on the α, $\dot{\alpha}$ plane alone. The conclusion to be drawn is that, in general, the variation of a number of the motion variables other than the angle of attack plays a significant role in determining the nature of the motion following an attempted recovery. This finding is in line with that of the preceding section.

The extent to which the curves in the α, $\dot{\alpha}$ plane for the multi-degree-of-freedom motion differs from those for an aircraft constrained to a pitching motion only also has some relevance to the above considerations. Accordingly we consider some aspects of this much simpler motion.

8. Motion with Freedom to Pitch Only

If the aircraft is free to pitch only the motion is described by the pitching moment equation of motion alone and so, for some chosen value of the airspeed, can be fully represented by the phase-plane plot $(\alpha, \dot{\alpha})$. The solution of the equation of motion is discussed in Section 4 and Appendix A. As explained there the $\alpha, \dot{\alpha}$ plane is subdivided into three regions by limiting trajectories known as the 'separatrix' curves. The three regions are characterised by the three possible forms of motion and the curves indicate the general nature of these motions.

Let us examine the effect on this single degree-of-freedom motion of varying the damping-in-pitch and speed for an aircraft with zero thrust moment. Consider in the first instance the effect of a change in the damping-in-pitch or with autostabiliser in and out. If the speed is fixed at that corresponding to steady level flight conditions at an angle of attack of 12 degrees and a height of 4000 m, the resulting curves are as in Figs. 71 and 72. Thus we again note (*see* also Appendix A and Section 4) that decrease of damping reduces the size of the region containing the normal recoveries, whilst it has the opposite effect on the extent of the region giving 'superstall' conditions. Also the less the damping the easier it is to convert a 'superstall' motion into a 'bounce' provided that at the instant this is attempted there is sufficient control power in pitch.

We next consider the effect of performing the same motions at a different constant speed.

Some qualitative assessment of the effect of this on the prospect of executing a normal recovery may be made by inspection of the equation of motion

$$\ddot{\alpha} = \frac{\rho V^2 S l}{2 I_y} C_m(\alpha, \eta) + \frac{\rho V \dot{\alpha} S l}{2 I_y} (C_{m_q} + C_{m_{\dot{\alpha}}}).$$

Both terms on the right-hand side are reduced numerically by a reduction in the speed. Hence for an initial angle of attack and fully-down elevon deflection for which the pitching moment coefficient, $C_m(\alpha, \eta)$, is negative or in the nose-down sense, the acceleration-in-pitch contribution may not be sufficient to overcome the effect of the initial rate of increase of the angle of attack. This tends to reduce the value of the rate of change in the angle of attack for a given value of the angle of attack for which normal recovery is possible.

More can be deduced about the effect of a change in the speed, if the form of the phase-plane trajectories is examined. For instance, it readily follows from the analysis of Appendix A that the slopes of the separatrix curves through the saddle-point are reduced numerically by a reduction in the speed and, furthermore, in proportion to it. Hence, since the saddle-point and the stable spiral point remain fixed in position for all speeds provided the thrust moment is zero, we anticipate that the separatrix curves for one speed would lie wholly inside those for a greater speed. Figs. 73a and b show this to be the case. We conclude that the reduction in speed, under the influence of the increasing drag coefficient, plays an important part in determining the nature of motion that ensues following an attempt to recover. In particular, loss of speed implies that at some given angle of attack there is a much more restricted range of the rate of change of the angle of attack for which normal recovery is possible.

On the other hand a full discussion of the motion in any particular case requires that account be taken of the changes in all variables, that is, α, Θ or γ, V and h, for the non-uniform atmosphere.

9. General Discussion and Conclusions

The present investigation, covering two quite distinct types of aircraft, shows that, in order to obtain a full understanding of the behaviour of a particular aircraft during longitudinal manoeuvres involving large changes in the angle of attack, it is necessary to consider the full three degrees of freedom. This is a reflection of the importance of the lift and drag characteristics as compared with the more fundamental part played by variation with the angle of attack of the pitching moment. For any aircraft, a manoeuvre, in which angle of attack is increased, implies an increasing drag coefficient and deceleration. The changes in the lift, hence the normal acceleration and inclination of the flight path, depends on whether the aircraft exhibits a stall (as characterized by an abrupt decrease in the lift coefficient within a few degrees of some value of the angle of attack) or not. In the former case the lift decreases on two accounts *viz.* the change in the lift coefficient and the decreasing speed, whilst in the latter case the reduction of the lift coefficient only comes about at very large angles of attack and then fairly gradually.

If, with the elevator deflected for recovery, the pitching moment coefficient is in the nose-up sense over some range of the angle of attack, three types of motion are possible following an attempt to recover from any moderately high angle-of-attack condition. These are listed in Section 2. The calculations show that, for a given aircraft, the motion falls into one or other of these categories according as the rate of change in the angle of attack is less than or exceeds a certain band of values depending on the angle of attack, at which the chosen elevator deflection for recovery is reached, and to some extent on the values of other variables describing the dynamic state.

It is, however, concluded from the present studies that a close affinity exists between the behaviour of an aircraft in a three degree of motion and in a single pitching degree-of-freedom motion. The choice of speed in the latter motion is arbitrary, but a reasonable choice would seem to be that which corresponds to the statically-unstable trim point of the curve of pitching-moment coefficient. Statically this defines a critical angle-of-attack. The effects of changes in the aircraft's moment-of-inertia in pitch, and changes of centre-of-gravity position are described qualitatively in Appendix A using the single degree-of-freedom motion results.

It is of interest to note that this single degree-of-freedom motion could easily form the subject of a wind-tunnel experiment using the apparatus outlined in Ref. 9. Such an experiment could shed some further light on the question of the adequacy of the usual representation of the aerodynamic forces in calculations such as those described herein. From a practical point of view interest centres mainly on the definition of the conditions from which normal recovery (*see* Section 2) is possible and for this purpose, only the initial stages of the other two types of motion need to be established.

However there are reasons for examining in rather more detail the 'superstall' and 'bounce' motions. Firstly the exercise serves to demonstrate the usefulness of the phase-plane presentation in problems of motion in a number of degrees of freedom. We have seen that the presentation not only has the merit of compactness, but also contributes to a better understanding of the nature of the large-angle non-linear motion.

Secondly, the abrupt nature of the return to modest angle of attack in the closing stages of the 'bounce' recovery invites the question of how difficult is it to regain control in a 'bounce' motion. From the cases examined in Section 3 we may conclude that it may be difficult to judge the earliest instant at which the stick should be pulled back without the aid of an instrument displaying the angle of attack. Apart from this there seems to be no problem and the height loss is modest.

There remains the question of whether a 'superstalled' motion can be converted to a 'bounce' recovery and thereby offer a means of avoiding the consequences of entering a 'superstall'. Before proceeding to demonstrate that this is theoretically possible, it is worth noting that it is not at all clear that the procedure is a practical proposition. Firstly the pilot must be convinced that he has reached flight conditions from which only a 'superstalled' motion can result, otherwise application of nose-up pitching moment may merely convert a sluggish normal recovery into a 'superstall'. To be certain on this score implies attaining angles of attack so large that the elevator may become too ineffective to bring about the increase in the rate of change of the angle of attack necessary to move the aircraft's motion from one régime to the other. The best compromise between these conflicting requirements is to settle for an angle of attack near the unstable trim point. For the aircraft of Part I (*see* Table 1) this of the order 34 degrees. To demonstrate that sufficient control power is retained at this angle of attack to effect the change from a 'superstalled' motion to a 'bounce', we consider the motion shown in Fig. 9 and the effect upon it of applying up-elevator at an angle of attack of about 37 degrees or at 15 seconds. If the elevator is held in the central position ($\eta = 0$ degrees) from 15 to 20 seconds before it is returned to the

5 degree down position we see from Fig. 75 that sufficient nose-up rotation, and hence sufficient increase in the rate of change in the angle of attack, is generated to convert the previously 'superstalled' motion to a 'bounce' recovery. To assess the sensitivity of the procedure two other values of η are considered (*see* Fig. 76), namely $\eta = -2{\cdot}5$ degrees and -5 degrees from 15 to 20 seconds. The most important difference is in the peak normal acceleration and it may be possible to come near to the structural limits if too much control is used. Other calculations, whose results are not displayed here, confirm the expected results that the elevator need not be held at zero or negative settings for as long as 5 seconds, whilst too late application fails to produce the desired result. Hence, we conclude that, although in theory it is possible to convert a 'superstalled' motion into a 'bounce', from which again control may be regained, the procedure may present piloting difficulties.

Aircraft which have characteristics similar to those of the aircraft used for the present study can present a potential hazard in flight over an extended angle-of-attack range. As basic aerodynamic redesign is usually out of the question it is necessary to supply additional means of protection. This will usually be in the nature of some automatic system and such devices may assume different forms according to the severity of the problem. In a severe case (as indicated by a very restrictive normal recovery régime) the best form of protection is probably provided by a 'stick-pusher' system, which applies down 'elevator' according to some law, which reflects the tendency to 'superstall' as the 'recovery' angle of attack is increased for some specified value of its rate of change and as the rate is increased at some fixed, but sufficiently large, 'recovery' angle of attack. Further, as the aircraft responds and the angle of attack decreases below some value, judged to be safe, the stick should be returned by the protective system towards a normal-flight position.

For less severe cases it may suffice to give a strong warning to the pilot of the increasing angle of attack and possibly aid his consequent recovery action by additional damping. In this context it is necessary, of course, to bear in mind the differing action of additional damping within the different régimes (*see* Sections 4 and 8 and Figs. 40, 41 and 71, 72, 73).

Undoubtedly the impact of calculations such as reported here on the requirements set down by the airworthiness authorities—should be examined (*see* Appendix A), but this is a subject for wider discussion. However, one general point may be made. There is merit in formulating the requirements in such a way that they are equally meaningful for both predications of the flight behaviour and for flight testing.

Finally we may set down our findings as regards the aerodynamic input for the calculation of the longitudinal motion and the calculations themselves, as follows:

(1) Whilst at present no hard-and-fast statement can be made on the aerodynamic data required, there are a number of indications that, over a range of angle of attack and its rate of change, the motion may be considered to proceed in a quasi-steady manner.

Hence the more immediate need is for

(i) the best available data (that is, data expected to be least subject to unknown scale and compressibility effects) for static conditions over a wide angle-of-attack range,

(ii) oscillatory dynamic derivatives again covering a wide range in the angle of attack.

In order that limits may be set, if necessary, on the validity of the above assumption it is desirable to study various pitching motions in wind tunnels, in particular the motion which is the subject of Appendix A, and a number of the features of some of the figures given here should be reproduced using apparatus such as that outlined in Ref. 9.

(2) The calculations for a specific aircraft should proceed as follows,

(i) Calculate the single degree-of-freedom motion in pitch for the speed corresponding to the statically unstable trim point.

(ii) On the basis of the results of (i) calculate the three degree-of-freedom motion for an appropriate range of inputs.

Acknowledgment

The authors wish to acknowledge the help given by Mr. H. Barnes in the preparation of and conduct of a number of computer programs needed for the present investigation.

LIST OF SYMBOLS

$\bar{c}$ Wing mean chord

c_0 Wing root chord

C_D Drag coefficient = drag/$\frac{1}{2}\rho V^2 S$

C_L Lift coefficient = lift/$\frac{1}{2}\rho V^2 S$

C_m Pitching-moment coefficient = moment/$\frac{1}{2}\rho V^2 Sl$

C_{m_q} Non-dimensional coefficient derivative

$$= \partial C_m / \partial \left(\frac{ql}{V}\right); \qquad M_q = \tfrac{1}{2}\rho V S l^2 C_{m_q}$$

$C_{m_{\dot{\alpha}}}$ Non-dimensional coefficient derivative

$$= \partial C_m / \partial \left(\frac{\dot{\alpha} l}{V}\right); \qquad M_{\dot{\alpha}} = \tfrac{1}{2}\rho V S l^2 C_{m_{\dot{\alpha}}}$$

F Engine thrust

g Acceleration due to gravity

h Height

h_i Indicated height

I_y Moment of inertia of aircraft in pitch

l Characteristic length (either $\bar{c}$ or c_0)

M Pitching moment

M_q Pitching-moment derivative with respect to rate of pitch

$M_{\dot{\alpha}}$ Pitching-moment derivative with respect to rate of change of the angle of attack

m The mass of the aircraft

n_i Apparent (or indicated) normal-acceleration factor

q Rate of pitch

Q Ratio of kinetic pressure at the tailplane position to the free-stream value

S Wing area

t Time

V Aircraft velocity relative to the air (airspeed)

V_E Equivalent airspeed = $\sqrt{\sigma} V$

V_{i_R} Indicated airspeed (recorder instrument)

α Angle of attack (or angle of incidence)

γ Flight-path angle (angle of climb)

Θ Inclination (attitude in pitch)

Θ_i Inclination indicated by the recorder

η Elevator deflection (total elevon angle in Part II)

η_P Elevon angle input due to the pilot

η_S Elevon angle due to autostabiliser

η_T	Tailplane deflection ($= \eta$, Part I)
ρ	Air density
ρ_0	Air density at sea-level
σ	$= \rho/\rho_0$ relative air density

Note on nomenclature

The terms normal, 'superstall' and 'bounce' have been introduced tentatively here for economy of description. It is not suggested that they are necessarily the most appropriate terms even though 'superstall' has been in use for some time with a somewhat less well-defined meaning.

Definitions, together with some explanation for the choice of words, are given below.

Normal

A normal recovery is a reversal of an excursion in angle of attack by use of elevator, which only involves a modest dynamic overshoot, that is, the aircraft is prevented from attaining large angles of attack.

Superstall

This term refers to a motion in which the aircraft tends to settle, or oscillate about, a very high angle-of-attack trimmed state.

Bounce

This term describes a recovery in which as a result of a high positive rate of change in the angle of attack the aircraft attains very high angles of attack, but eventually returns to flight at more normal values of the angle of attack.

In effect the aircraft 'bounces' out of the very high angle-of-attack conditions. Under certain circumstances there exists the possibility of converting a 'superstalled' condition into a 'bounce' recovery, or of bouncing the aircraft out of the locked-in state.

REFERENCES

No.	*Author(s)*	*Title, etc.*
1	G. J. Hancock	Problems of aircraft behaviour at high angles of attack. AGARDograph 136 (1969).
2	R. S. Shevell and R. D. Schaufele ..	Aerodynamic design features of the D.C.9. Journal of Aircraft, Vol. 3, No. 6 (1966).
3	D. J. Kettle and D. A. Kirby ..	Low-speed wind-tunnel tests on the effects of tailplane and nacelle position on the superstall characteristics of transport aircraft. R.A.E. Technical Report 67197 A.R.C. 29 746 (1967).
4	R. T. Taylor and E. J. Ray ..	A systematic study of the factors contributing to post-stall longitudinal stability of T-tail transport configurations. Paper presented at A.I.A.A., Aircraft Design and Technology Meeting, Los Angeles, California (1965).
5	H. H. B. M. Thomas	A study of the longitudinal behaviour of an aircraft at near-stall and post-stall conditions. A.G.A.R.D. Conference Proceedings, International A.G.A.R.D. C.P.17 (1966).
6	Ph. Poisson-Quinton and E. Erlich	Analysis of stability and control of an aircraft near its maximum lift. A.G.A.R.D. Conference Proceedings, International A.G.A.R.D. C.P.17 (1966).
7	H. G. Wiley	The significance of non-linear damping trends for current aircraft configurations. A.G.A.R.D. Conference Proceedings, International A.G.A.R.D. C.P.17 (1966).
8	H. H. B. M. Thomas and A. Jean Ross	On the reconstruction of the history of the dynamic behaviour of a high-tailed aircraft during stalling tests. R.A.E. Technical Memorandum Aero 1087, A.R.C. 30923 (1968).
9	C. O. O'Leary and H. H. B. M. Thomas	Proposals for investigating the stalling dynamics of aircraft. R.A.E. Technical Memorandum Aero 1188, A.R.C. 32255 (1970).
10	R. C. Montgomery and M. J. Moul	Analysis of deep-stall characteristics of T-tailed aircraft configurations and some recovery procedures. A.I.A.A. Paper 66–13 (1966).

APPENDIX A

Stability over the Extended Angle-of-Attack Range of the Aircraft Motion with Freedom to Pitch Only

Consider the constrained motion which only involves pitching about the flight path. This motion is governed solely by the equation in the pitching moments,

$$I_y\dot{q} = \tfrac{1}{2}\rho V^2 Sl\left\{C_m(\alpha,\eta) + C_{m_q}\frac{ql}{V} + C_{m_{\dot\alpha}}\frac{\dot\alpha l}{V}\right\}.$$

Here we shall for simplicity omit the thrust moment and ignore the variation of ρ. In such a motion Θ and α may only differ by a constant (the flight path angle, γ). Hence

$$\dot\alpha = q,$$

so that the equation of motion may be rewritten

$$\ddot\alpha = \frac{\rho V^2 Sl}{2I_y}\left\{C_m(\alpha,\eta) + \left(C_{m_q} + C_{m_{\dot\alpha}}\right)\frac{\dot\alpha l}{V}\right\}$$

$$= F_1(\alpha,\eta) + F_2(\alpha)\dot\alpha, \quad \text{say,}$$

or alternatively as

$$q\frac{dq}{d\alpha} = F_1(\alpha,\eta) + F_2(\alpha)q.$$

Both forms are useful. The first permits us to calculate the motion in the time domain, either with some inputs of η as functions of time, or examine the nature of the motion for some fixed positive value of the elevator deflection, η, for various initial conditions specified by prescribed values of α and $\dot\alpha$. To present the solutions in the phase-plane it is necessary to determine the values of α and $\dot\alpha$ at corresponding times. On the other hand in the second form the solution is directly in the form q (or $\dot\alpha$) as a function of α. The only drawback arises when the solution is obtained by numerical integration. At points defined by $q = 0$, $\alpha = \alpha_0$, for which $F_1(\alpha,\eta) \neq 0$, the slope $dq/d\alpha$ becomes infinite. To continue the solution across the α-axis it then becomes necessary to obtain a series solution to the equation.

If the last point determined by the numerical integration procedure is q_1, α_1, and q_1 is not very small—the above form of the equation may be used and q expressed as a series in $\theta = (\alpha - \alpha_1)$,

$$q = q_1 + a_1\theta + a_2\theta^2 + \ldots,$$

whilst for very small values of q_1 it is desirable to invert the differential and obtain

$$\frac{d\theta}{dq} = \frac{q}{F_1 + F_2 q}$$

and assume

$$\theta = a_2 q^2 + a_3 q^3 + \ldots .$$

A disadvantage of the equation of motion in the time domain lies in the difficulty of obtaining evenly spaced points with respect to their angle-of-attack values, whereas this is a natural consequence of the second. Use of the two forms may be combined to obviate the need for the series solutions.

We wish especially to consider the motion following an attempt to recover, that is, with full-down deflection of the elevator. For the first subject aircraft the nature of the motion is discussed in Section 4 of the main text. There are two singular points within the positive angle-of-attack range. At least one additional singular point lies on the negative α-axis, but this need not concern us here.

Application of Poincaré's criteria readily discriminates between the different types of singularity. That for the lower of the two positive values of the angle of attack is a col or saddle-point, whilst that for the higher of the two angles of attack is a spiral point, stable or unstable according to the sign of the damping-in-pitch. The slope of the separatrix (or boundary curve between stable and unstable regions) through the saddle-point is indeterminate, but easily follows from application of l'Hospital's rule. Thus at the saddle-point $\alpha = \alpha_c$, $q = 0$,

$$\left(\frac{dq}{d\alpha}\right)_{\alpha_c} = \lim_{\alpha \to \alpha_c} \left\{\frac{F_1(\alpha) + F_2(\alpha)q}{q}\right\}$$

$$= \frac{(F_2(\alpha))_{\alpha_c}\left(\frac{dq}{d\alpha}\right)_{\alpha_c} + \left(\frac{dF_1}{d\alpha}\right)_{\alpha_c}}{\left(\frac{dq}{d\alpha}\right)_{\alpha_c}},$$

which yields a quadratic for the slope $(dq/da)_{\alpha_c}$. Provided a sufficiently small value of q is assumed this slope may be used to determine initial values of α and q (or $\dot{\alpha}$) to be taken in the numerical solution for the separatrix. It is, perhaps, on the whole advisable to start the computation further away from the singular point. To do this the initial values are obtained from a series solution,

$$q = a_1\theta + a_2\theta^2 + a_3\theta^3 + \ldots$$

with the function $F_1(\alpha)$ and $F_2(\alpha)$ likewise expanded in ascending powers of $\theta = (\alpha - \alpha_c)$, in this instance.

To show how variation of the damping with increasing angle of attack affects the motion we may combine a linear decay of damping with the orginal shape of the function, $F_1(\alpha)$. Three cases are considered

(1) Damping becomes zero beyond the second trim point.
(2) Damping becomes zero at the second trim point.
(3) Damping becomes zero ahead of the second trim point.

The results of the computations are shown in Figs. 43, 44 and 45 respectively. For the second case the nature of the singularity does not follow directly from Poincaré's criteria and we must consider the behaviour of the solution in the neighbourhood of the trim point. We transfer the origin to this point and again denote the perturbation in α by θ. Then near $\theta = 0$ (and more generally if F_1 is linear over a range of α, *see* Fig. 46) the equation of motion is

$$\frac{dq}{d\theta} = \frac{F_1 + F_2 q}{q}$$

$$= -\frac{\alpha\theta + b\theta q}{q};$$

an equation which is immediately integrable by separation of the variables

$$\int \frac{q\,dq}{1 - (b/a)q} + \frac{a\theta^2}{2} = \text{constant},$$

or

$$\frac{a\theta^2}{2} - \frac{a^2}{b^2}\log_e\left(1 - \frac{b}{a}q\right) - \frac{a}{b}q = \text{constant}.$$

For the range $a/b > q \geqslant -a/b$ the log term may be expanded so that we finally obtain

$$a\theta^2 + q^2\left(1 + \frac{2b}{3a}q + \frac{b^2}{2a^2}q^2 \ldots\right) = \text{constant},$$

which in the limiting case $q \ll 3a/2b$ is approximately

$$a\theta^2 + q^2 = \text{constant.}$$

The trajectories not too far removed from the origin are thus symmetrical with respect to the axis $\theta = 0$ and almost so with respect to the $q = 0$ axis, *see* Fig. 45. Furthermore the analysis shows the origin to be a centre for a limited range of θ and q.

In the case of the F_1 and F_2 functions shown in Fig. 46 the above form of solution holds for the whole region within the closed trajectory shown. The analytic solution is compared with that given by the numerical integration.

For the slender tailless aircraft the solutions of the corresponding equation of motion are displayed in Figs. 71, 72, 73a and b. We may also use the above motion to illustrate the effects of changes in the moment of inertia, in the position of the centre of gravity, or the closely allied effect of changes in the shape of the pitching-moment curve.

A change in the moment of inertia has an effect very like the effect of changing the speed except that it leaves unaffected the influence of the rate of change in the angle of attack. Increase in the inertia makes normal recovery more difficult, as would be expected.

Consider now three positions of the centre of gravity such that for the assumed downward deflection of the elevon we obtain the variations of pitching moment coefficient with angle of attack shown in Fig. 74a, b and c. The trajectories in the α, $\dot{\alpha}$ plane of the aircraft motion, with freedom to pitch only, are as shown beneath each curve of pitching-moment coefficient. The first set of trajectories (*see* also Section 8) contain the three types of motion, namely, the normal recovery contained between the two left-hand branches of the separatrix, 'the superstall' or trajectories which spiral into the upper trim point, and lastly the 'bounce' recovery which lies outside the outer right-hand branch of the separatrix.

When the curve of $C_m(\alpha, \eta_0)$ just touches the α-axis the right-hand branches of the above separatrix are evanescent and the separatrix now ends in a cusp as shown. The entire plane is, in this case, divided into two regions only and all trajectories are recoveries: those to the left of the separatrix are normal, whilst those to the right of it are 'bounce' type recoveries.

As the centre of gravity of the aircraft is moved to a forward position the pitching-moment coefficient becomes more negative at a given angle of attack and the curve of the pitching-moment coefficient against the angle of attack lies wholly below the α-axis. Accordingly all trajectories are of the normal type except that as we move to the right, or for increase in the angle of attack, the trajectories indicate progressively more sluggish recovery.

Although the variation in behaviour pattern shown in Fig. 74 applies strictly to the effect of changing the centre-of-gravity location for a given aircraft it can to a large measure be interpreted as applying to different aircraft with the pitching-moment characteristics shown. Thus we conclude that for aircraft having pitching moment of type (a) the usable flight régime is defined by the desire to keep well within the limits of the normal region specified in the particular motion of this Appendix by certain values of α and $\dot{\alpha}$, but more generally by α, $\dot{\alpha}$, Θ and V. On the other hand for aircraft whose characteristics resemble those in Fig. 74b and c the limiting conditions relate to the possible height losses.

APPENDIX B

Constant Speed Manoeuvre

If the longitudinal motion takes place at constant speed it is governed by the following set of equations

$$0 = F\cos\alpha - \tfrac{1}{2}\rho V^2 S C_D(\alpha, \eta) - mg\sin\gamma,$$

$$mV\dot{\gamma} = F\sin\alpha - \tfrac{1}{2}\rho V^2 S C_L(\alpha, \eta) - mg\cos\gamma$$

and

$$I_y\dot{q} = \tfrac{1}{2}\rho V^2 S l\left\{C_m(\alpha, \eta) + C_{m_q}\frac{ql}{V} + C_{m_{\dot{\alpha}}}\frac{\dot{\alpha}l}{V}\right\},$$

(where the moment arising from the engine thrust is neglected) together with the kinematic relationships

$$\Theta = \alpha + \gamma$$

and

$$\dot{\Theta} = q.$$

Elimination of the thrust force, F, from the first two equations yields,

$$mV\dot{\gamma}\cos\alpha = \tfrac{1}{2}\rho V^2 S C_N(\alpha, \eta) - mg\cos\Theta.$$

This equation can be written either in terms of α and Θ or in terms of α and γ thus,

$$mV(\dot{\Theta} - \dot{\alpha})\cos\alpha = \tfrac{1}{2}\rho V^2 S C_N(\alpha, \eta) - mg\cos\Theta$$

or

$$mV\dot{\gamma}\cos\alpha = \tfrac{1}{2}\rho V^2 S C_N(\alpha, \eta) - mg\cos(\alpha - \gamma).$$

Either form of this equation in the normal force together with the equation

$$I_y\ddot{\Theta} = \tfrac{1}{2}\rho V^2 S l\left\{C_m(\alpha, \eta) + C_{m_q}\frac{ql}{V} + C_{m_{\dot{\alpha}}}\frac{\dot{\alpha}l}{V}\right\}$$

defines the constant speed manoeuvre.

These equations of motion may be appropriate to the study of rapid pull-up manoeuvres executed by combat aircraft particularly for those aircraft whose pitching moment characteristics exhibit a strong 'pitch-up' trend.

In the light of the usefulness of the single degree-of-freedom motion in the interpretation of the general motion discussed in the main text, it could be that the above equations would define a motion having even a closer affinity to the full three degree-of-freedom motion. This speculation has not been explored further at present.

APPENDIX C

On the Nature of the Aircraft Motion in the Superstall After a Long Time

If we refer to the equations of motion it is immediately seen by inspection that the only true steady state for the case of a non-uniform atmosphere is a level flight condition defined by,

$$F \cos \alpha = \tfrac{1}{2}\rho V^2 S C_D(\alpha, \eta),$$

$$F \sin \alpha + \tfrac{1}{2}\rho V^2 S C_L(\alpha, \eta) = mg,$$

$$\tfrac{1}{2}\rho V^2 S l C_m(\alpha, \eta) + Fd = 0,$$

$$\frac{dh}{dt} = 0 \quad \text{or} \quad h = \text{constant}, \qquad \gamma = 0.$$

However for a uniform atmosphere, ρ = constant, an inclined steady rectilinear flight is possible. In this case steady values of the equivalent airspeed, $V_E = \sqrt{\sigma} V$, the flight path angle, γ, and the angle of attack, α, are determined by the equations

$$F \cos \alpha - mg \sin \gamma = \tfrac{1}{2}\rho_0 V_E^2 S C_D(\alpha, \eta),$$

$$-F \sin \alpha + mg \cos \gamma = \tfrac{1}{2}\rho_0 V_E^2 S C_L(\alpha, \eta)$$

and

$$\tfrac{1}{2}\rho_0 V_E^2 S l C_m(\alpha, \eta) + Fd = 0$$

for given values of F and η, with

$$\frac{dh}{dt} = V \sin \gamma = \frac{V_E}{\sqrt{\sigma}} \sin \gamma$$

$$= \text{constant}.$$

If we denote the solutions to these equations by V_{E_S}, α_S and γ_S the extent to which the motion in a non-uniform atmosphere differs from that in the uniform atmosphere may be judged by returning to the full equations of motion

$$m\dot{V} = F \cos \alpha - mg \sin \gamma - \tfrac{1}{2}\rho_0 V_E^2 S C_D(\alpha, \eta),$$

$$mV\dot{\gamma} = F \sin \alpha - mg \cos \gamma + \tfrac{1}{2}\rho_0 V_E^2 S C_L(\alpha, \eta)$$

and

$$I_y \dot{q} = \tfrac{1}{2}\rho_0 V_E^2 S l \left\{ C_m(\alpha, \eta) + C_{m_q} \frac{ql}{V} + C_{m_{\dot{\alpha}}} \frac{\dot{\alpha} l}{V} \right\} + Fd.$$

With V_E = constant = V_{E_S} it follows that V must vary and by differentiation of the equation

$$V_E = \sqrt{\sigma} V$$

we obtain

$$\frac{dV_E}{dt} = 0 = \sqrt{\sigma} \frac{dV}{dt} + V \frac{d\sqrt{\sigma}}{dt}$$

which yields

$$\frac{dV}{dt} = -\frac{V}{\sqrt{\sigma}}\frac{d\sqrt{\sigma}}{dt}$$

$$= -\frac{V_{Es}^2}{\sigma\sqrt{\sigma}}\frac{d\sqrt{\sigma}}{dh}\sin\gamma_S.$$

Thus an imbalance of the first equation comes about as the altitude changes and so the motion must depart from the steady rectilinear motion that occurs in the uniform atmosphere. The difference depends on the speed and the density ratio for the portion of the atmosphere traversed. Hence in the present study the effect is not large, since at about 2000 m the factor $(1 - V_{Es}^2 d\sqrt{\sigma}/dh/g\sigma\sqrt{\sigma})$ is around 1·01. This explains the closeness of the variables to their steady-state values for uniform atmosphere as indicated on the right-hand side of the figures, where appropriate.

Apart from the solution of the equations of motion as given above, the only other course open is to consider the possibility of obtaining approximate analytic solutions for the non-uniform atmosphere case. In the present context the matter is not of such importance as to warrant investigation along these lines.

TABLE 1

Characteristics of the High-Tail Aircraft

wing area = 1358·3 ft^2 = 126·19 m^2

mean chord of wing = 15·12 ft = 4·61 m

$$\frac{\rho_e S\bar{c}}{2m} = 0{\cdot}007723$$

$$\frac{F_e}{mg} = 0{\cdot}04039$$

$$\frac{\rho_e S\bar{c}^3}{2I_y} = 0{\cdot}002655$$

$$\frac{\partial C_L}{\partial \eta} \equiv \frac{\partial C_L}{\partial \eta_T} = 1{\cdot}3 \text{ per radian*}$$

$$\frac{\partial C_m}{\partial \eta} \equiv \frac{\partial C_m}{\partial \eta_T} = -3{\cdot}63 \text{ per radian.*}$$

* Longitudinal control consists of all-moving tailplane with geared elevator.

TABLE 2

Characteristics of the Slender-Wing Tailless Aircraft

wing area = 358·25 m^2

root chord (c_0) = 27·66 m

$$\frac{\rho_e S c_0}{2m} = 0{\cdot}0427$$

$$\frac{F_e}{mg} = 0{\cdot}1562 \text{ (CG at } 0{\cdot}52c_0)$$

$$\frac{\rho_e S c_0^3}{2I_y} = 0{\cdot}2756$$

thrust moment arm = $0{\cdot}025c_0$

$$C_{m_q} = -0{\cdot}201 + 0{\cdot}91\Delta x/c_0$$

$$C_{m_{\dot{\alpha}}} = -0{\cdot}101 + 0{\cdot}46\Delta x/c_0$$

where Δx is the distance of the centre of gravity of the aircraft aft of $0{\cdot}5c_0$.

In the above tables the suffix e refers to the initial conditions.

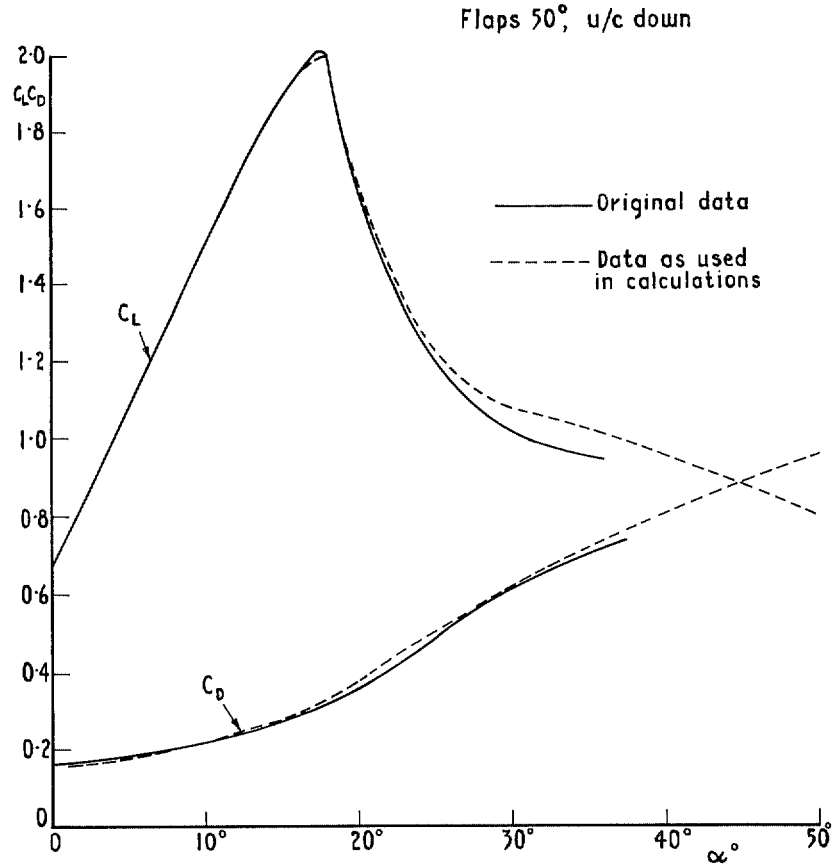

FIG. 1. Variation of lift and drag coefficients with angle of attack.

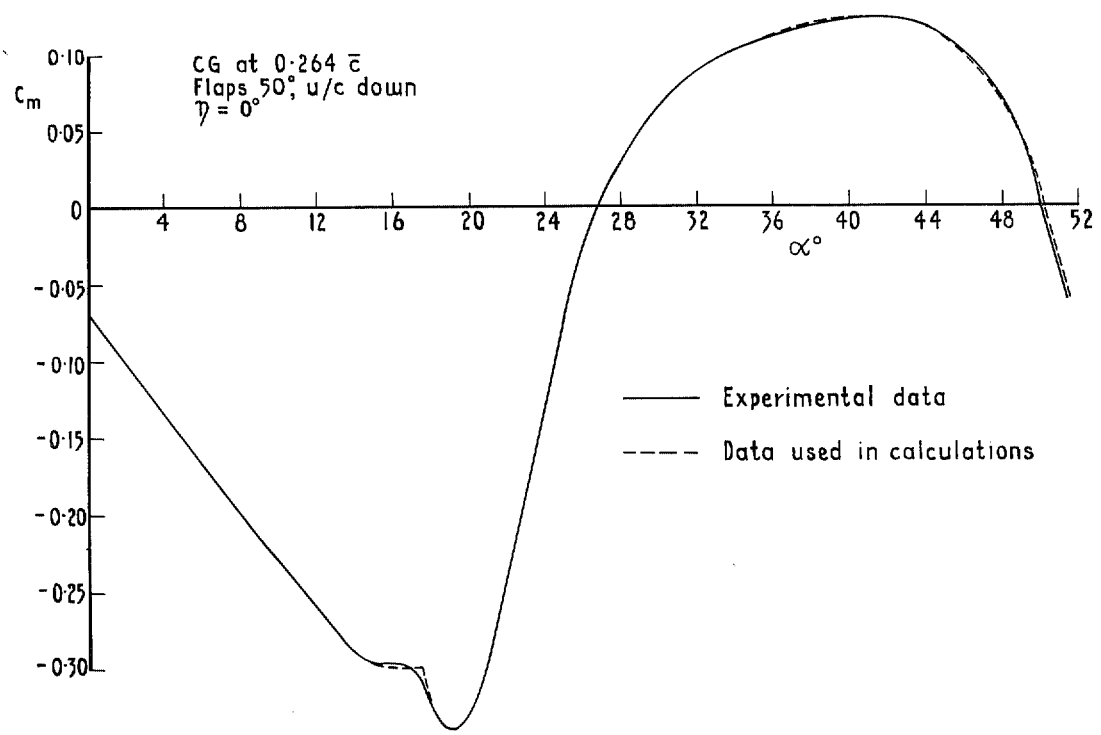

FIG. 2. Pitching moment due to angle of attack.

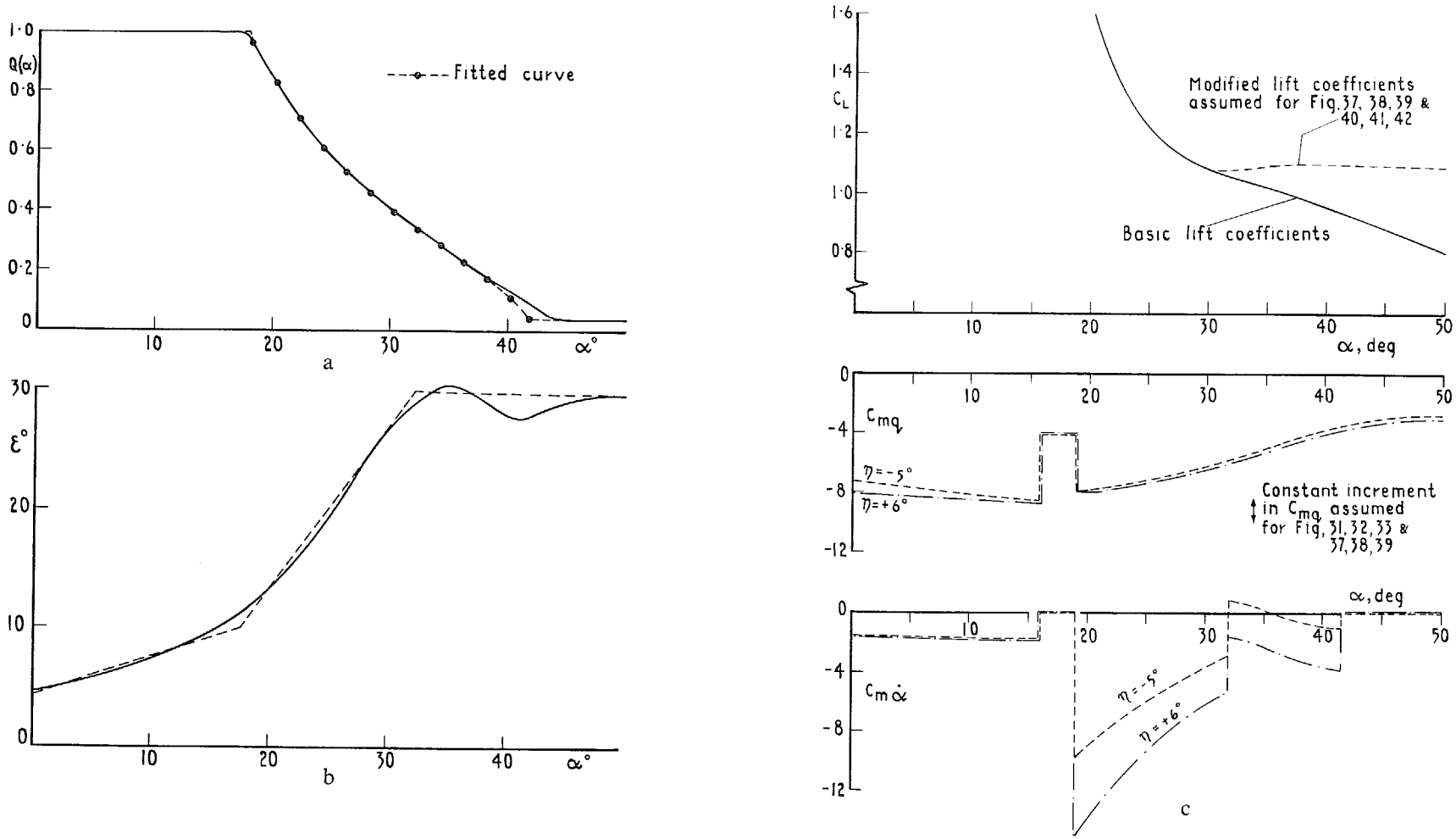

FIG. 3a & b. Kinetic pressure factor Q, and the downwash at the tailplane ε.

FIG. 3c. Typical variation of damping-in-pitch and lift characteristics assumed in basic study with modifications to give increased damping particularly at large angles of attack.

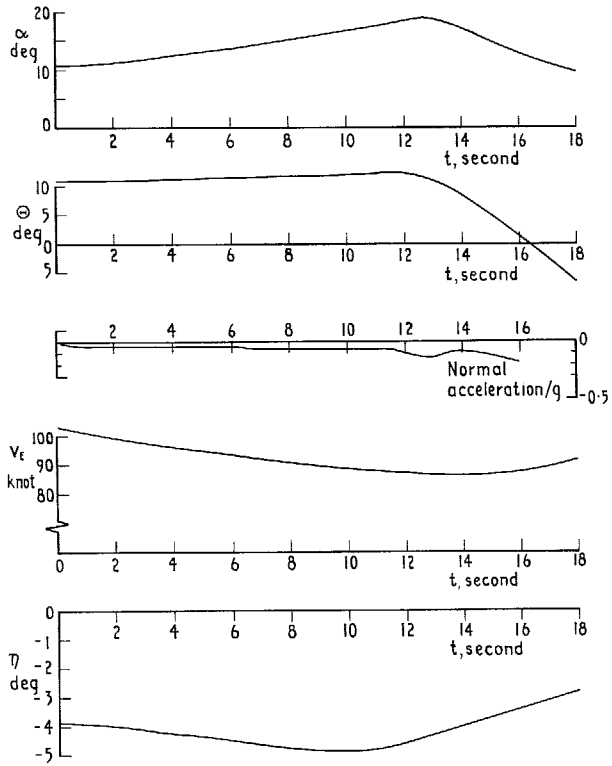

a

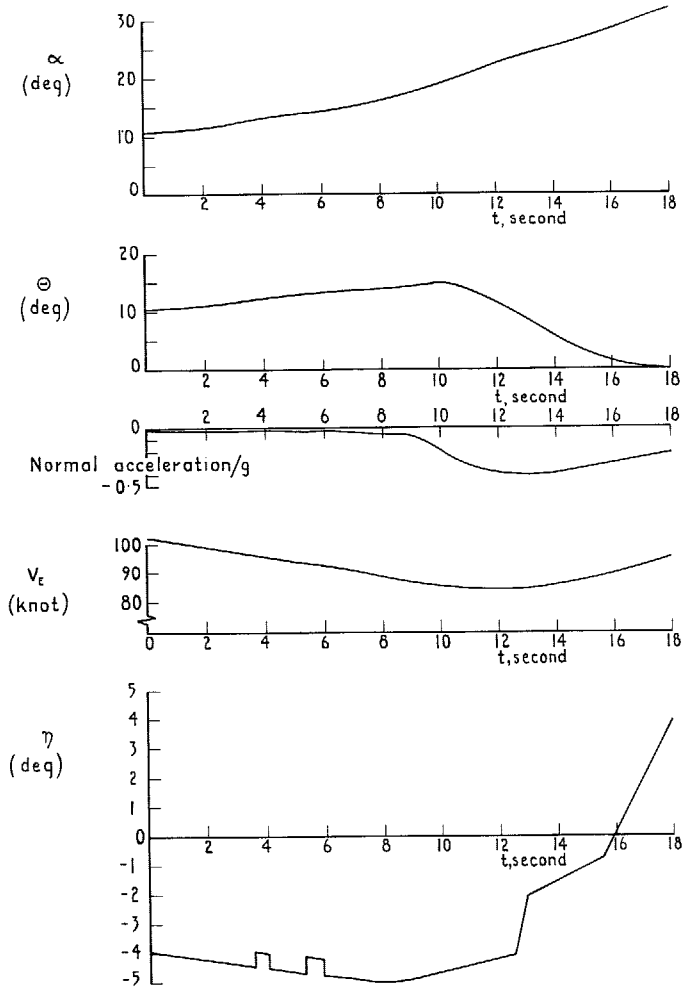

b

FIG. 4a. Stall and recovery following early reduction in the amount of up-elevator.

FIG. 4b. Stall and failure to make normal recovery due to too late application of sufficient down-elevator (*see* also Figs. 5 to 7).

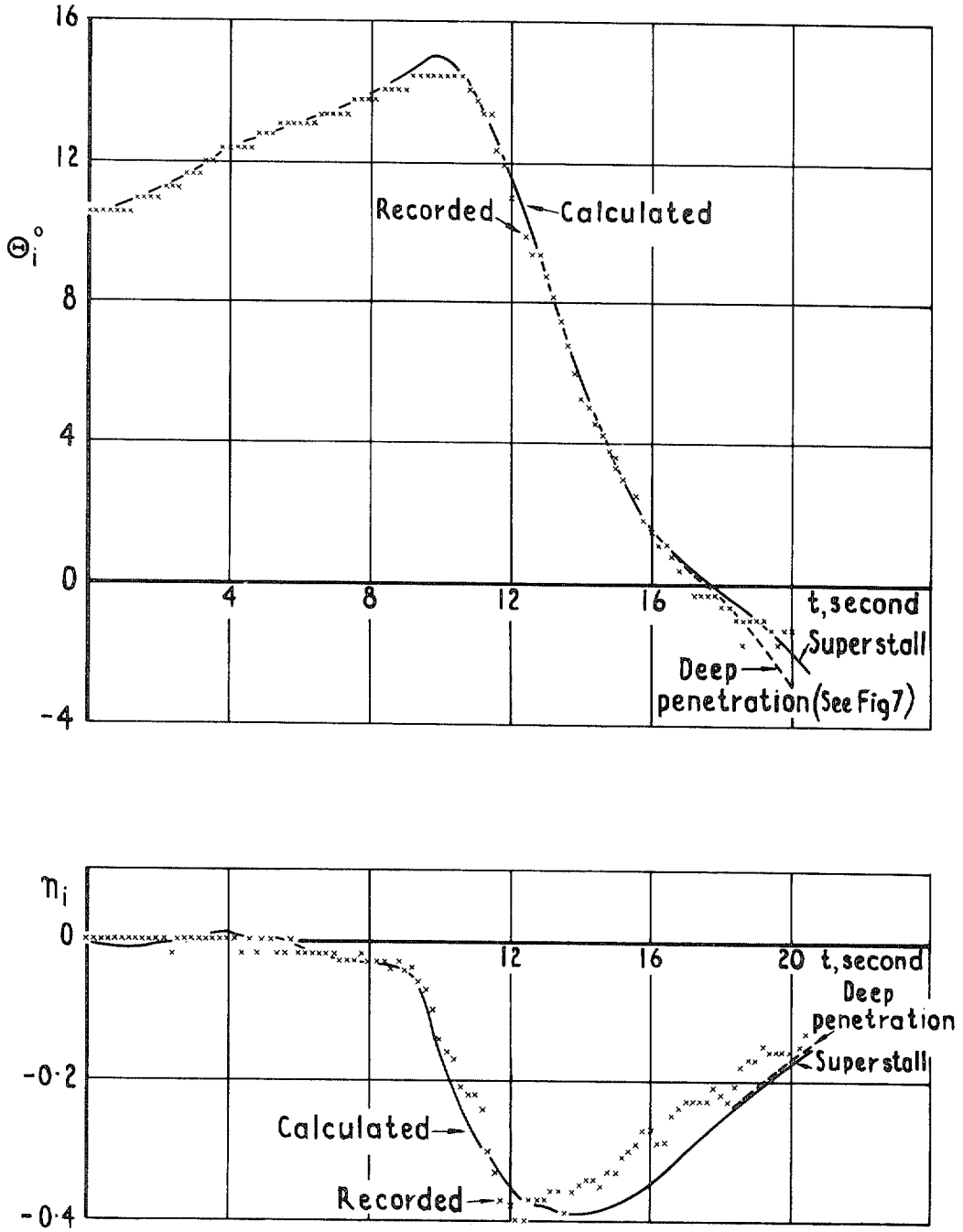

FIG. 5. Pitch attitude (angle of inclination), Θ_i, and indicated normal acceleration factor, n_i.

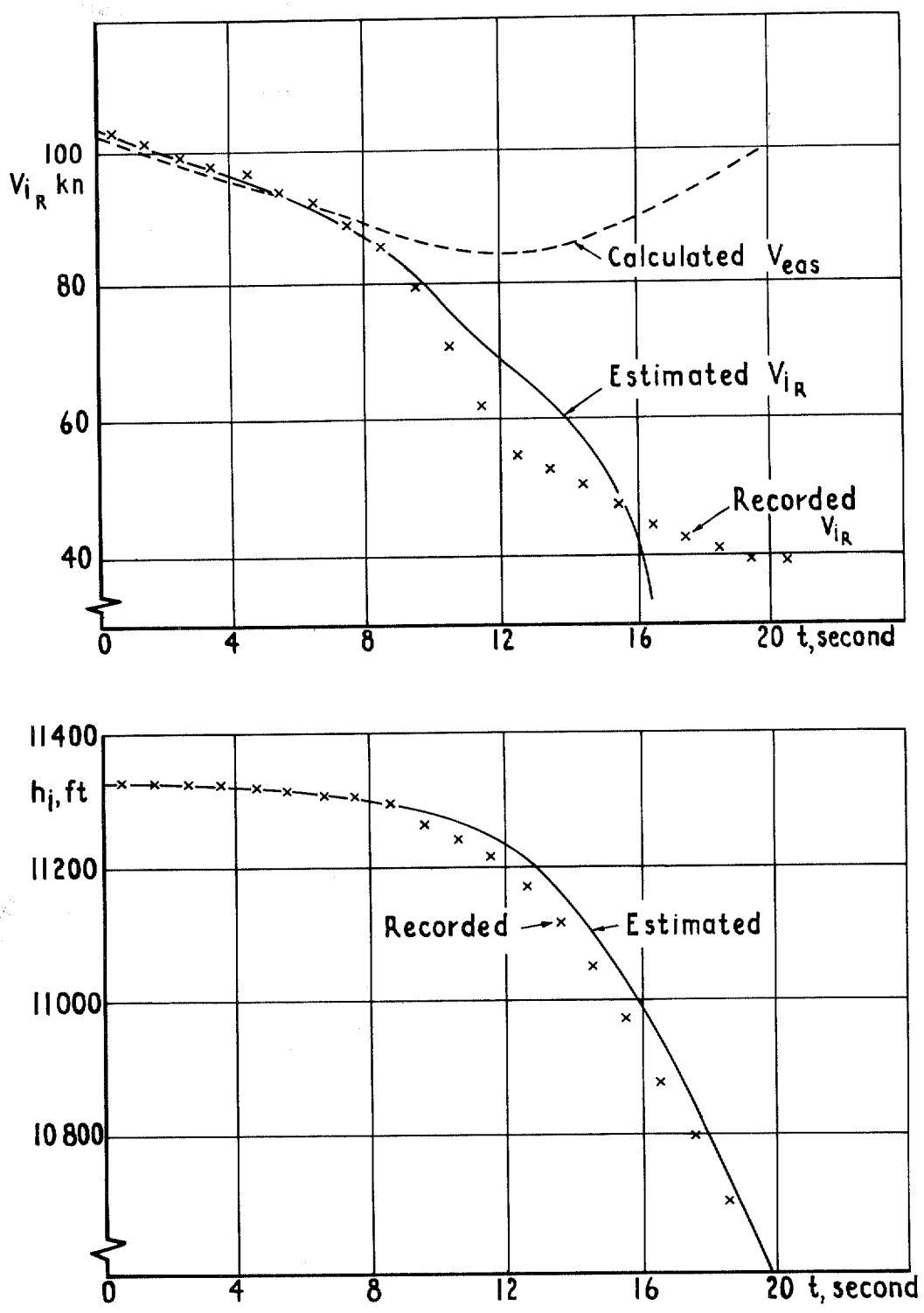

FIG. 6. History of the recorded indicated velocity V_{i_R} and indicated height, h_i.

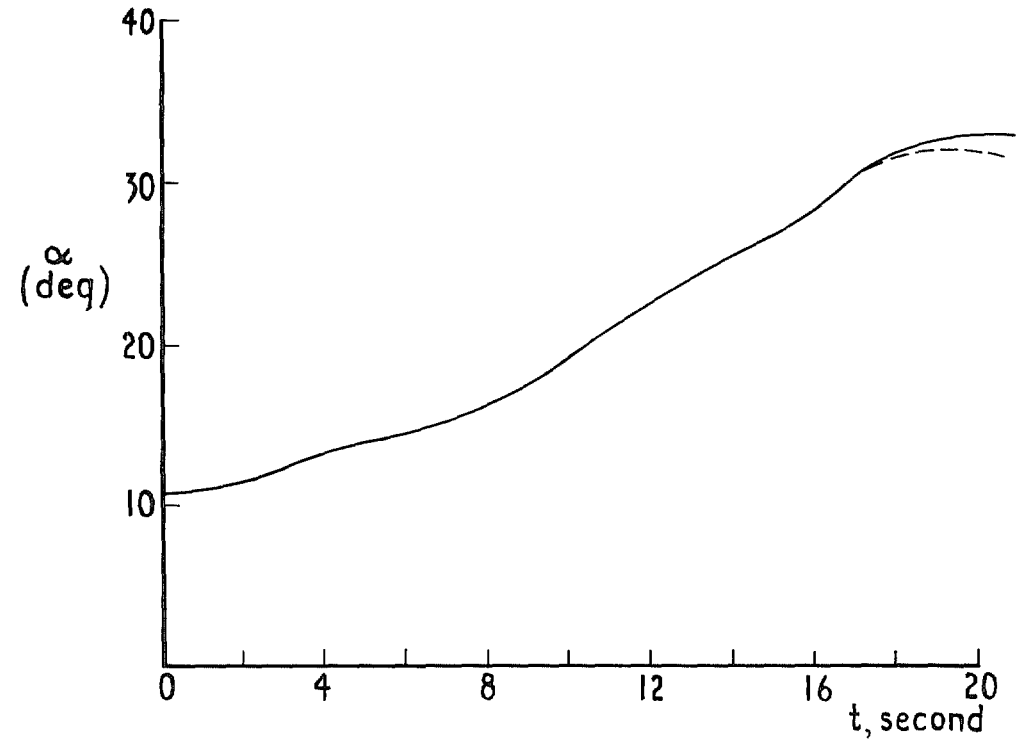

a

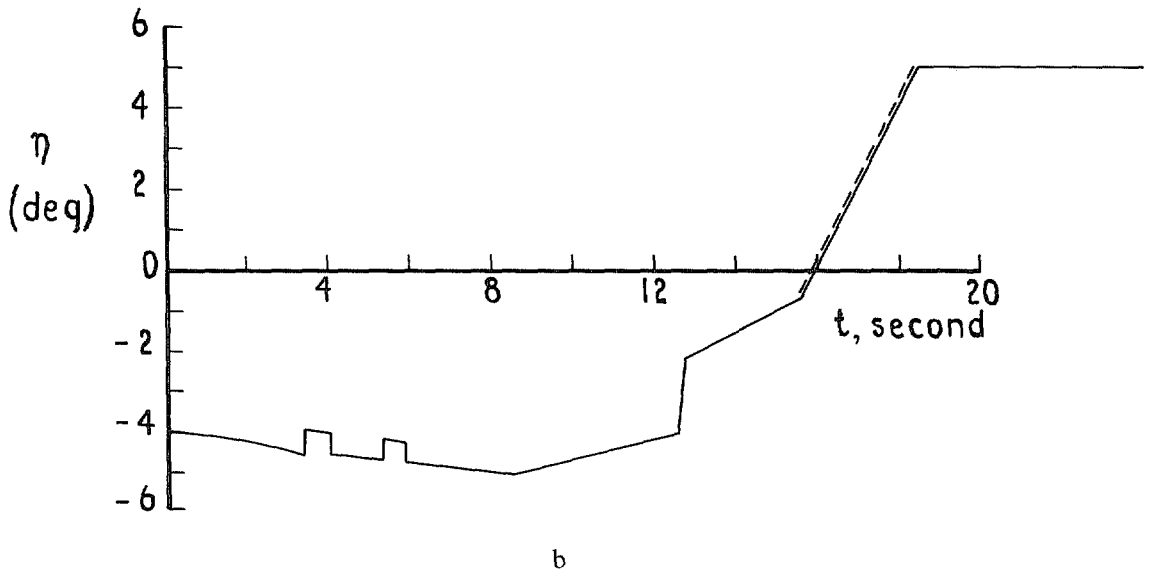

b

FIG. 7a. Angle of attack history for elevator input shown below.

FIG. 7b. Elevator input which gives response closely approximating the given response in Θ, n_i, V_i and h (*see* Figs. 5 and 6).

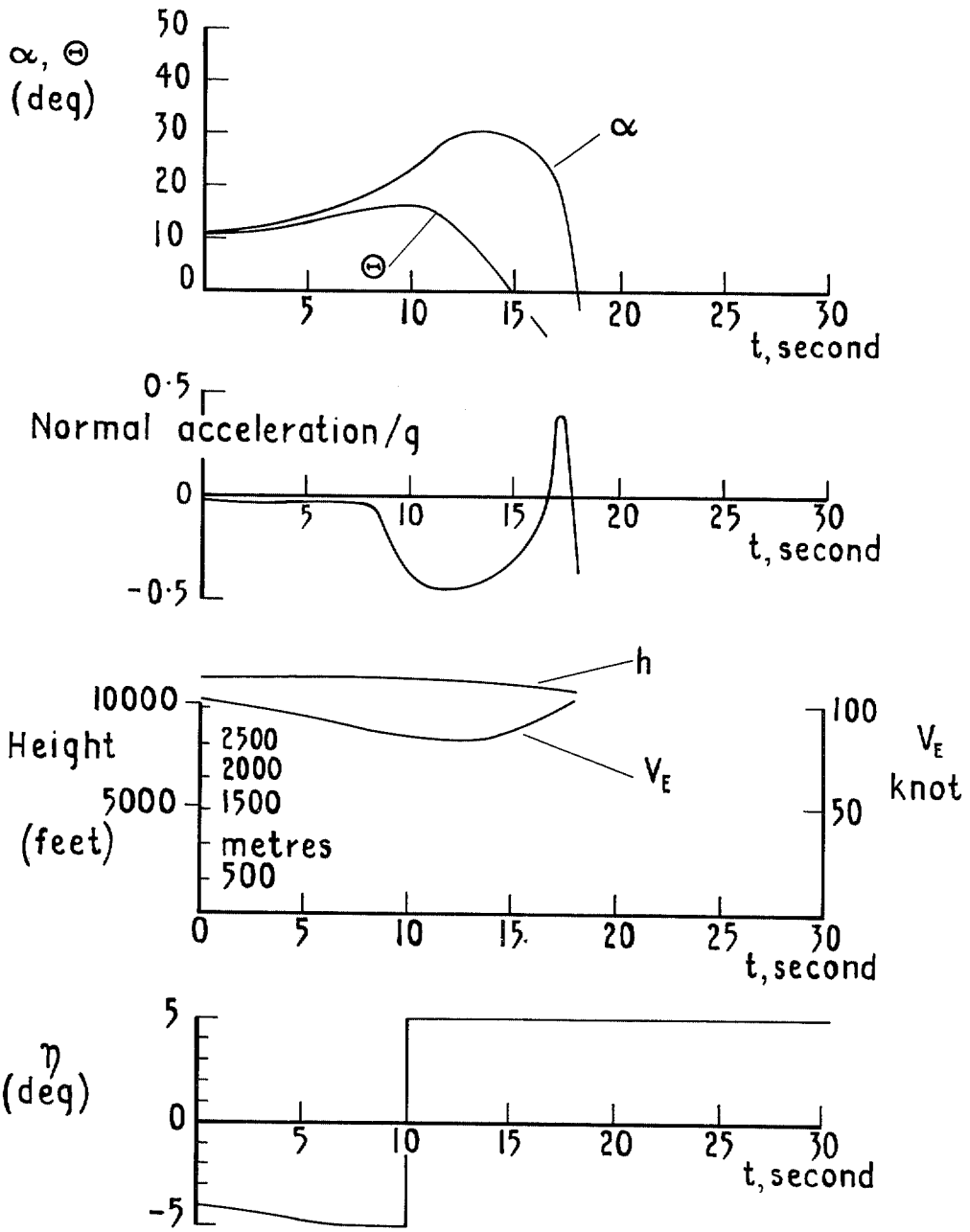

FIG. 8. Typical aircraft motion illustrating a normal recovery (near the limiting conditions).

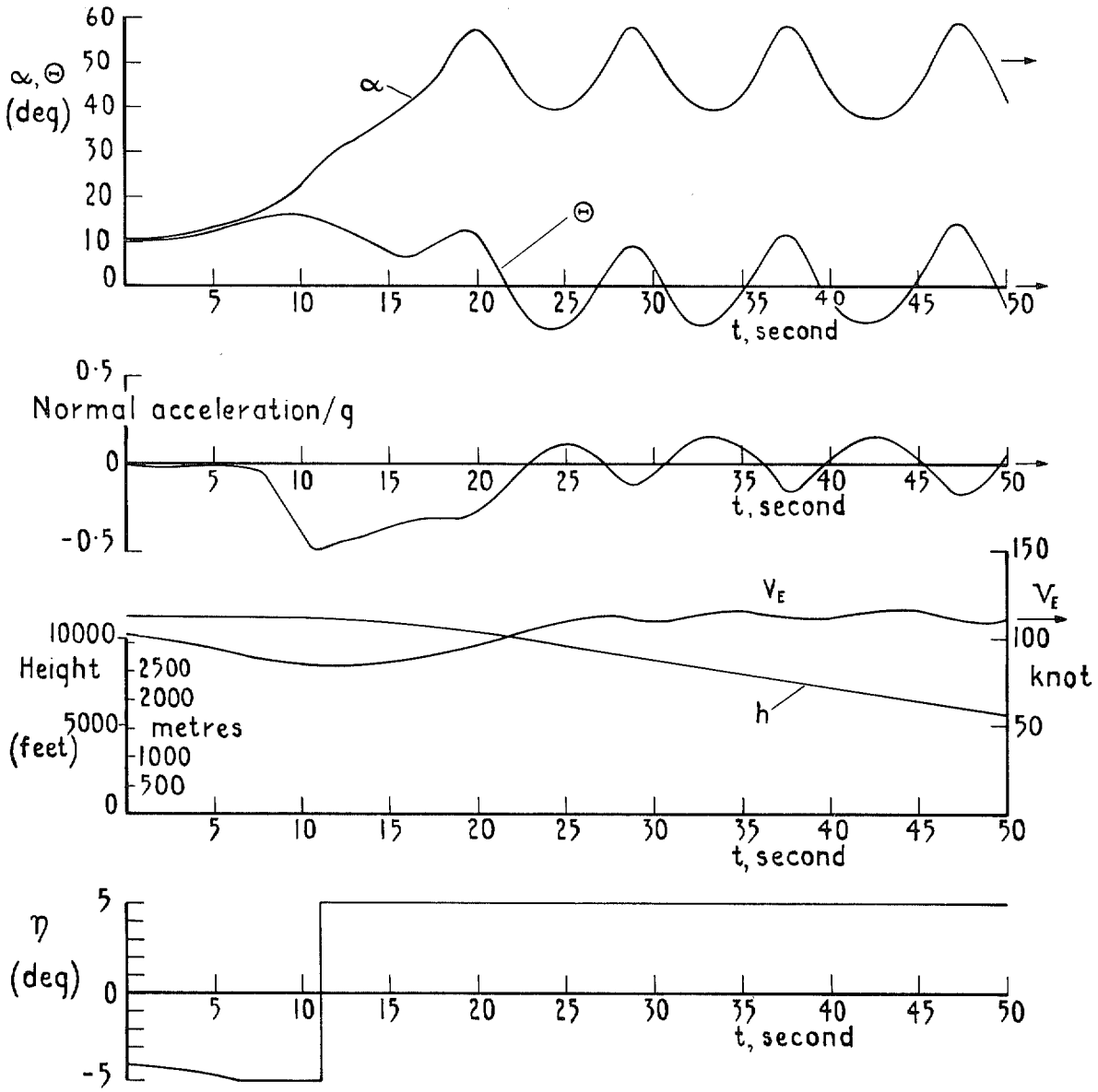

FIG. 9. Typical aircraft motion illustrating a 'superstalled' condition.

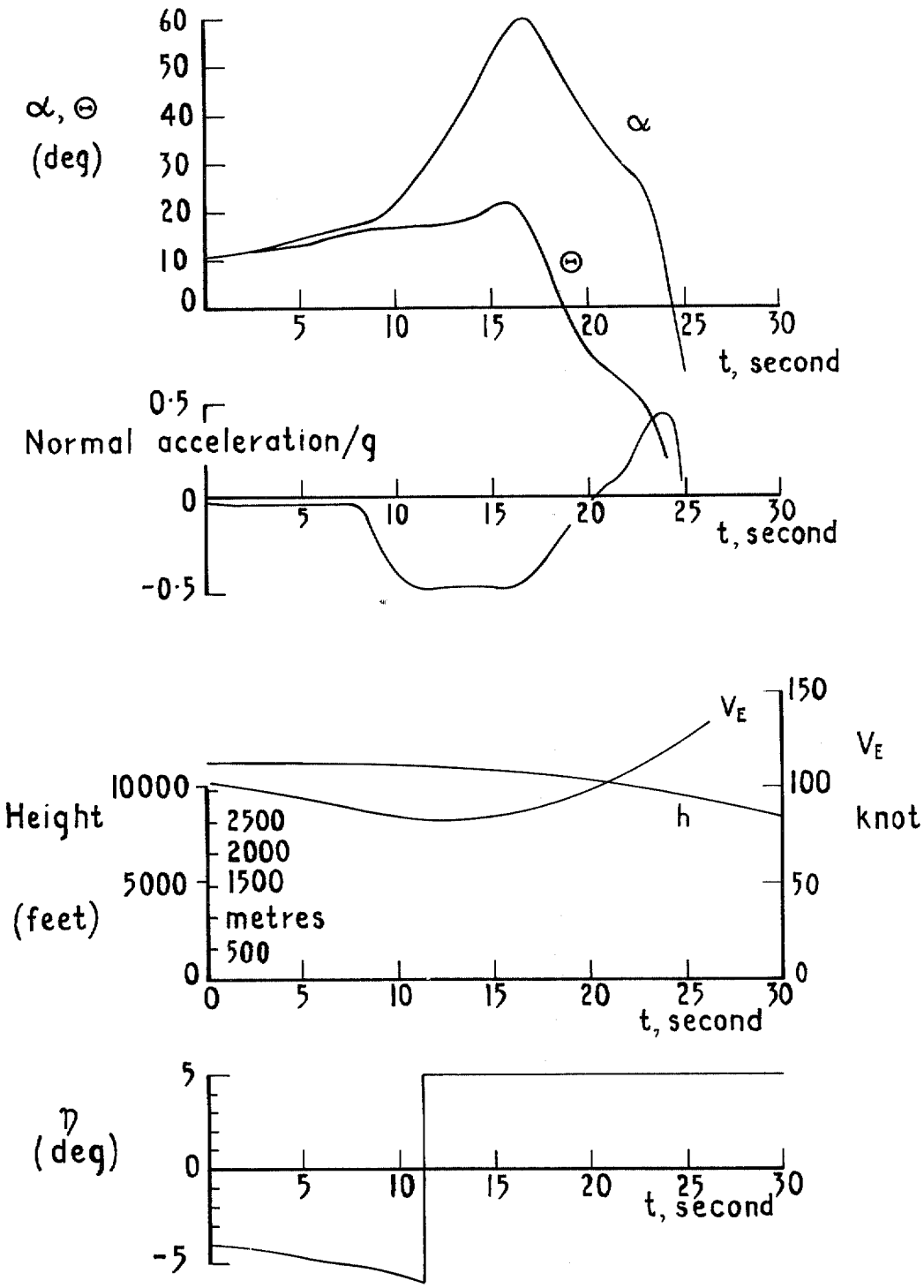

FIG. 10. Typical aircraft motion illustrating a 'bounce' type recovery.

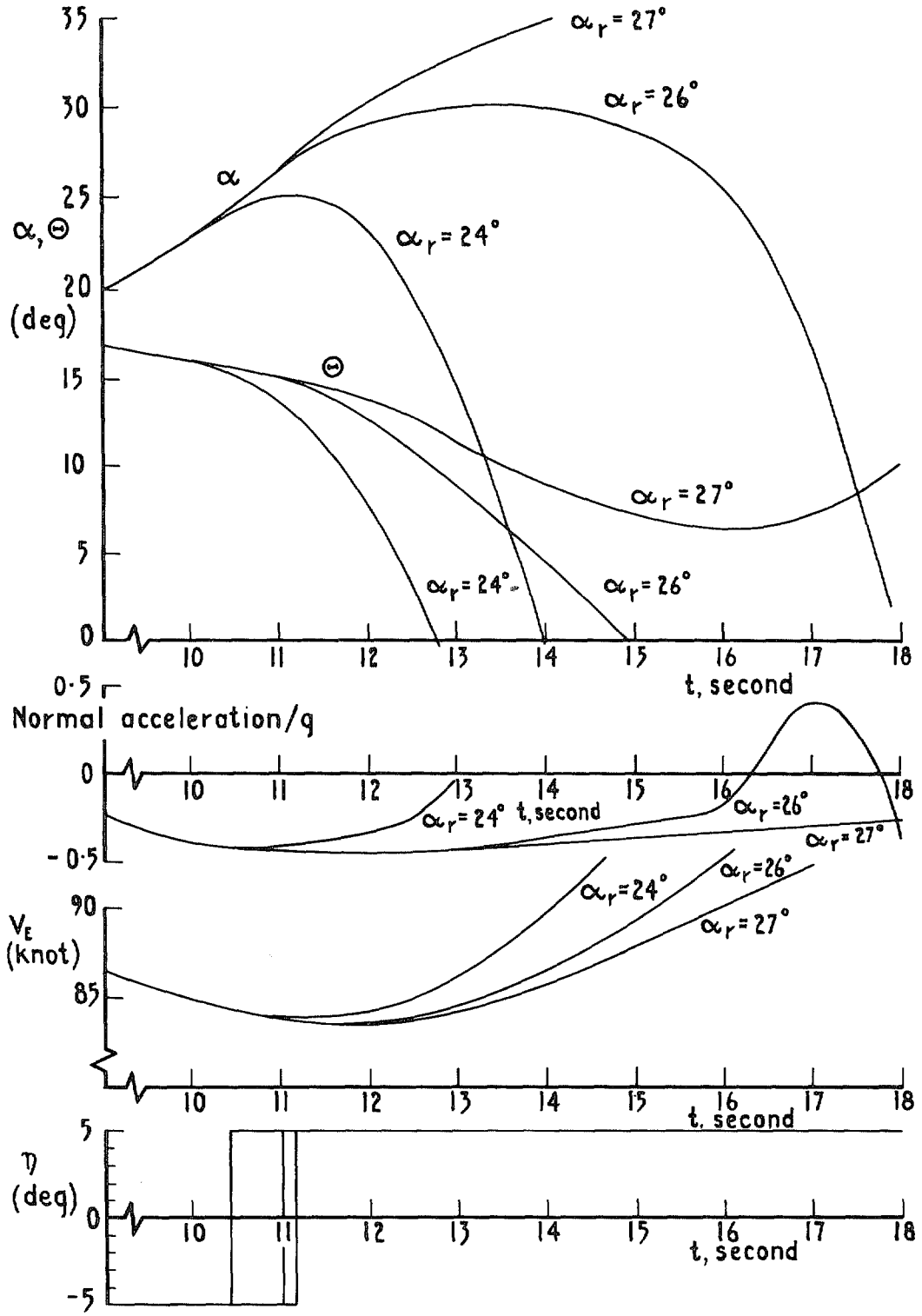

FIG. 11. Effect of delaying recovery attempt till a specified angle of attack is reached.

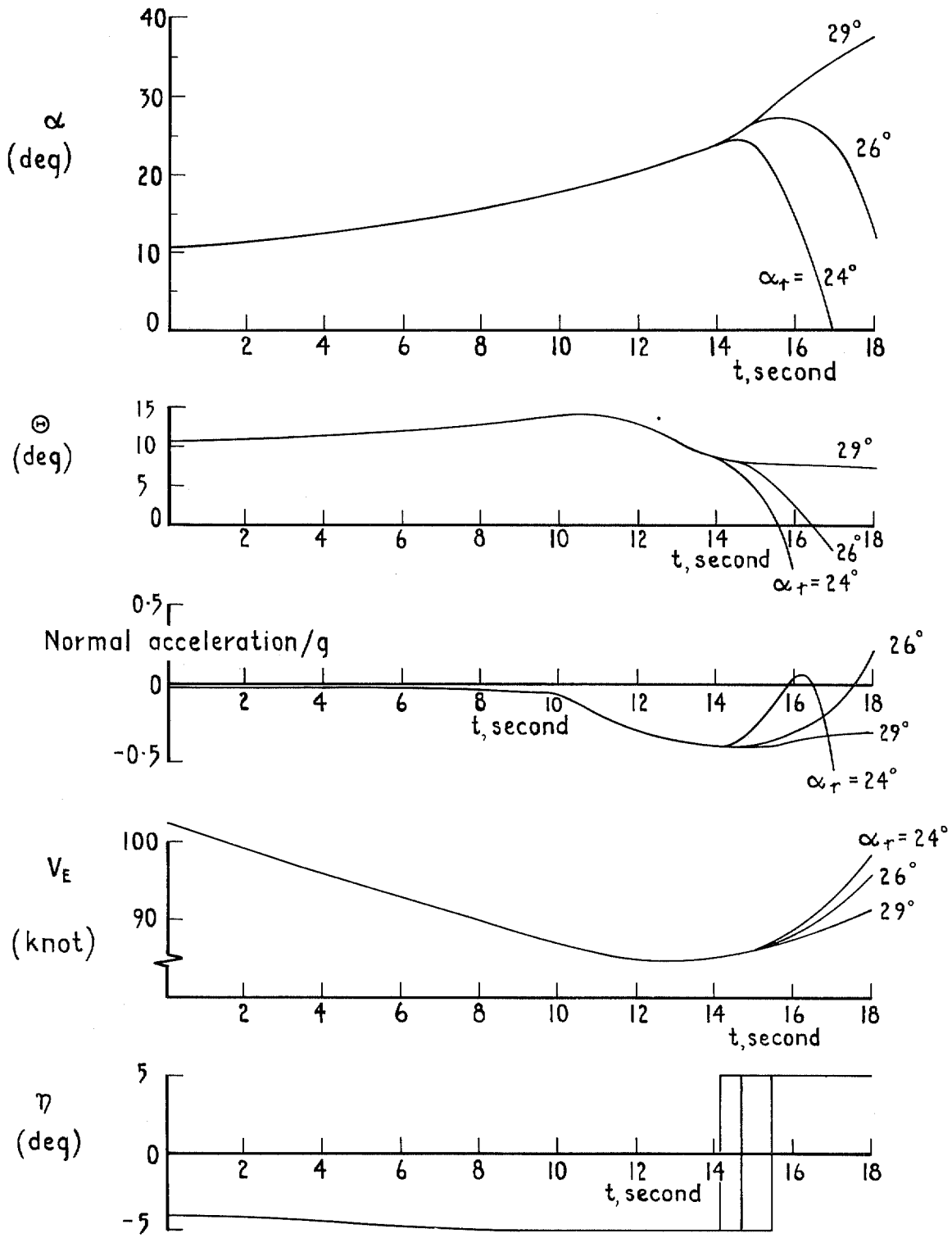

FIG. 12. Effect of delaying recovery attempt till a specified angle of attack is reached.

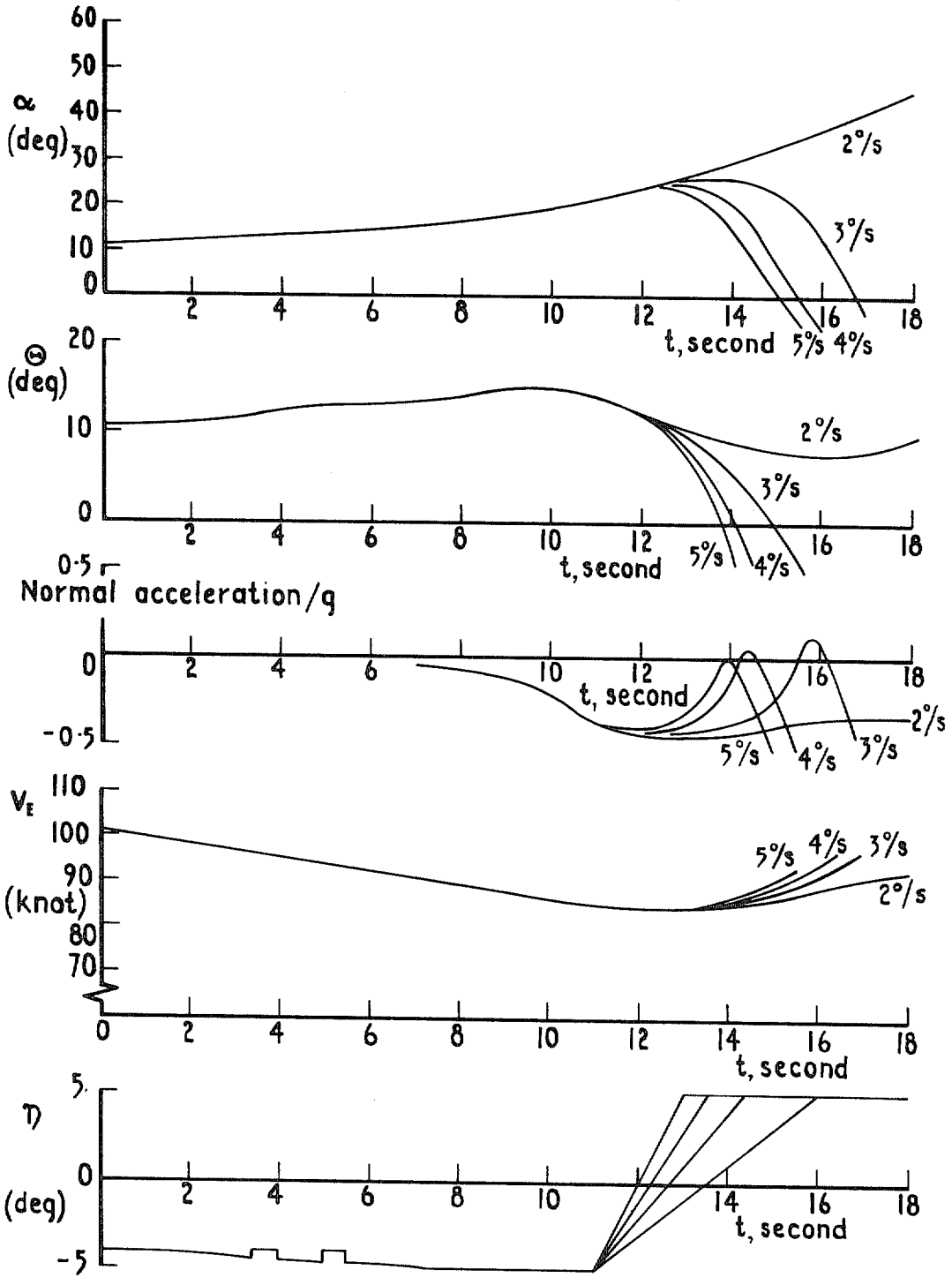

FIG. 13. Effect of rate of application of down-elevator on aircraft motion following recovery attempts initiated at the same instant (or recovery angle of attack).

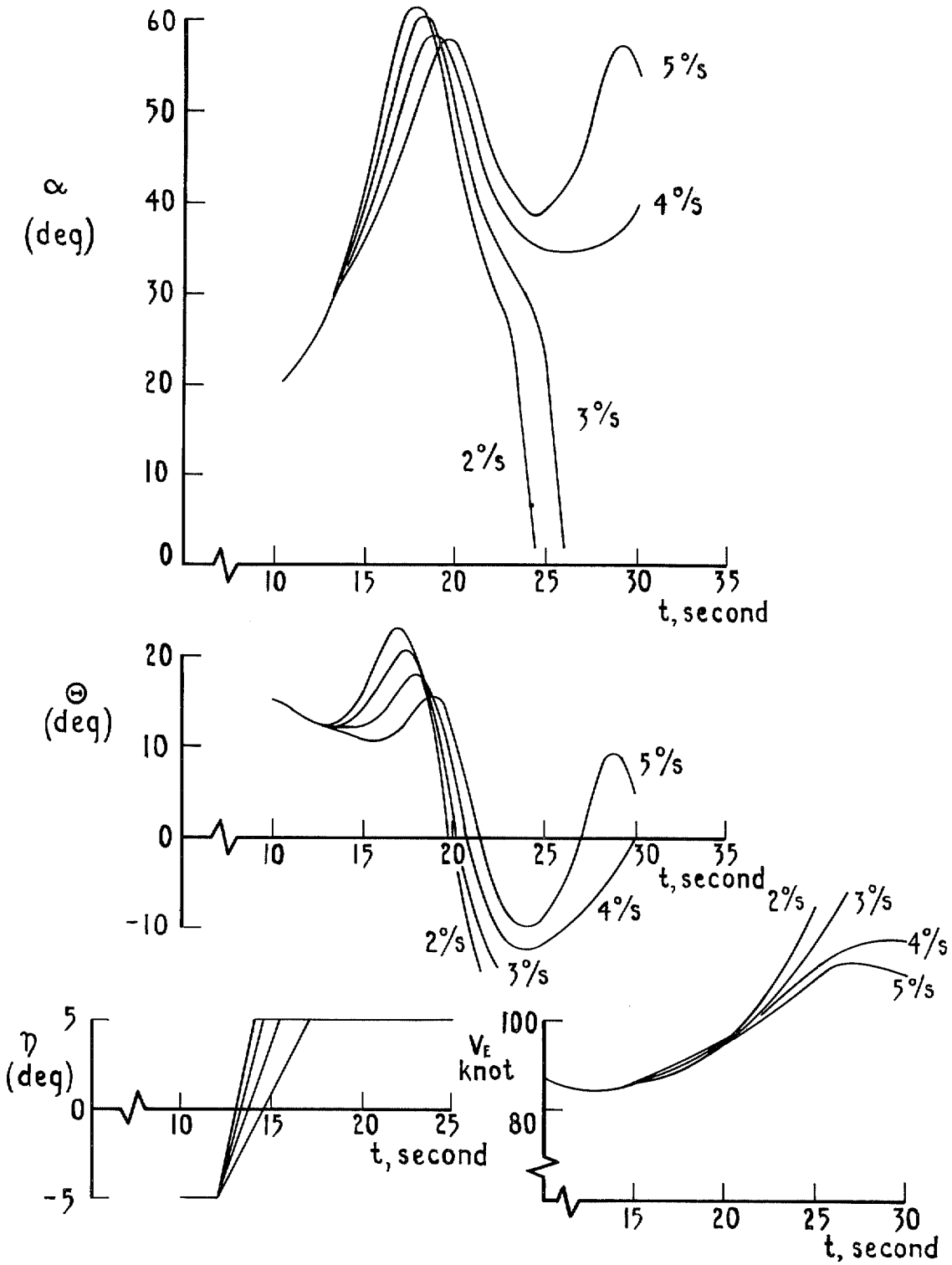

FIG. 14. Effect of rate of application of down-elevator in an abortive attempt resulting in either a 'superstall' or 'bounce' motion.

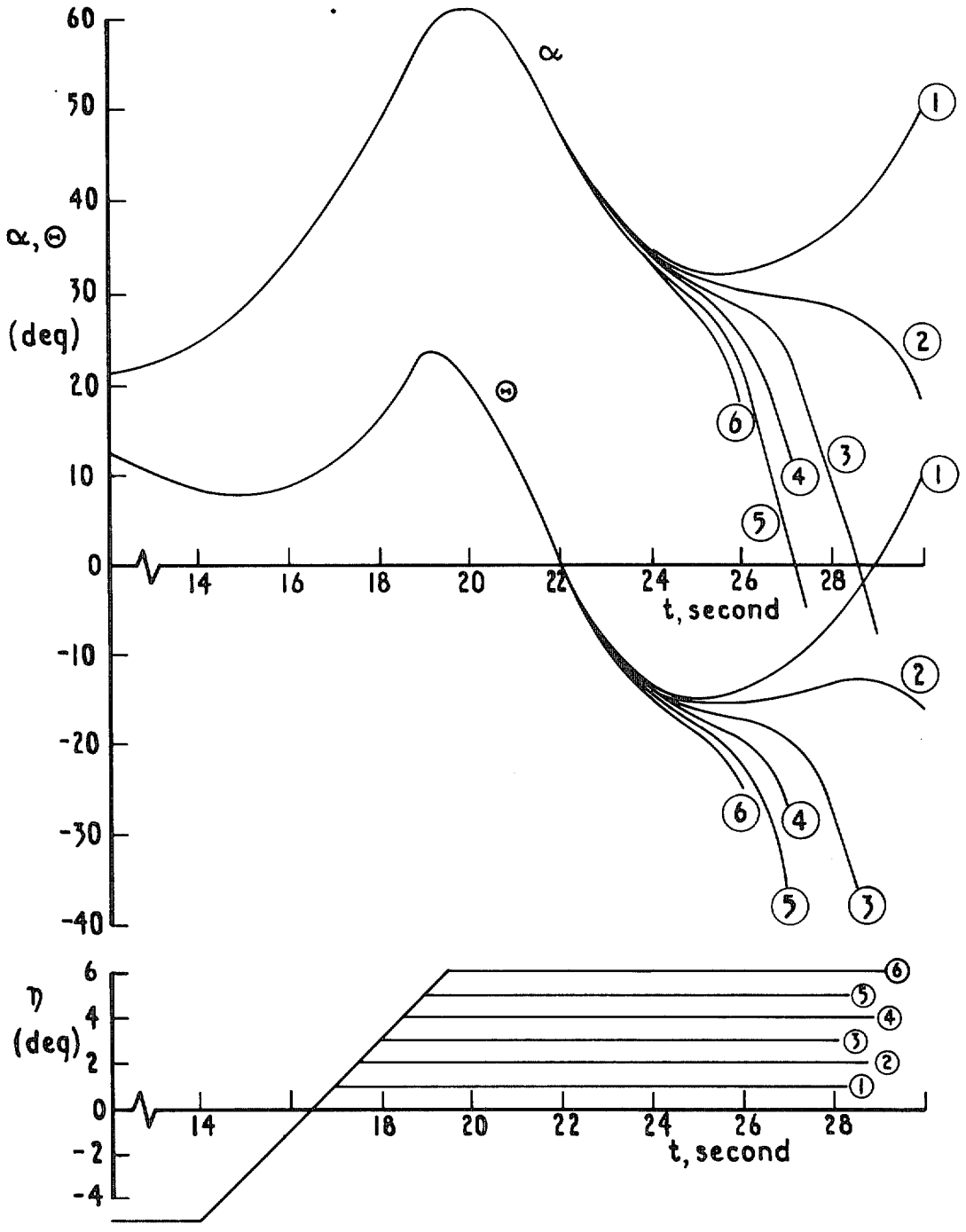

FIG. 15. Effect of various amounts of down-elevator on later stages of a manoeuvre in which rate of application is low.

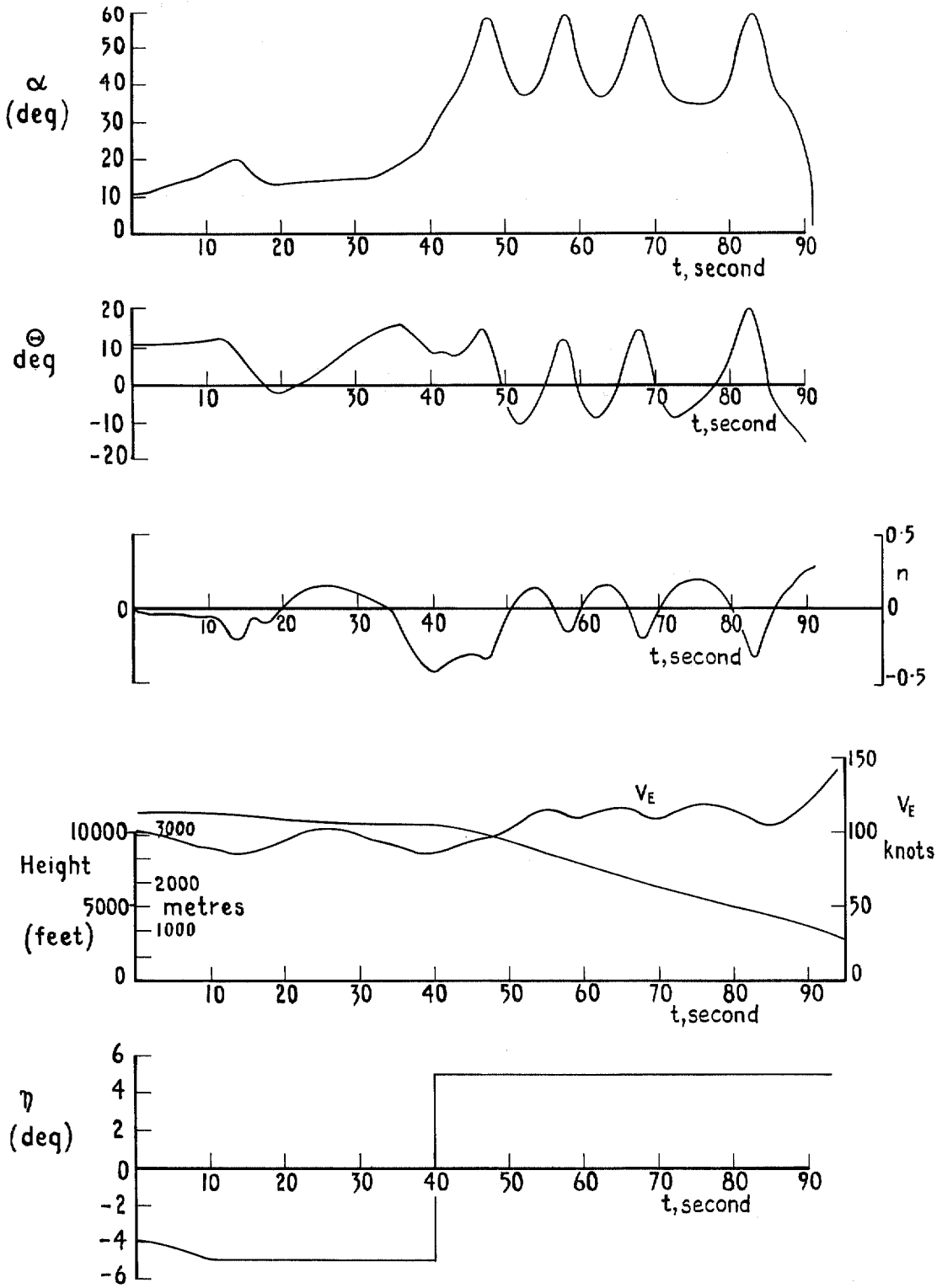

FIG. 16. Longitudinal motion in which a partial recovery is followed by an oscillation about the 'superstall' and finally a recovery ($\alpha_r = 27°$).

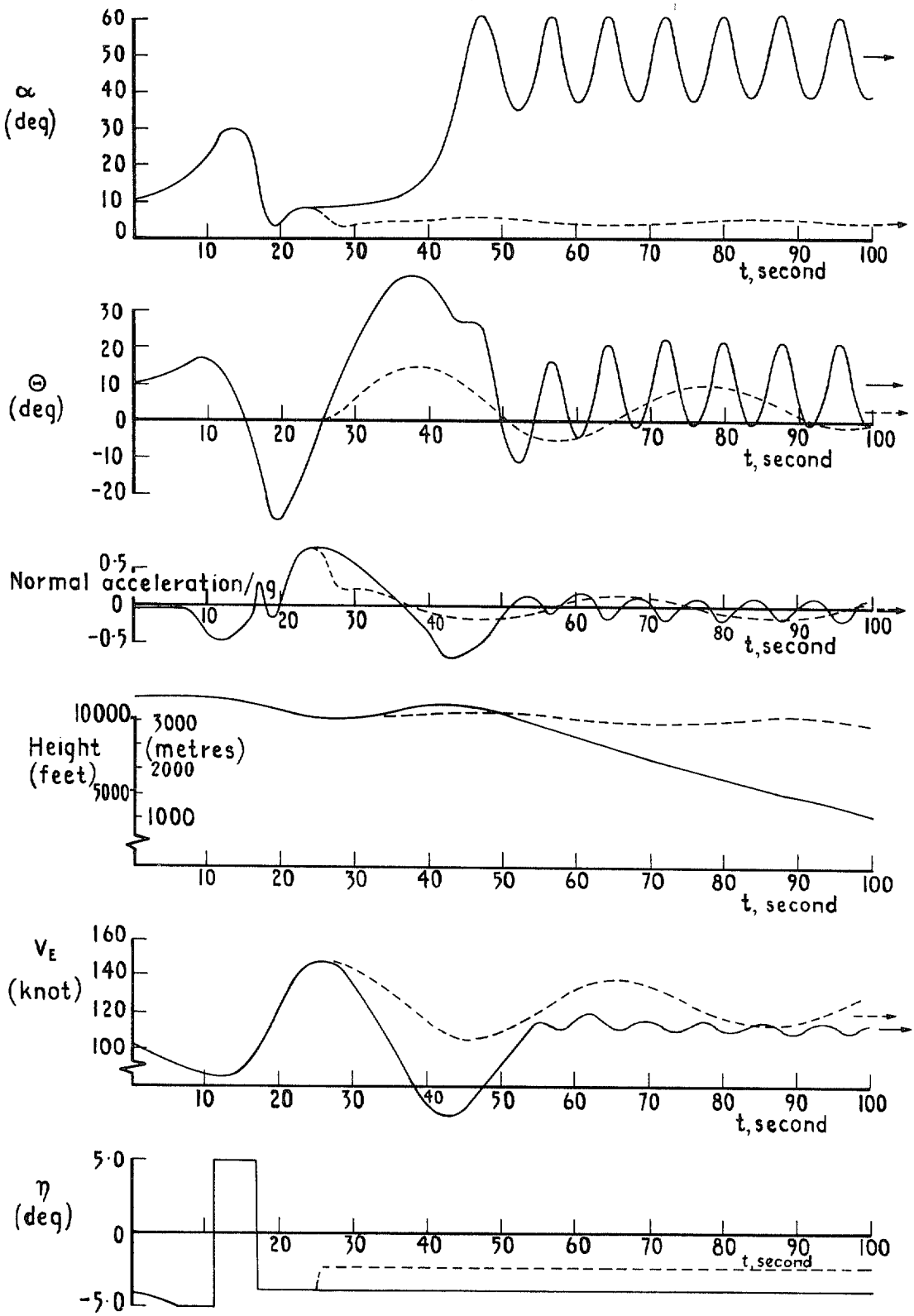

FIG. 17. Effect of two values of up-elevator on the final stages of a marginal recovery (high thrust level beyond $t = 16{\cdot}5$ second).

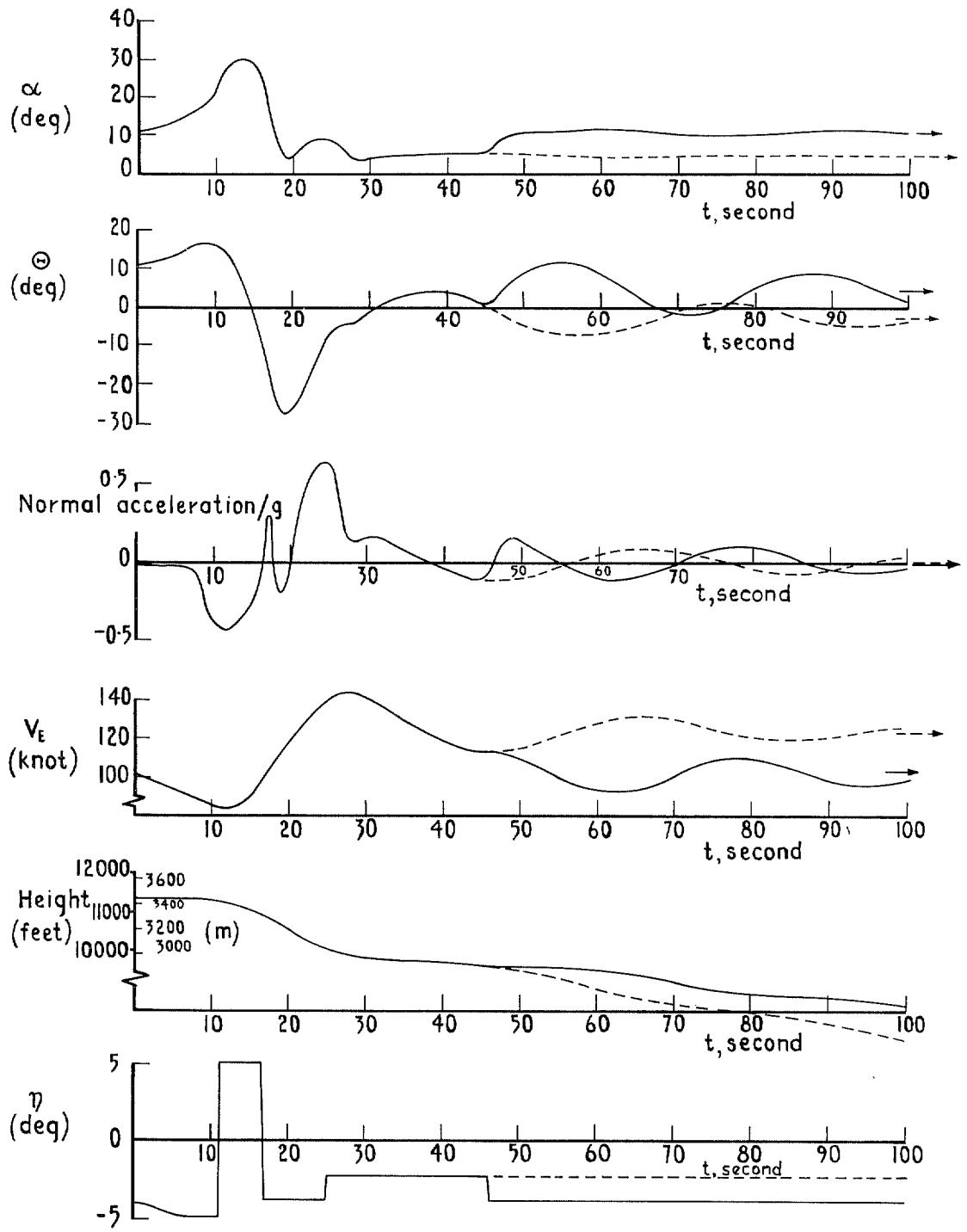

FIG. 18. Effect of different elevator inputs on return to normal flight after a marginal recovery.

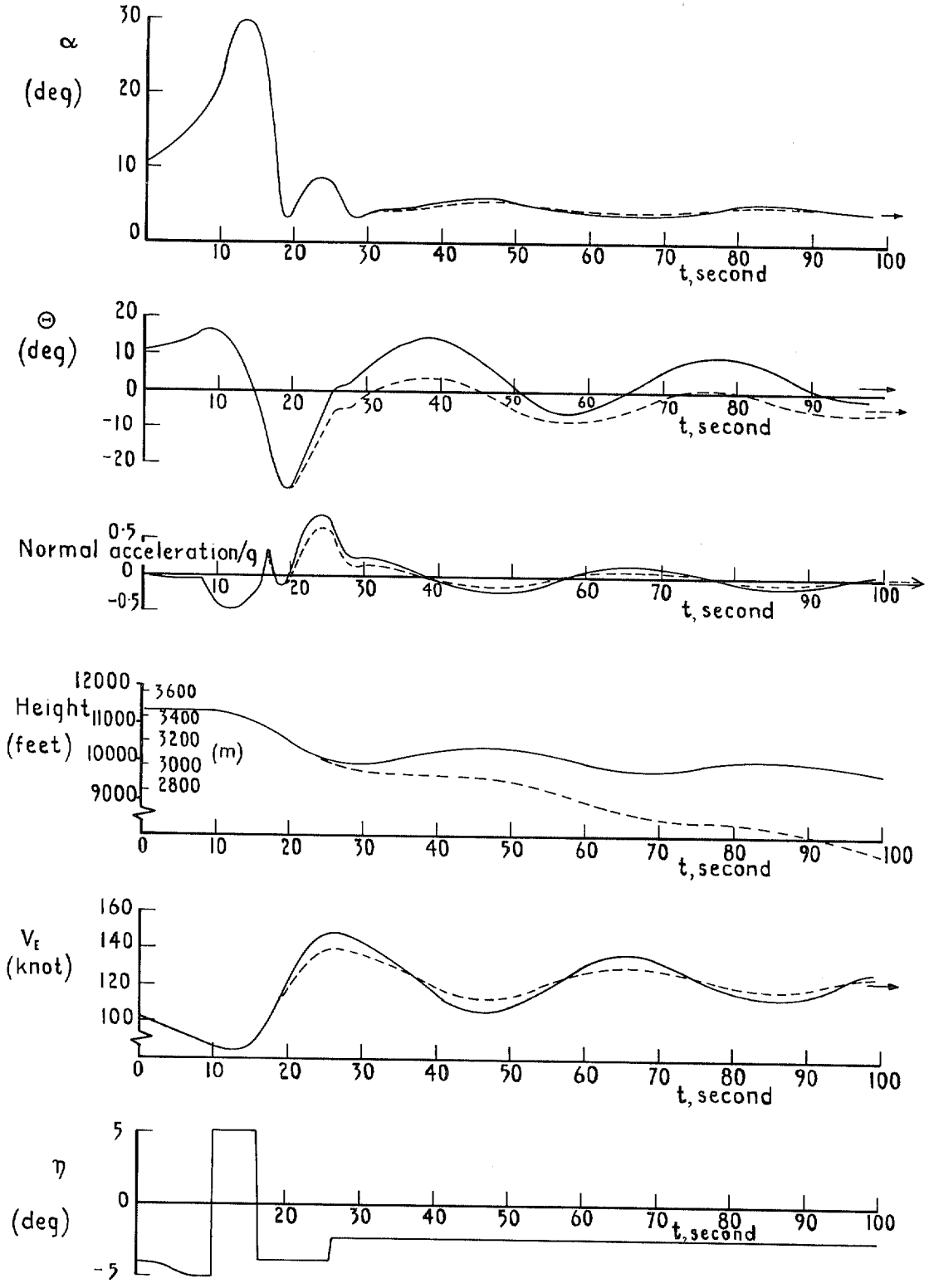

FIG. 19. Effect of increasing thrust at the same instant as elevator is reversed ($t = 16{\cdot}5$ second).

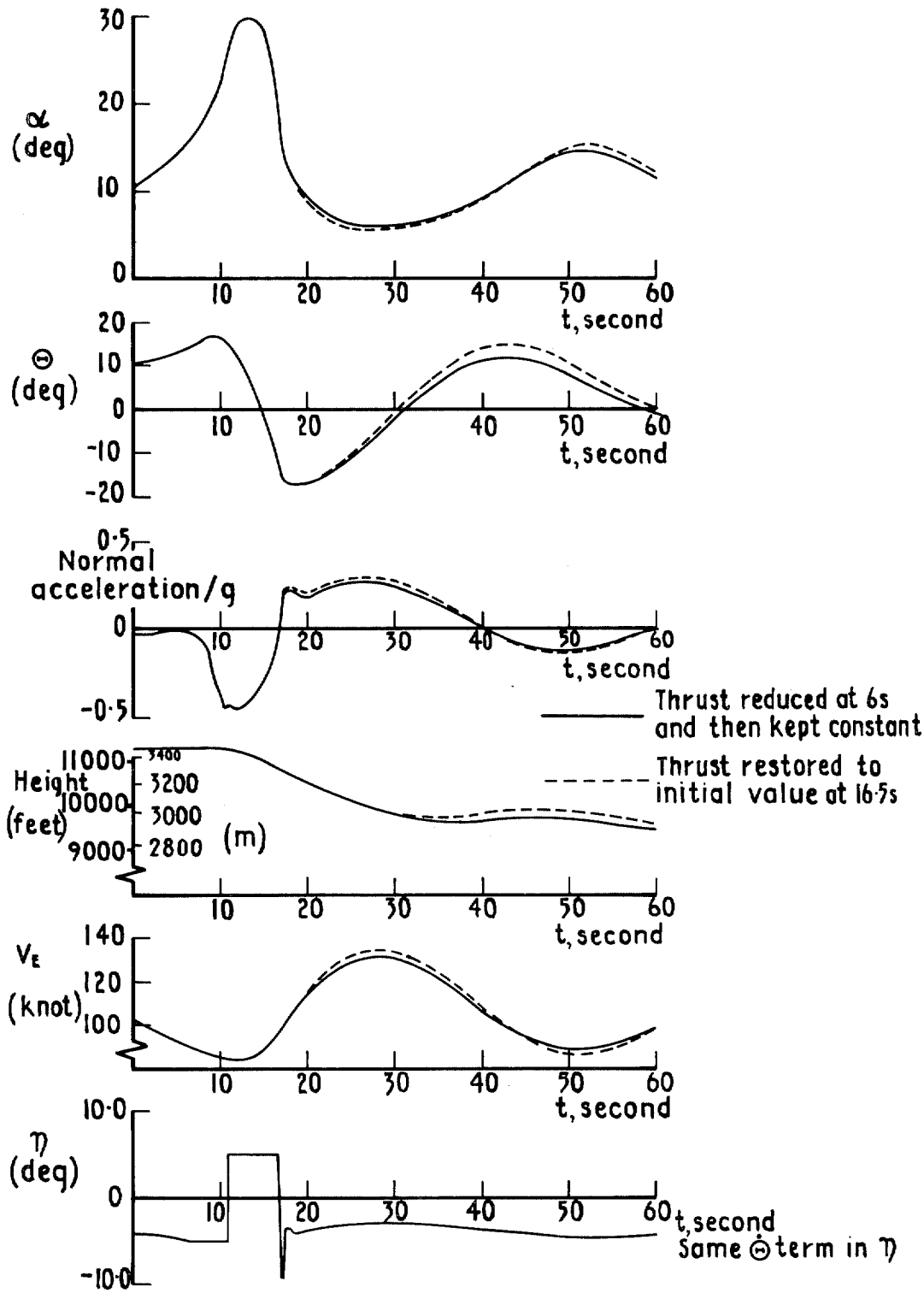

FIG. 20. Effect of restoring the engine thrust to its initial value on the recovery motion.

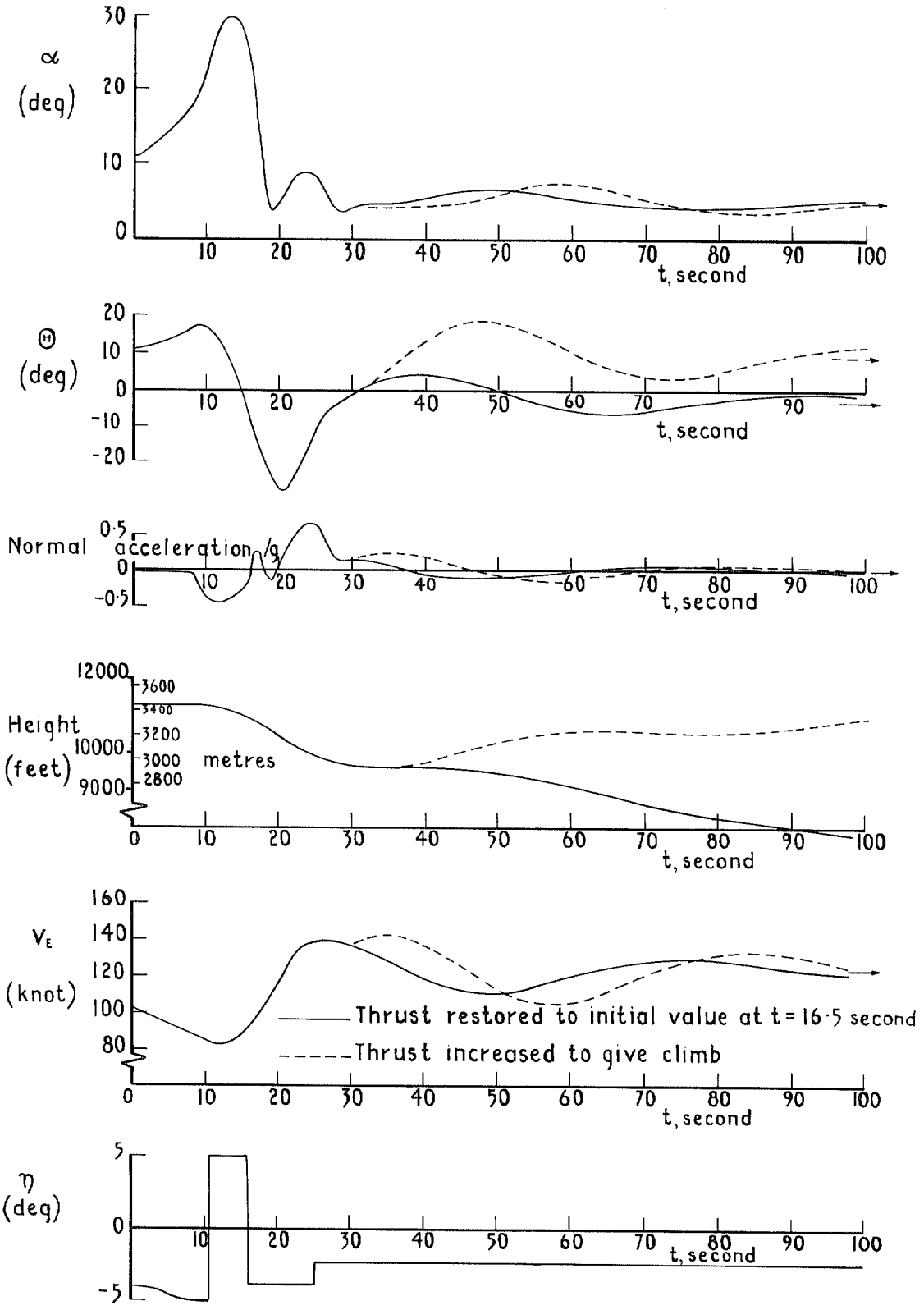

FIG. 21. Effect of a large increase in thrust following reversal of elevator (in the case shown at $t = 30$ second).

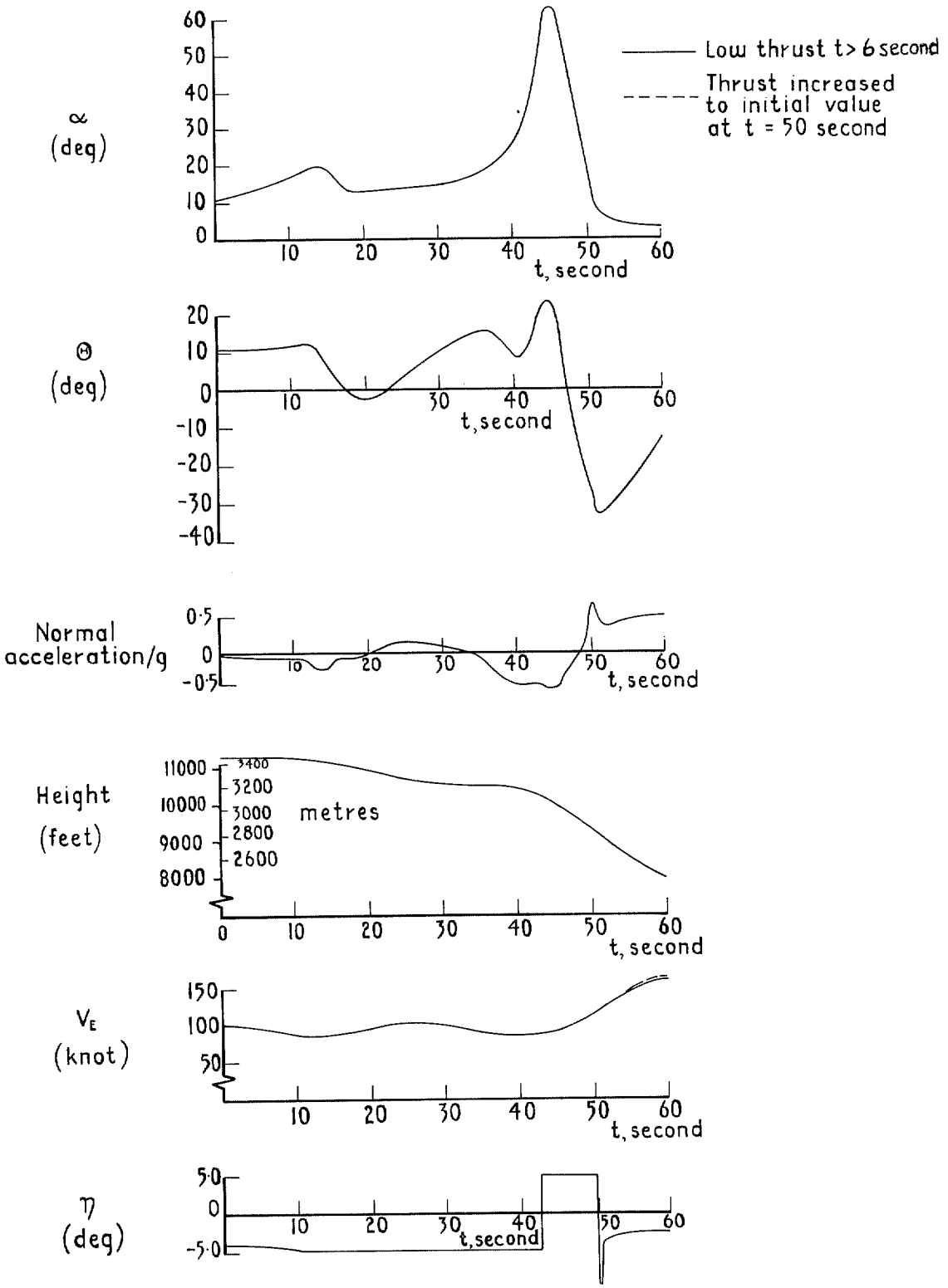

FIG. 22. Effect of an increase in thrust after the aircraft has passed through a 'bounce' recovery.

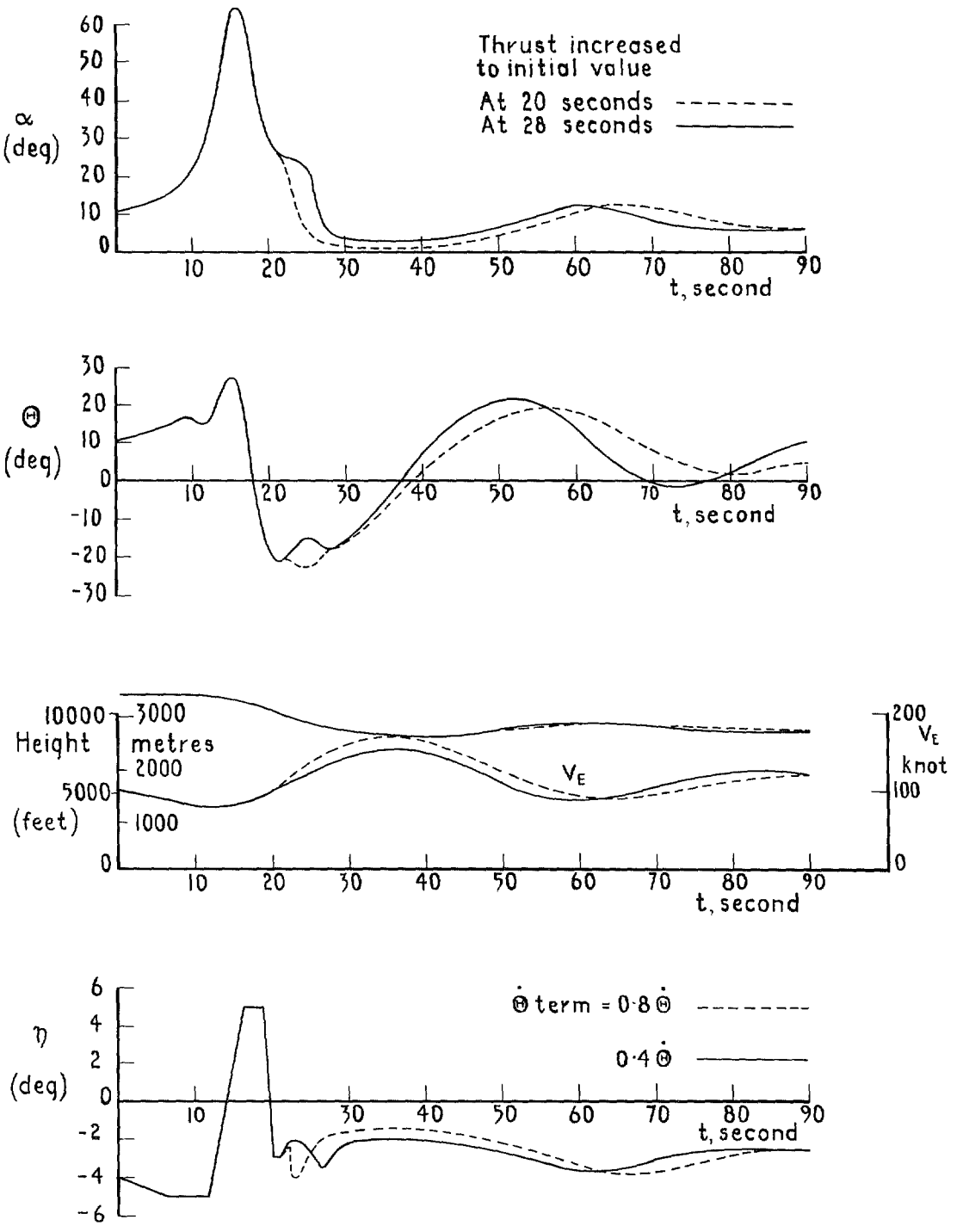

FIG. 23. Return to normal flight after a 'bounce' recovery.

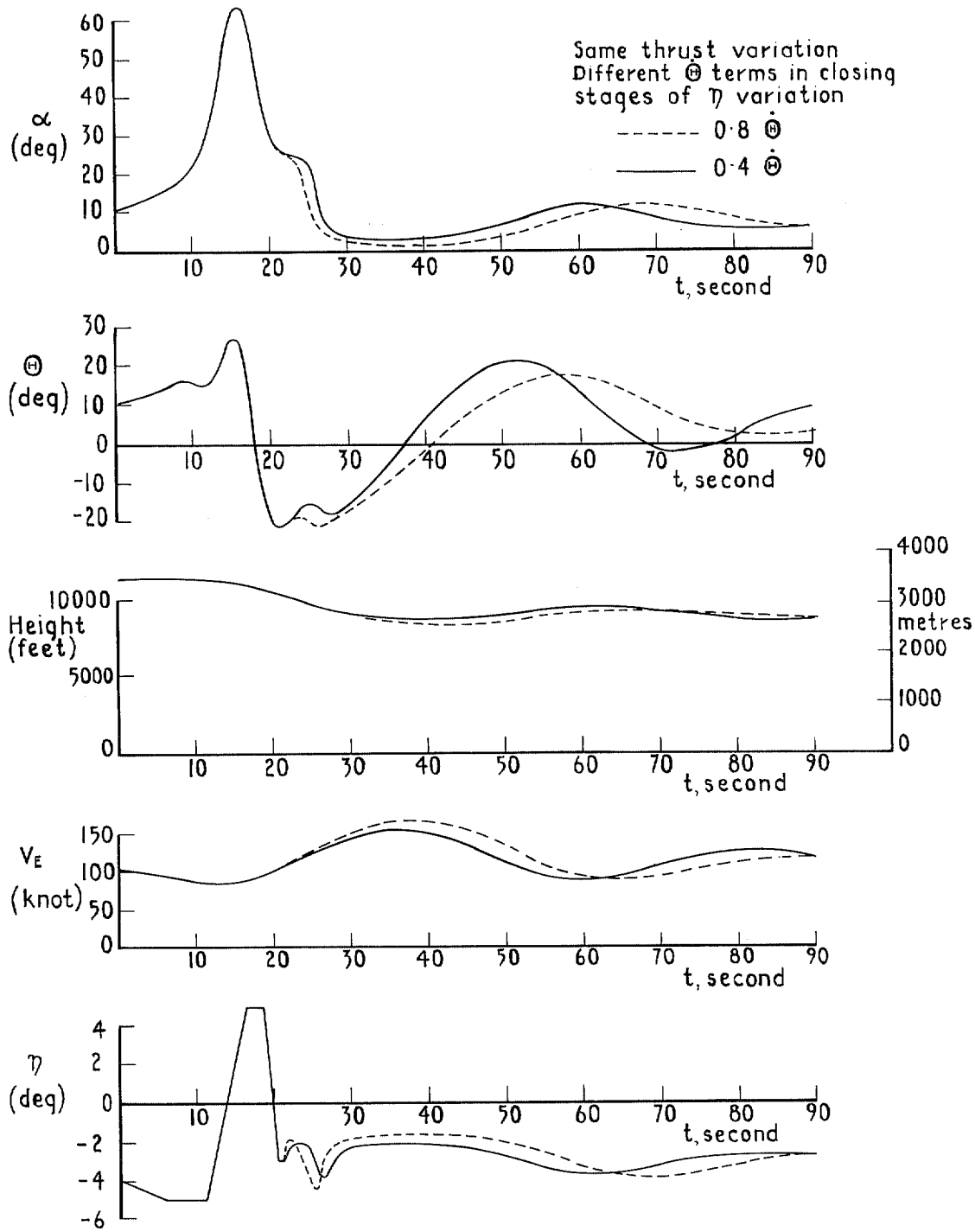

FIG. 24. Effect of increasing term proportional to rate of pitch in the pilot's input on closing stages of a 'bounce' recovery (*cf.* Fig. 23).

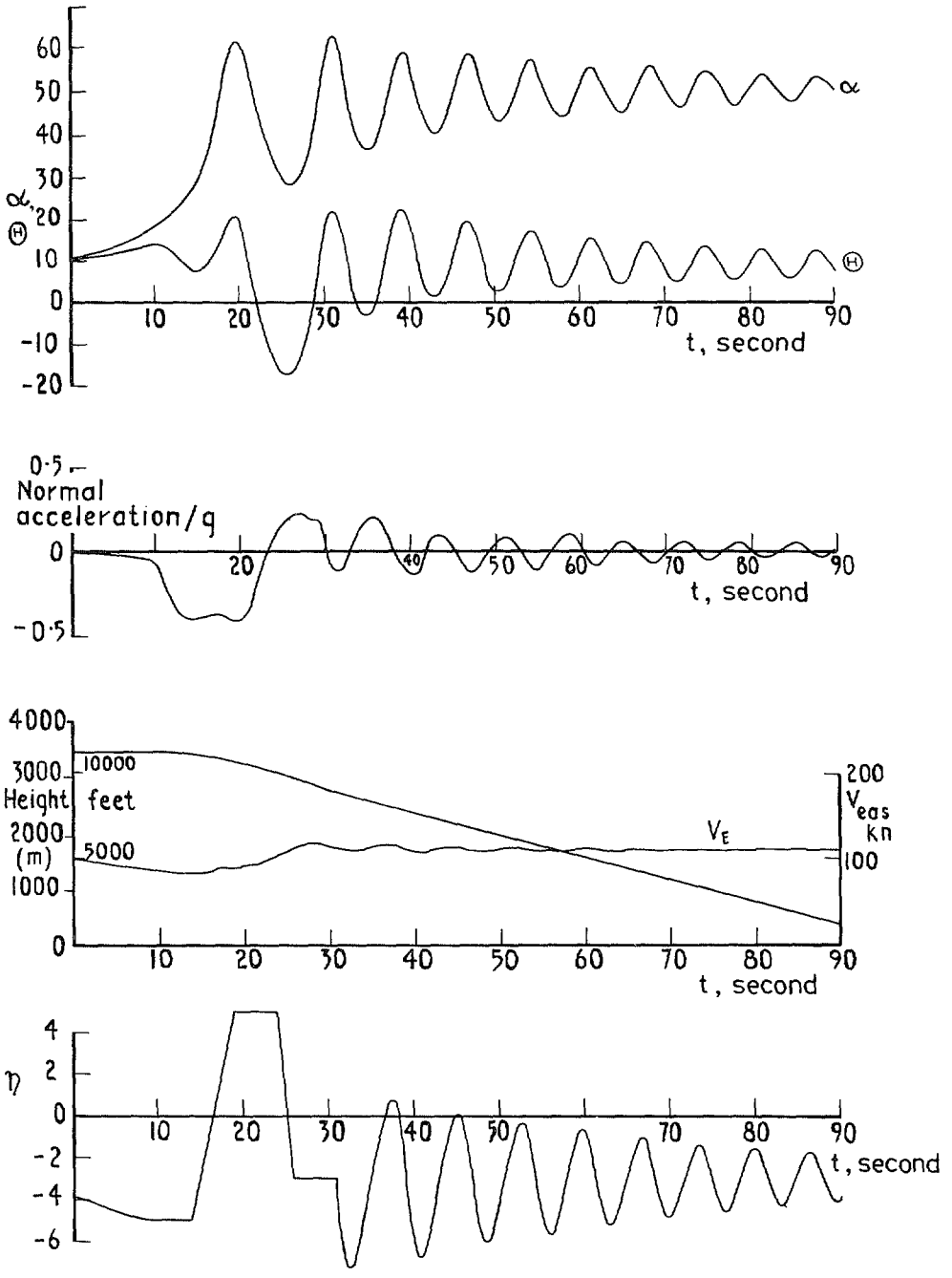

FIG. 25. A manoeuvre in which a 'bounce' recovery is followed by convergence into the stable high angle-of-attack condition.

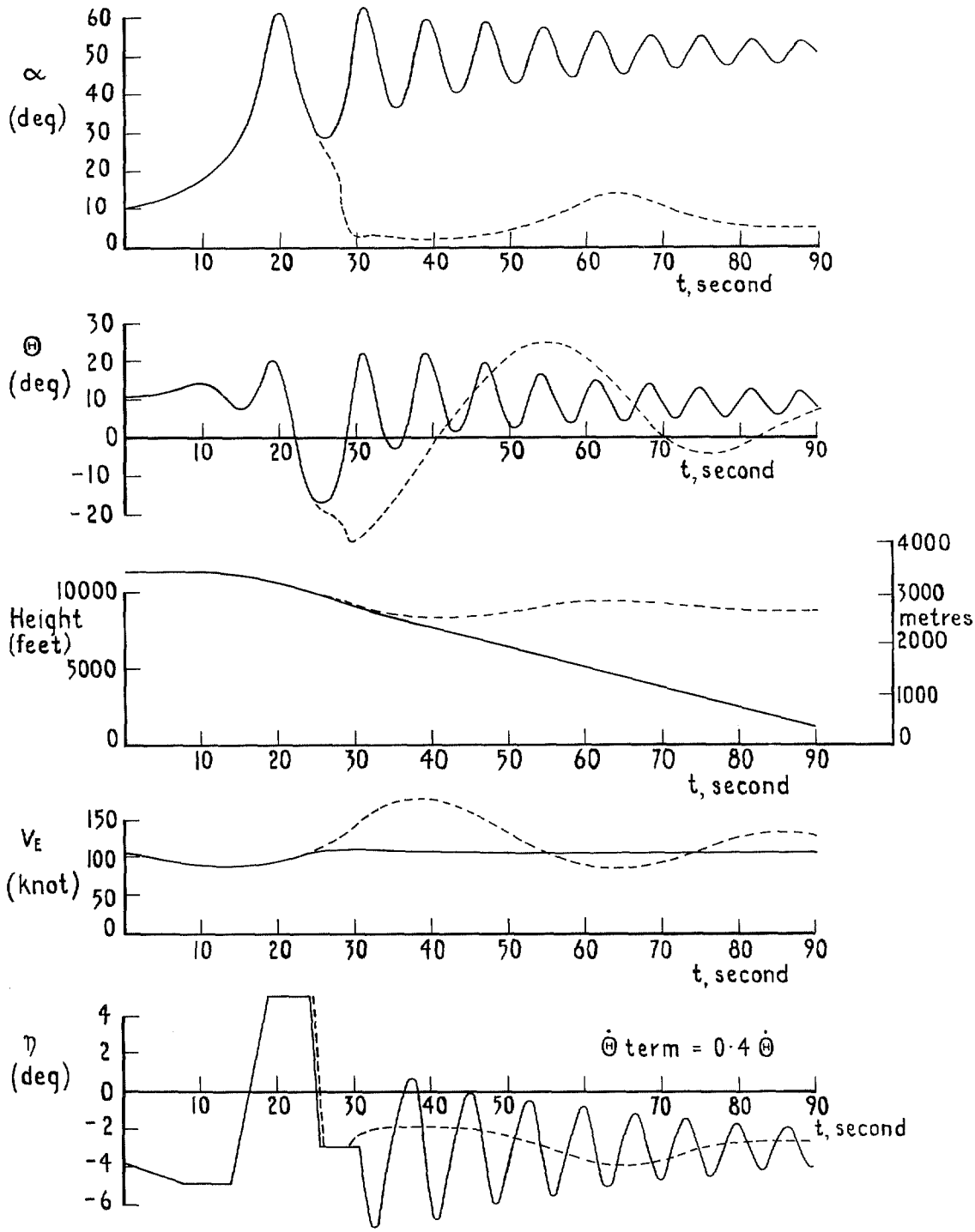

FIG. 26. Effect of delaying reversal in the elevator input and reducing the time for which reversed elevator is held constant.

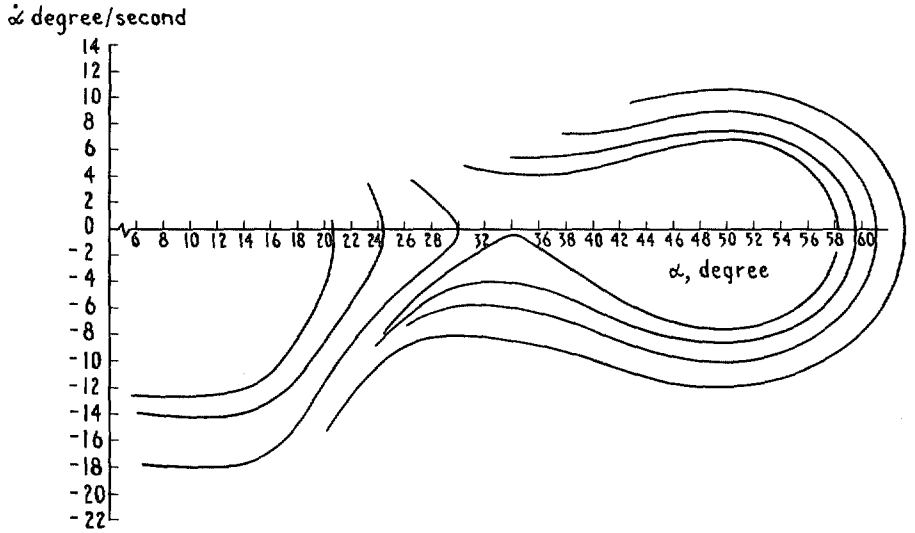

FIG. 27. $\dot{\alpha}, \alpha$ plots showing a number of normal and 'bounce' recoveries for aircraft motion with three degrees of freedom.

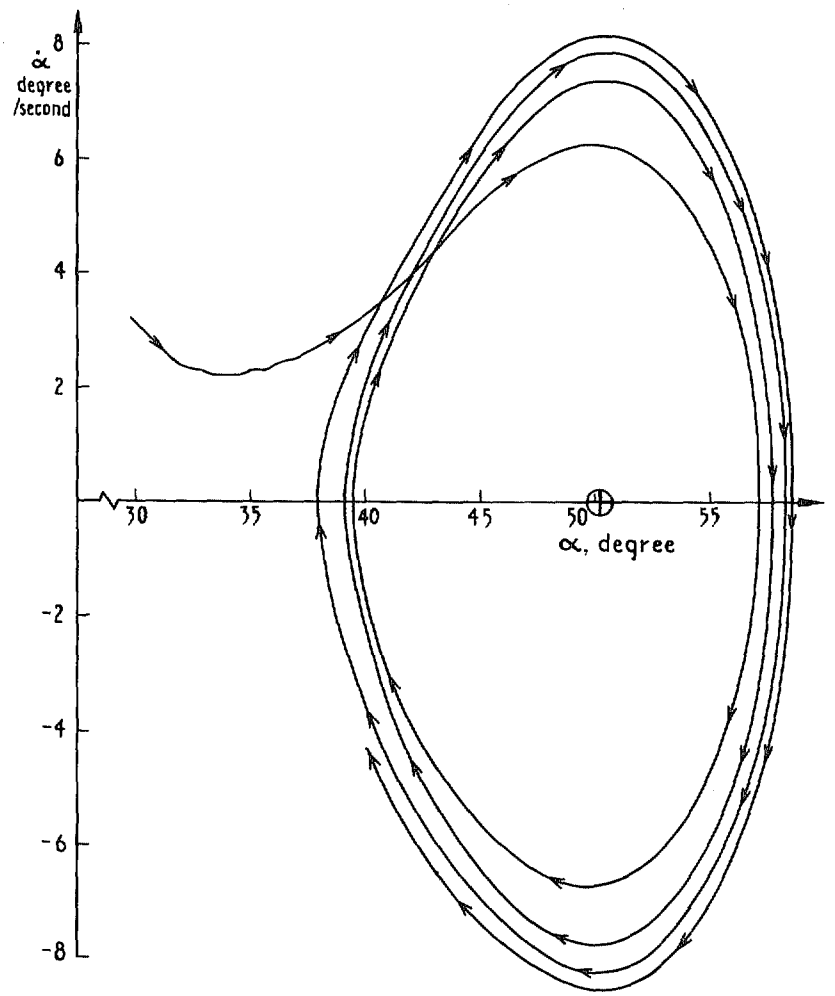

FIG. 28. $\dot{\alpha}, \alpha$ plot for 'superstalled' motion of the aircraft with its given characteristics.

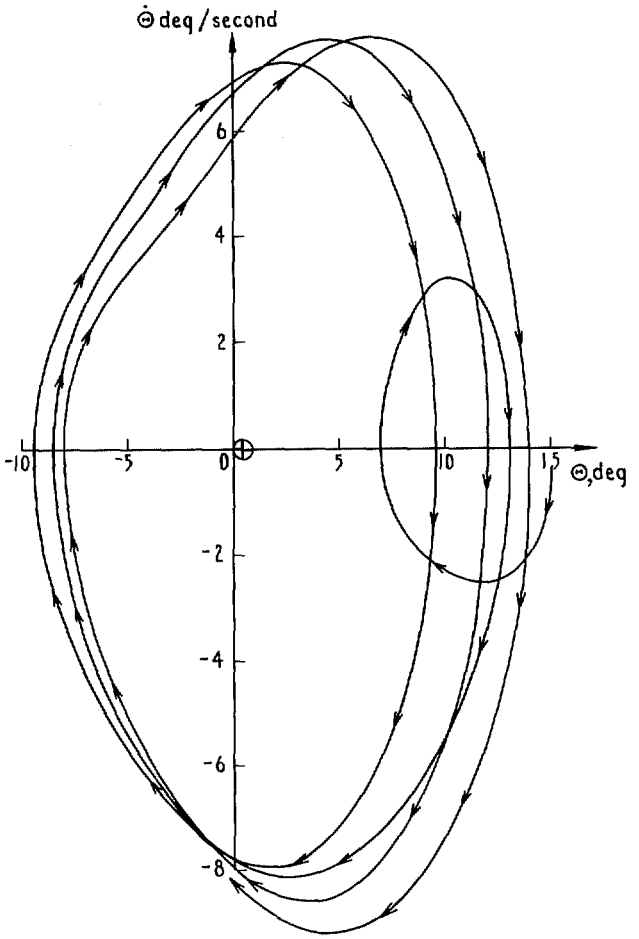

FIG. 29. $\dot{\Theta}$, Θ plot for 'superstalled' motion of the aircraft with its given characteristics.

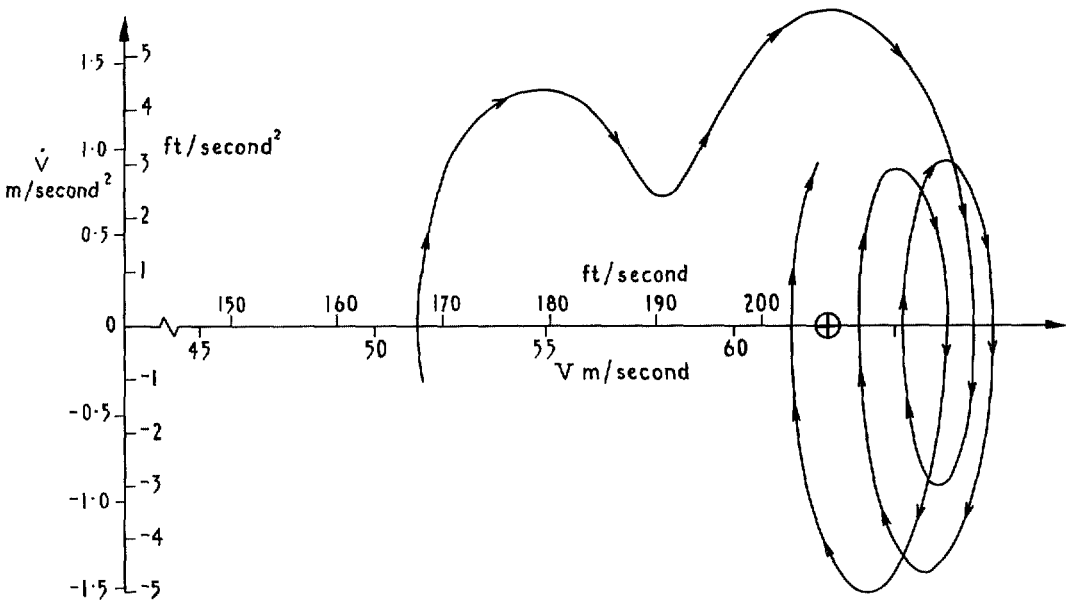

FIG. 30. $\dot{V}$, V plot for 'superstalled' motion of the aircraft with its given characteristics.

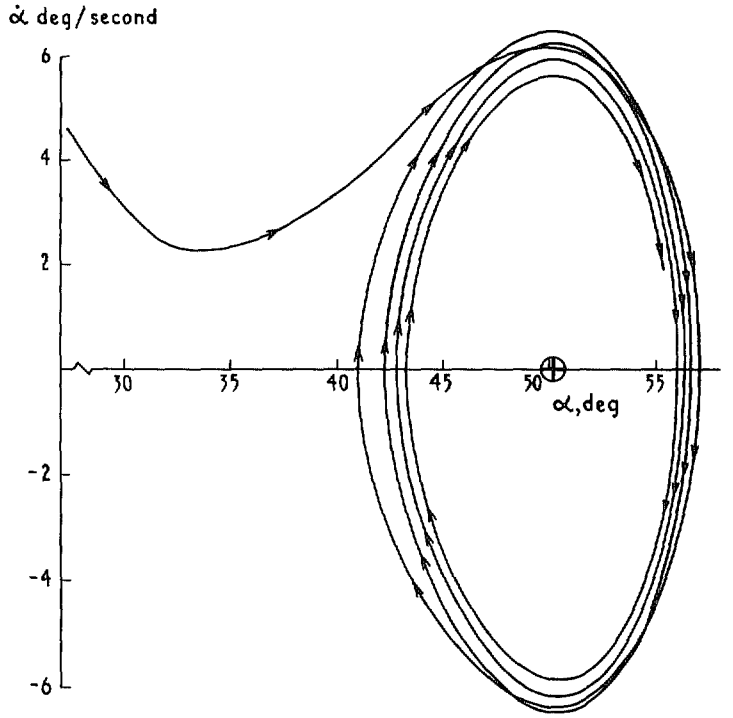

FIG. 31. $\dot{\alpha}$, α plot for 'superstalled' motion of the aircraft with increased damping in pitch (*see* Section 4).

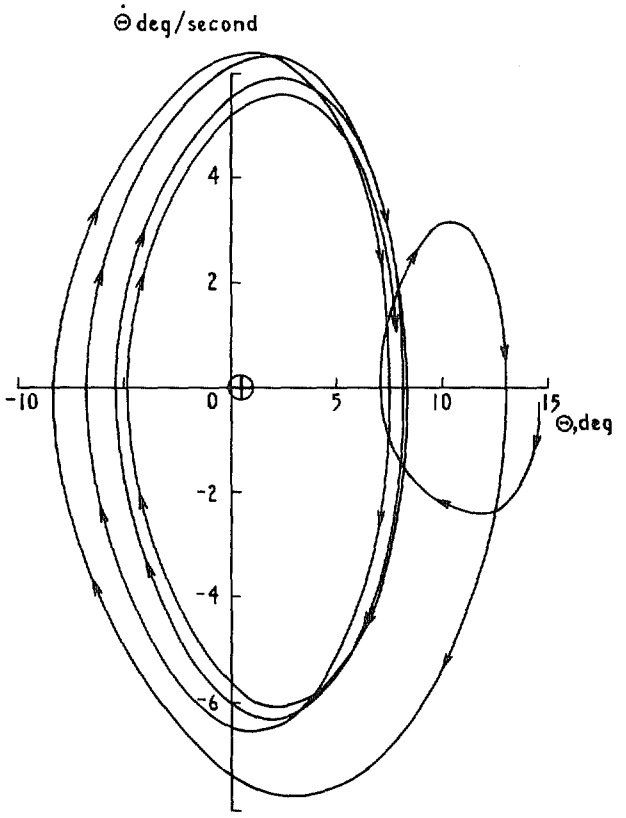

FIG. 32. $\dot{\Theta}$, Θ plot for 'superstalled' motion of the aircraft with increased damping in pitch (*see* Section 4).

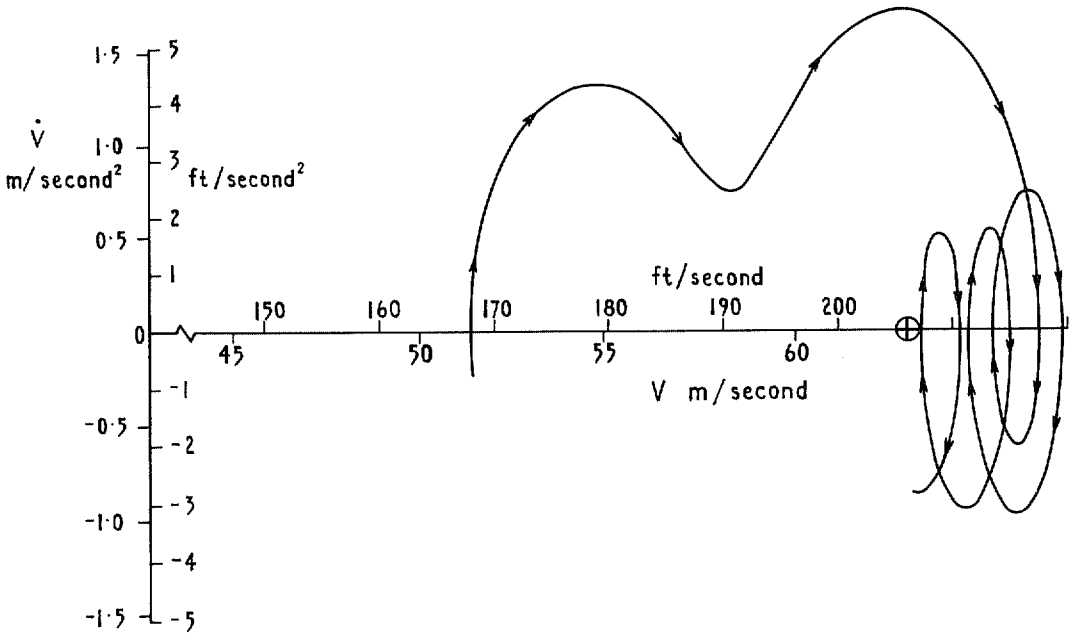

FIG. 33. $\dot{V}$, V plot for 'superstalled' motion of the aircraft with increased damping in pitch (*see* Section 4).

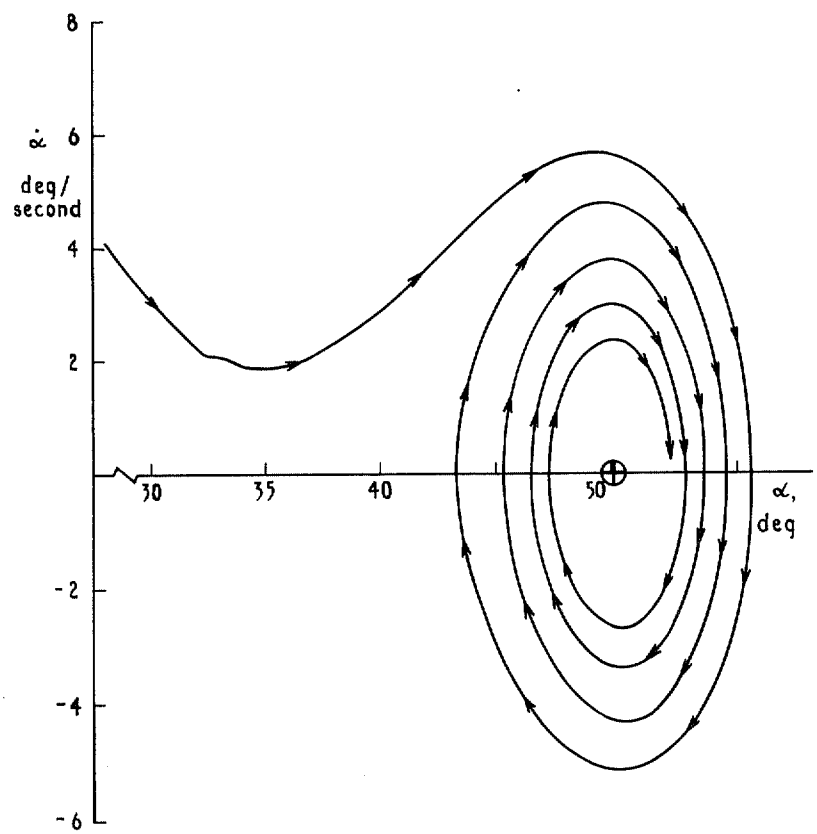

FIG. 34. $\dot{\alpha}$, α plot of the 'superstalled' motion of the aircraft with modified lift characteristics (*see* Section 4).

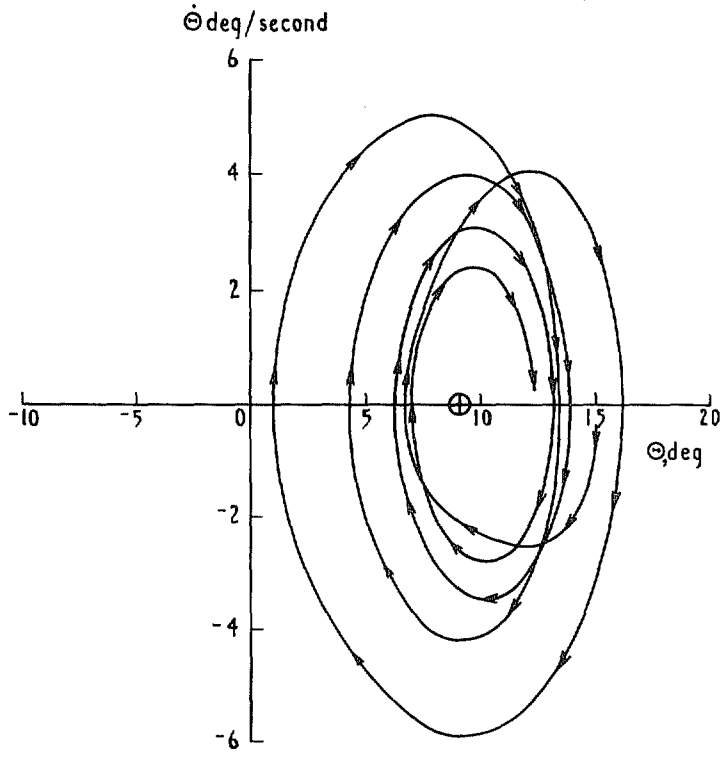

FIG. 35. $\dot{\Theta}$, Θ plot for the 'superstalled' motion of the aircraft with modified lift characteristics (*see* Section 4).

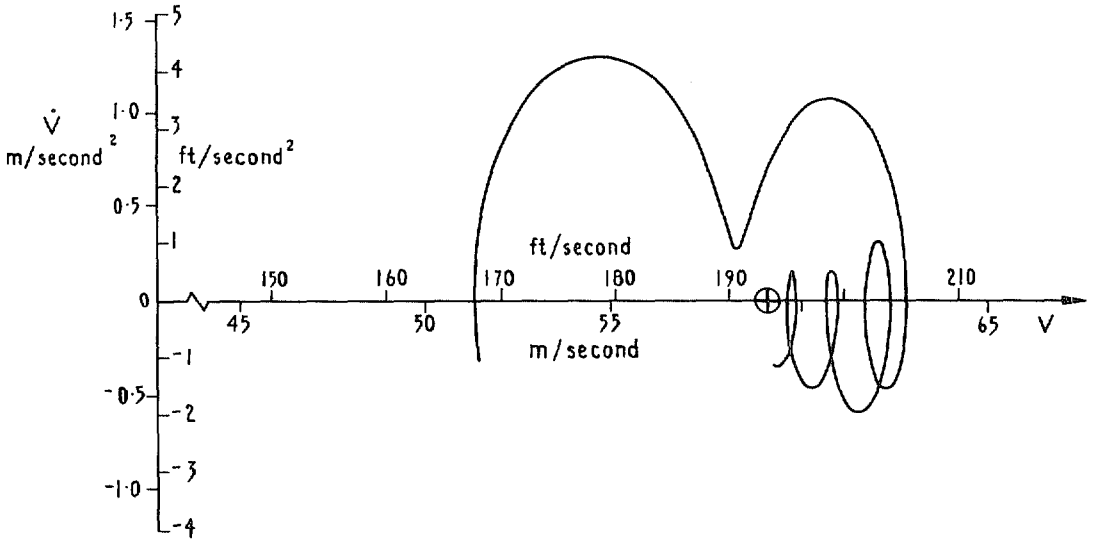

FIG. 36. $\dot{V}$, V plot for the 'superstalled' motion of the aircraft with modified lift characteristics (*see* Section 4).

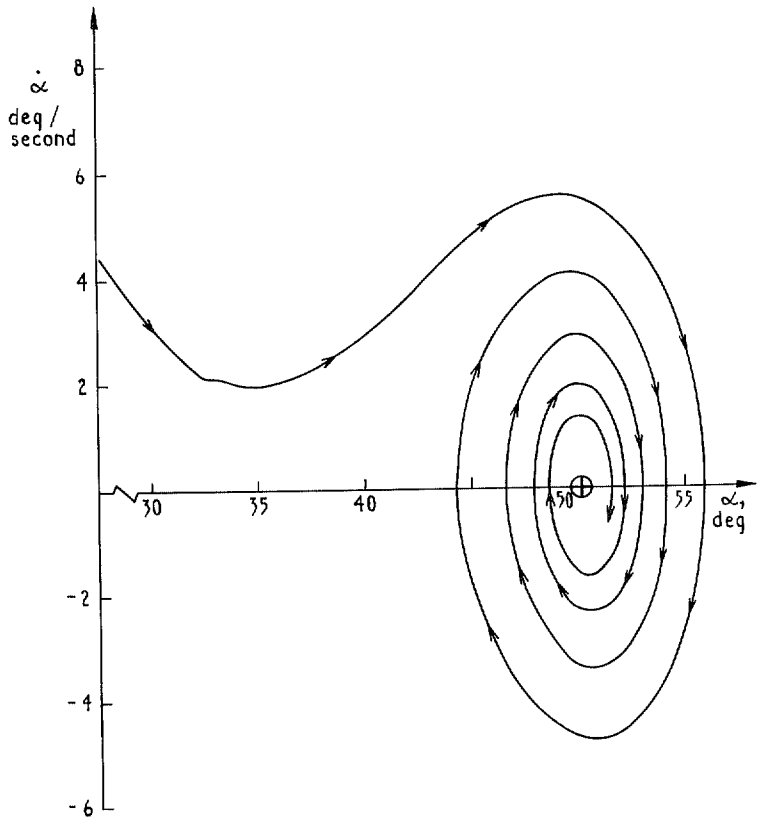

FIG. 37. $\dot{\alpha}$, α plot of 'superstalled' motion of aircraft with increased damping in pitch and modified lift characteristics (*see* Section 4).

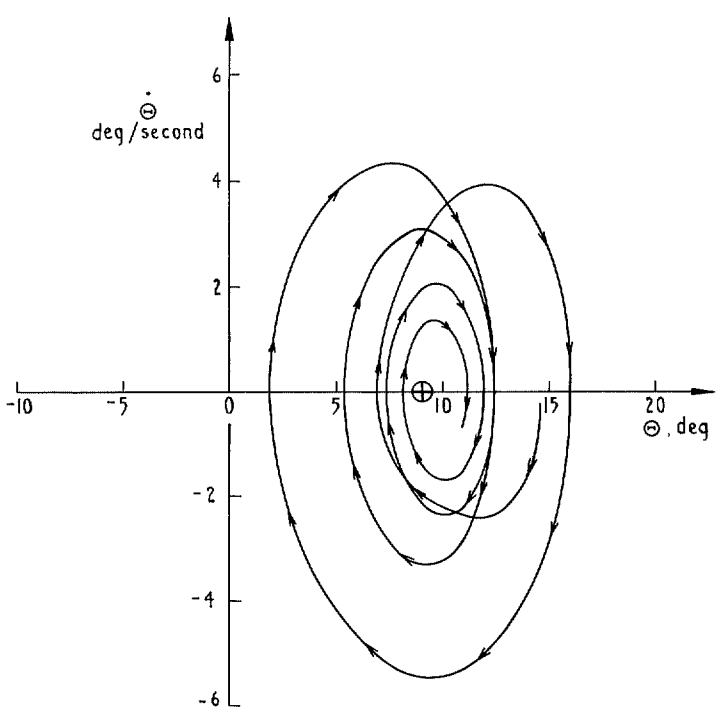

FIG. 38. $\dot{\Theta}$, Θ plot of 'superstalled' motion of aircraft with increased damping in pitch and modified lift characteristics (*see* Section 4).

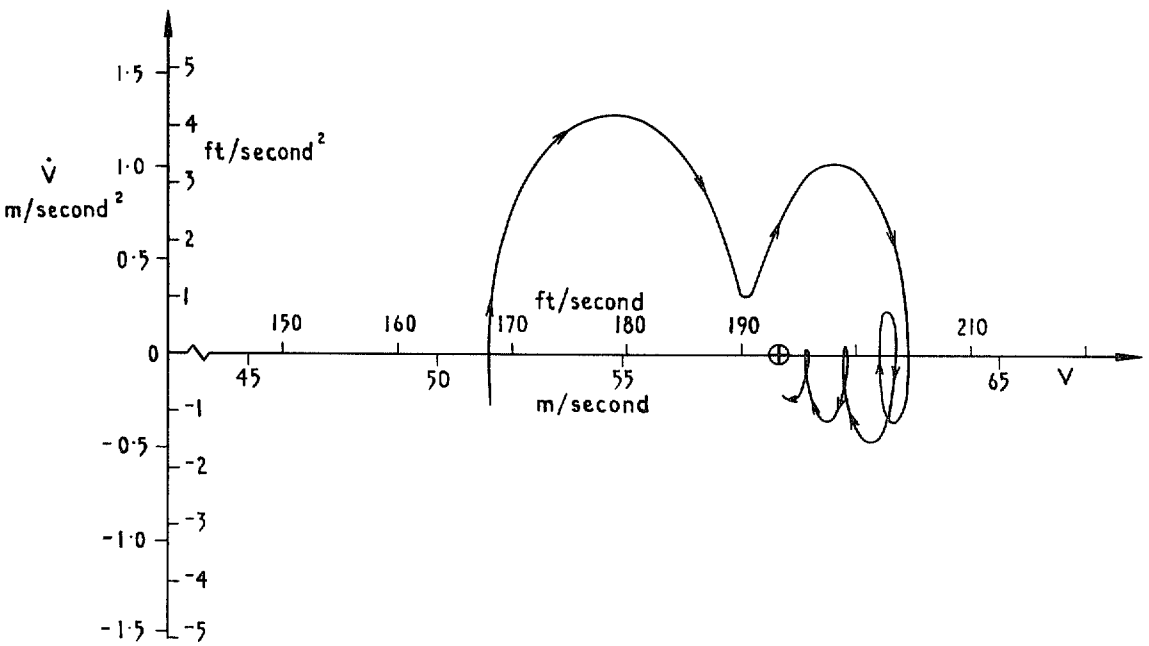

FIG. 39. $\dot{V}$, V plot of 'superstalled' motion of aircraft with increased damping in pitch and modified lift characteristics (*see* Section 4).

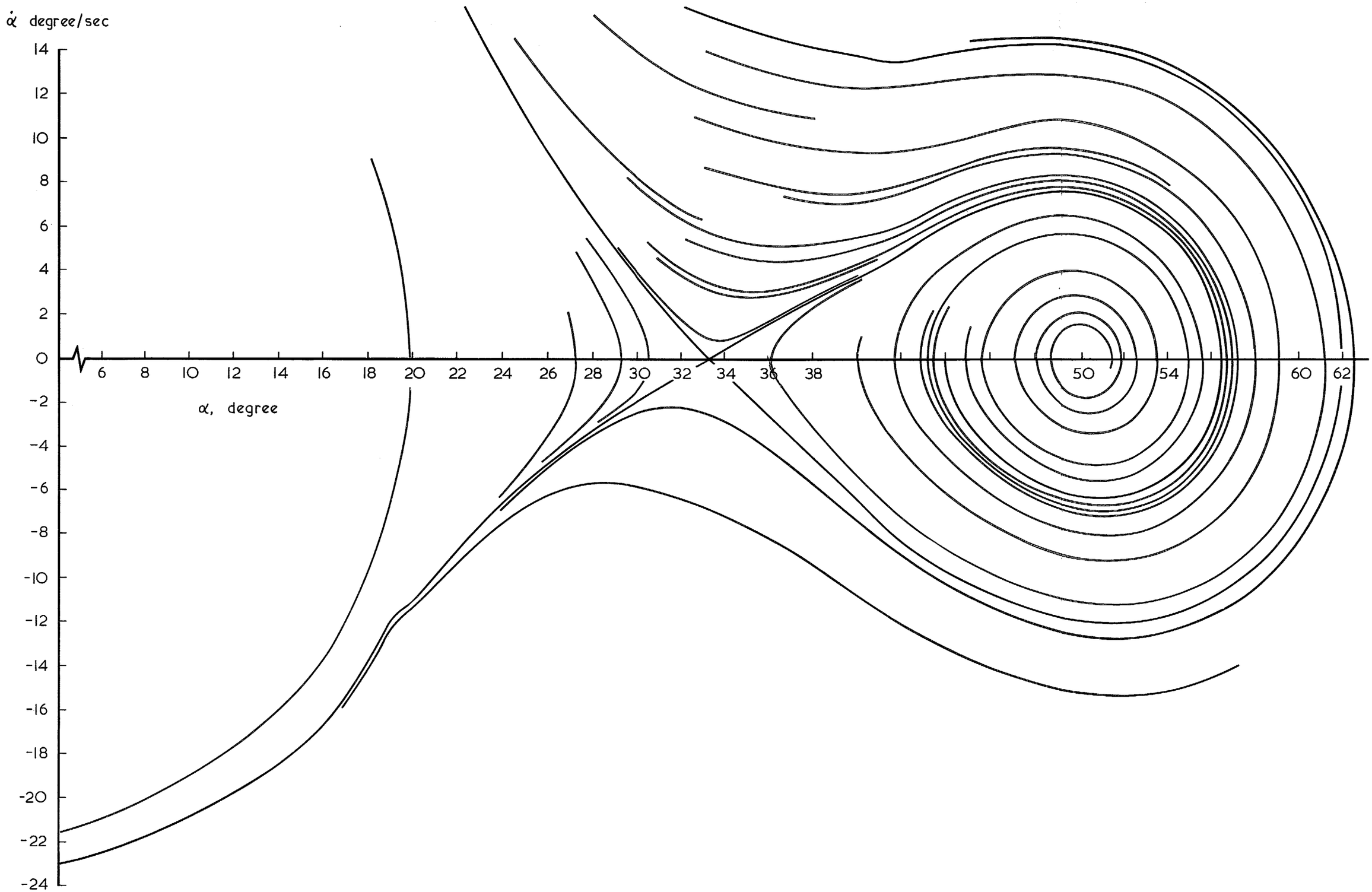

FIG. 40. Single degree of freedom motion (variable damping).

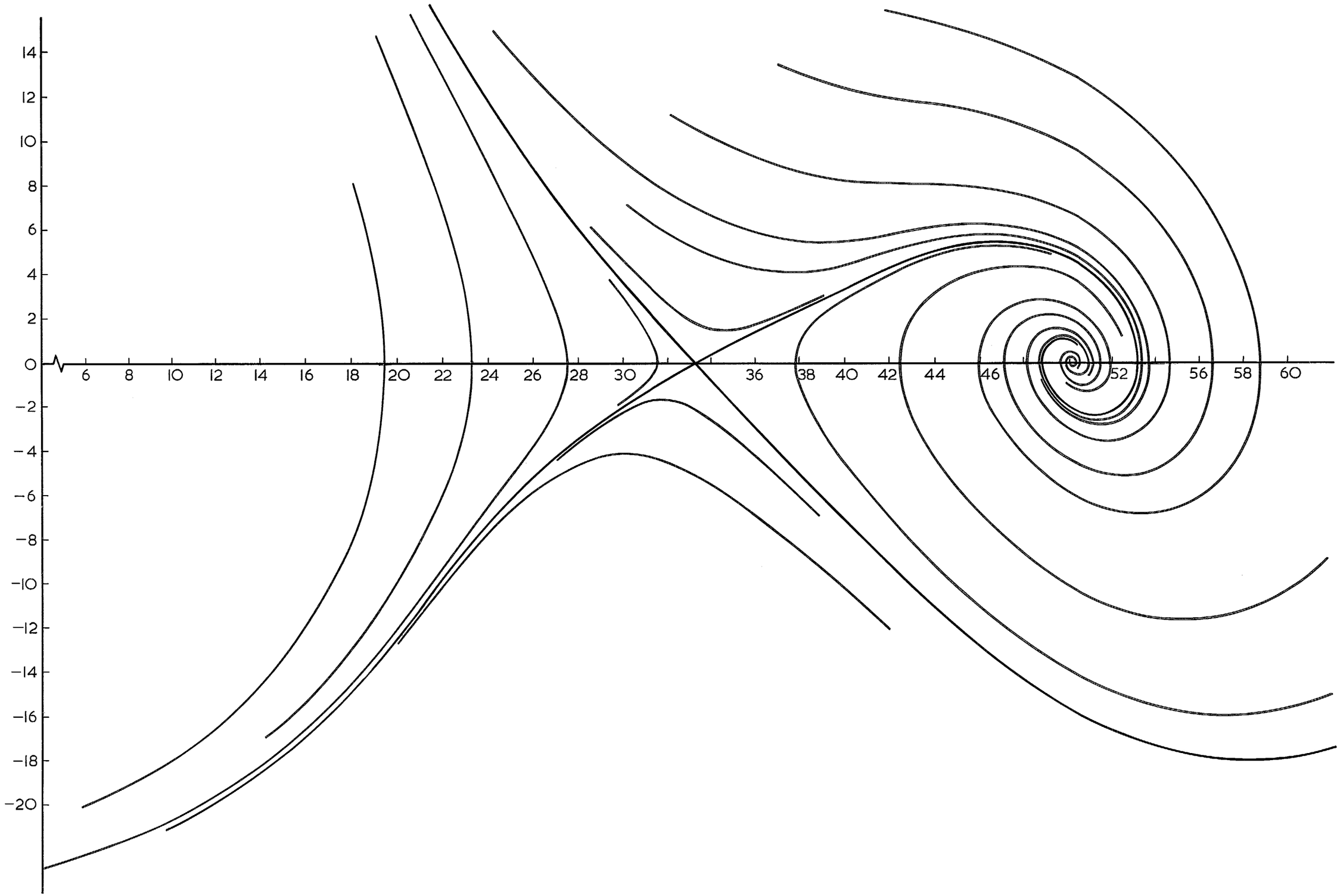

FIG. 41. Single degree of freedom motion (constant damping).

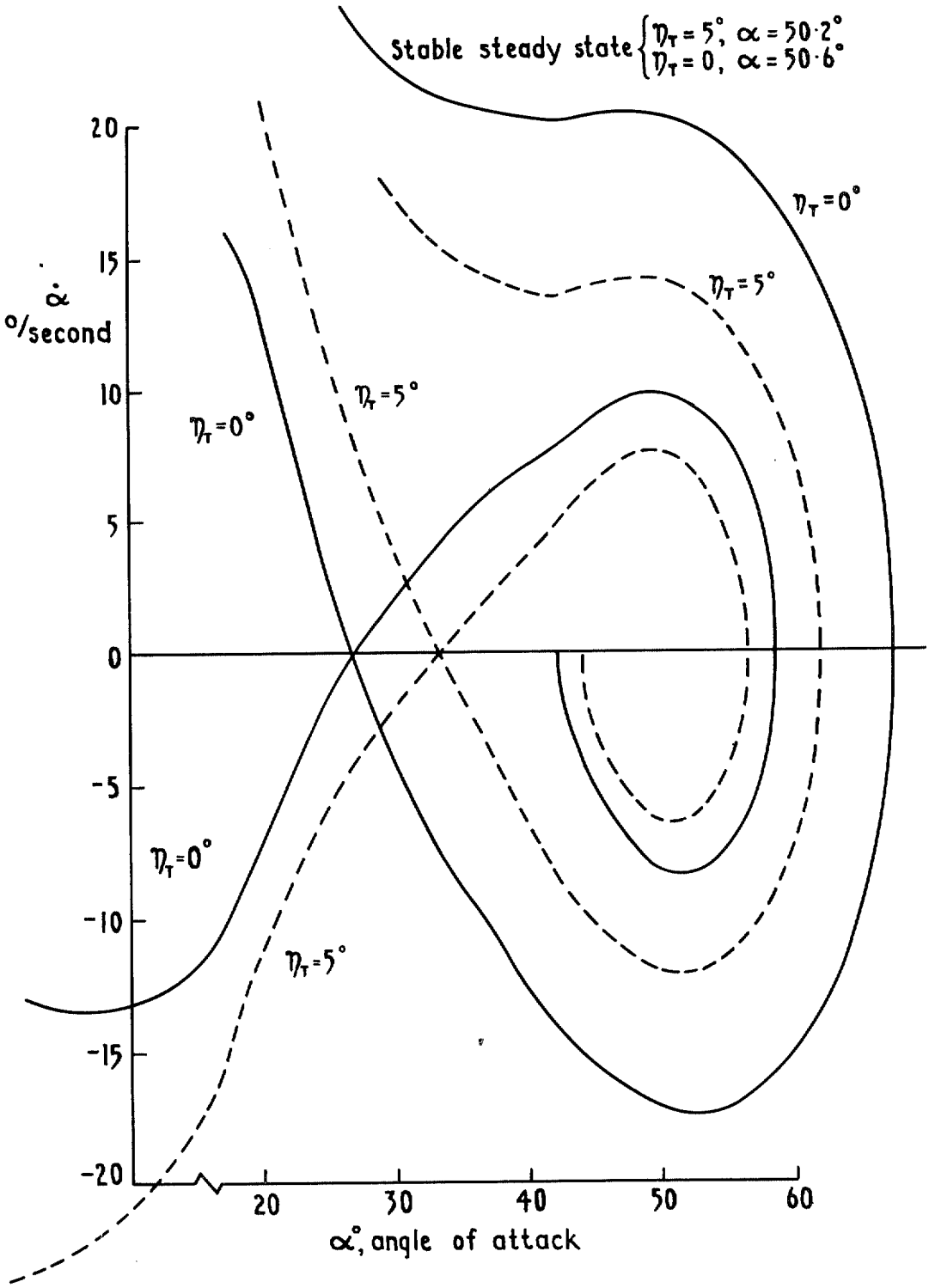

FIG. 42. Separatrix curves for aeroplane with elevator neutral and 5° down elevator (single degree-of-freedom motion)

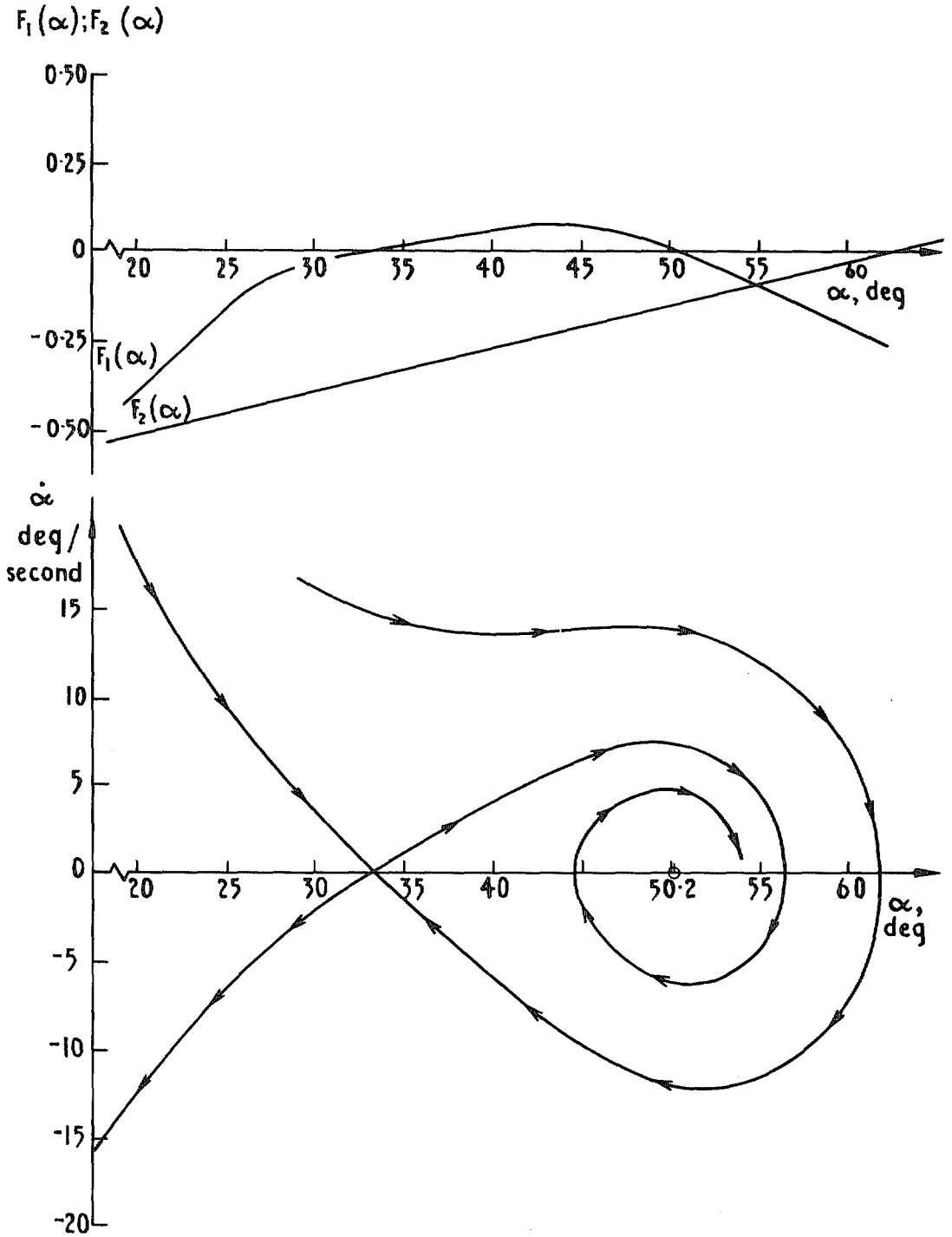

FIG. 43. Single degree-of-freedom motion in pitch with reversal of damping beyond the trim angle of attack ($\alpha = 50{\cdot}2°$)

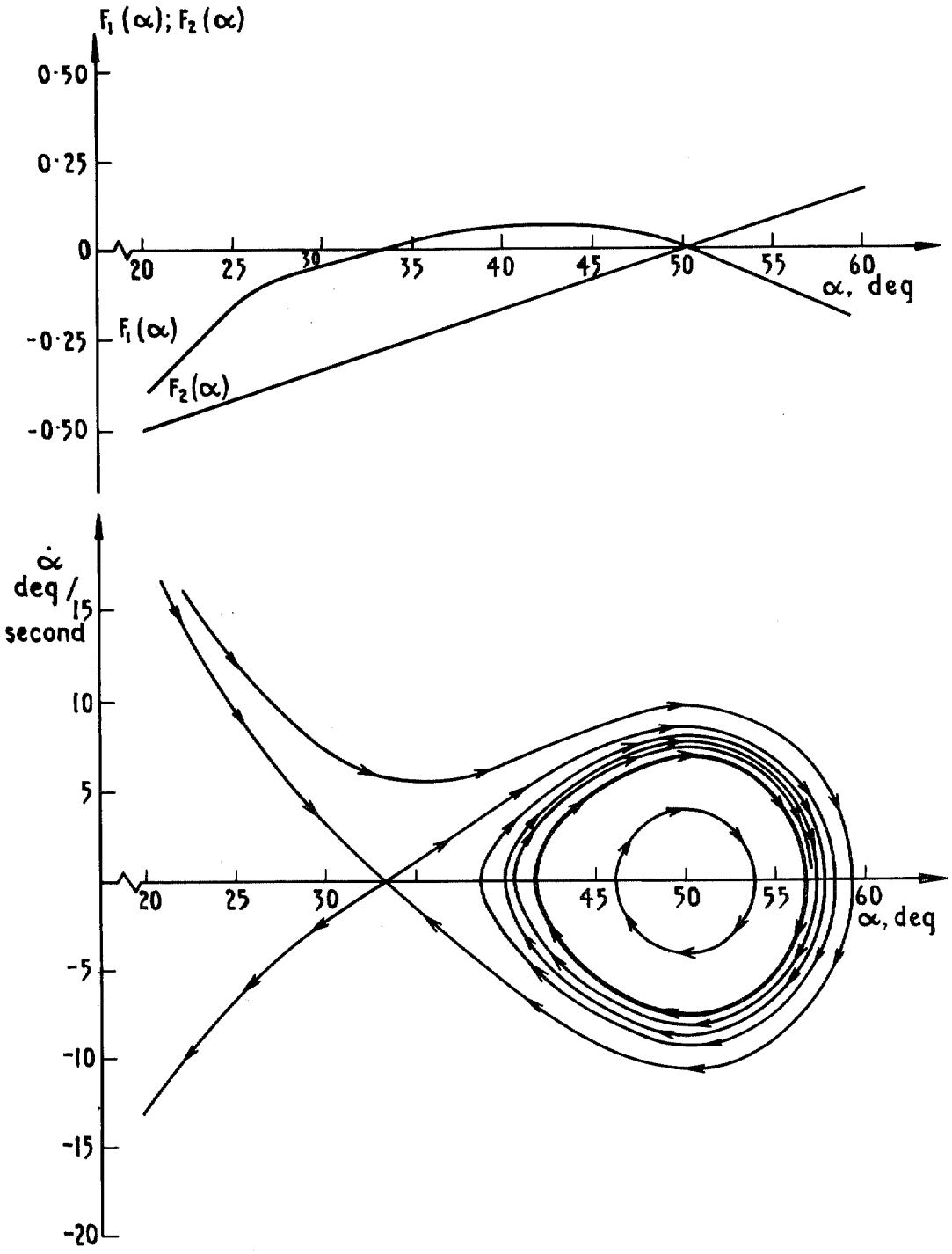

FIG. 44. Single degree-of-freedom motion in pitch with zero damping at the trim angle of attack ($\alpha = 50{\cdot}2°$).

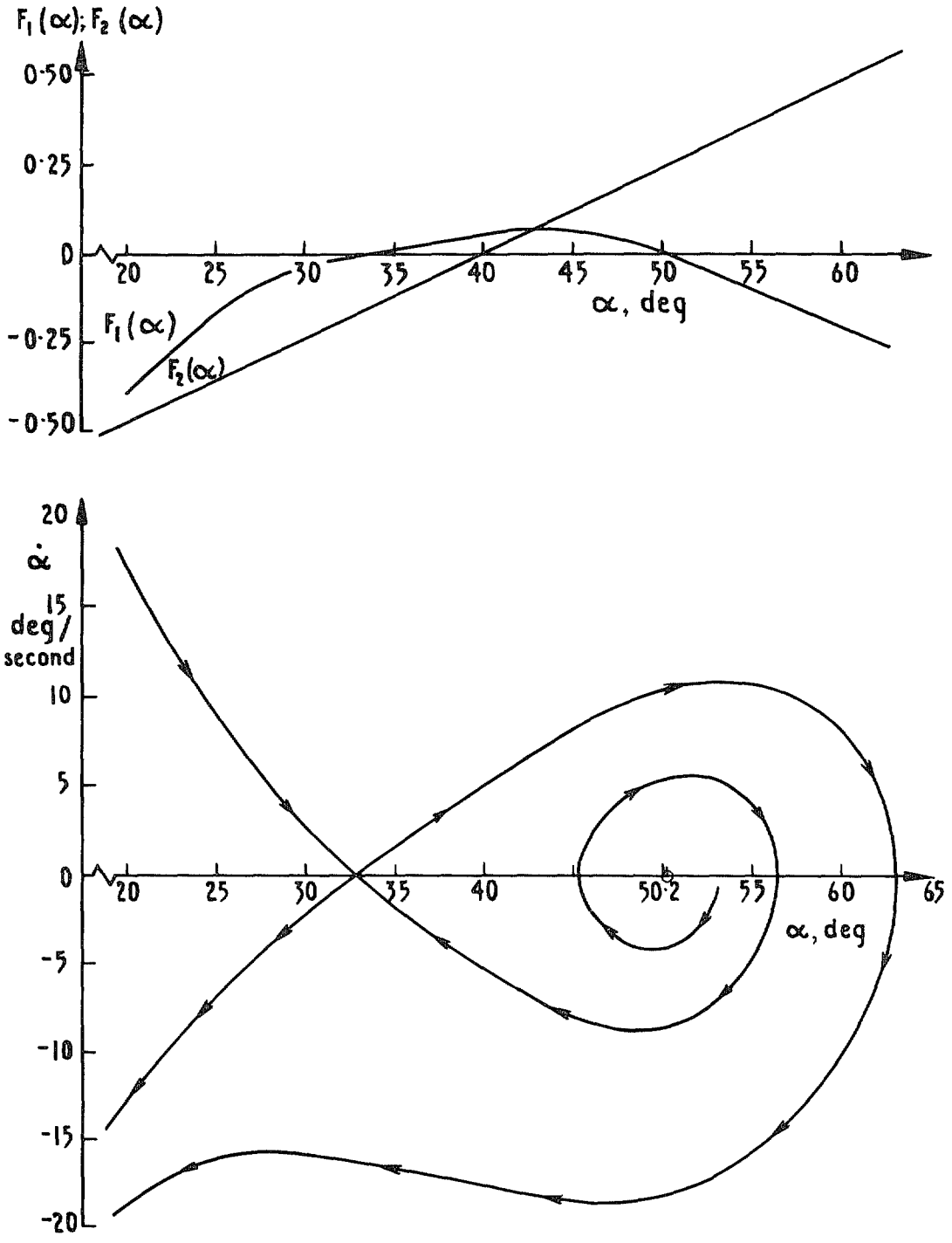

FIG. 45. Single degree-of-freedom motion in pitch with reversal of damping ahead of the trim angle of attack ($\alpha = 50{\cdot}2°$)

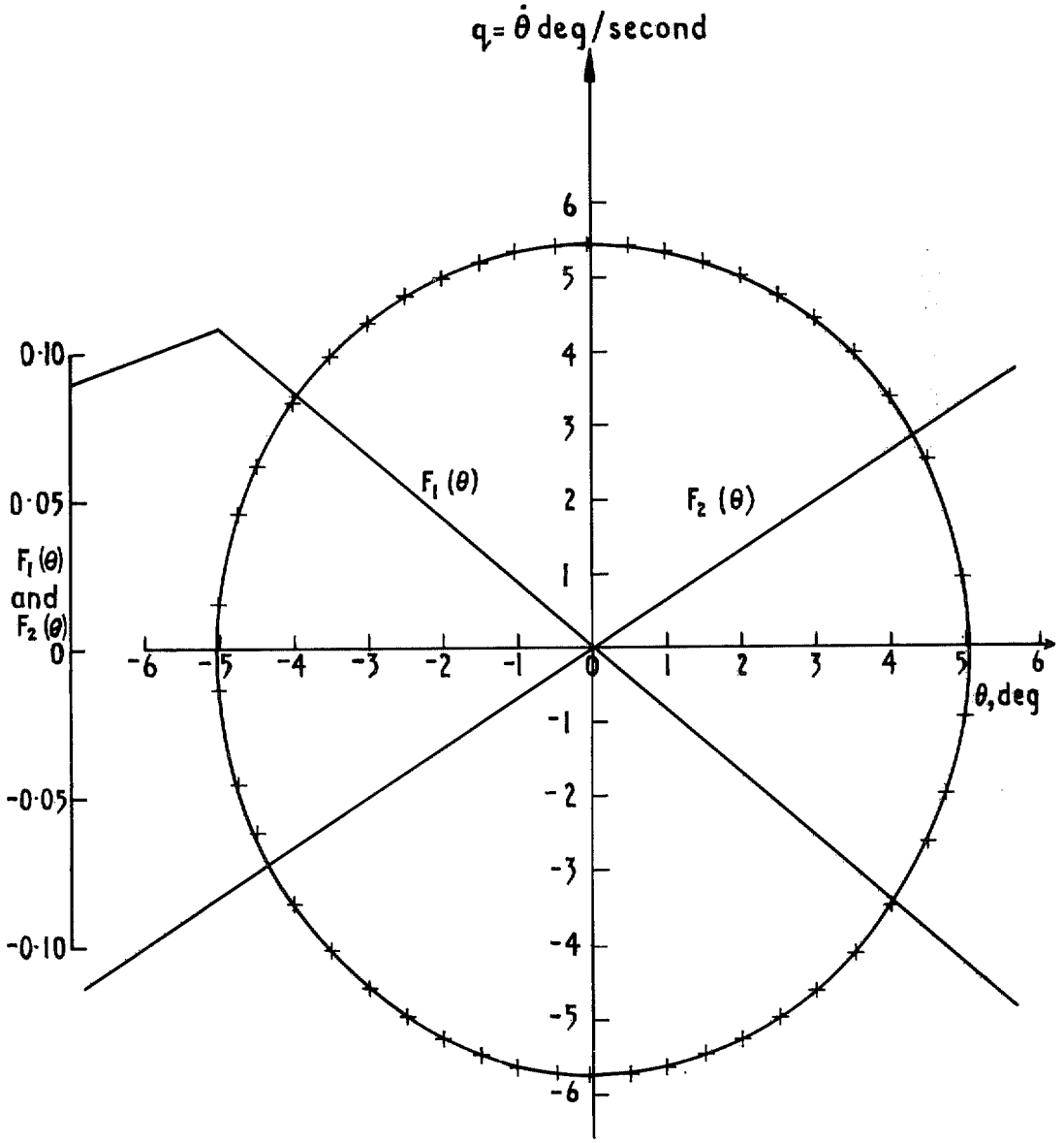

FIG. 46. Comparison of analytic and computed solutions for limiting cycle (single-degree-of-freedom motion with damping and stiffness characteristics shown).

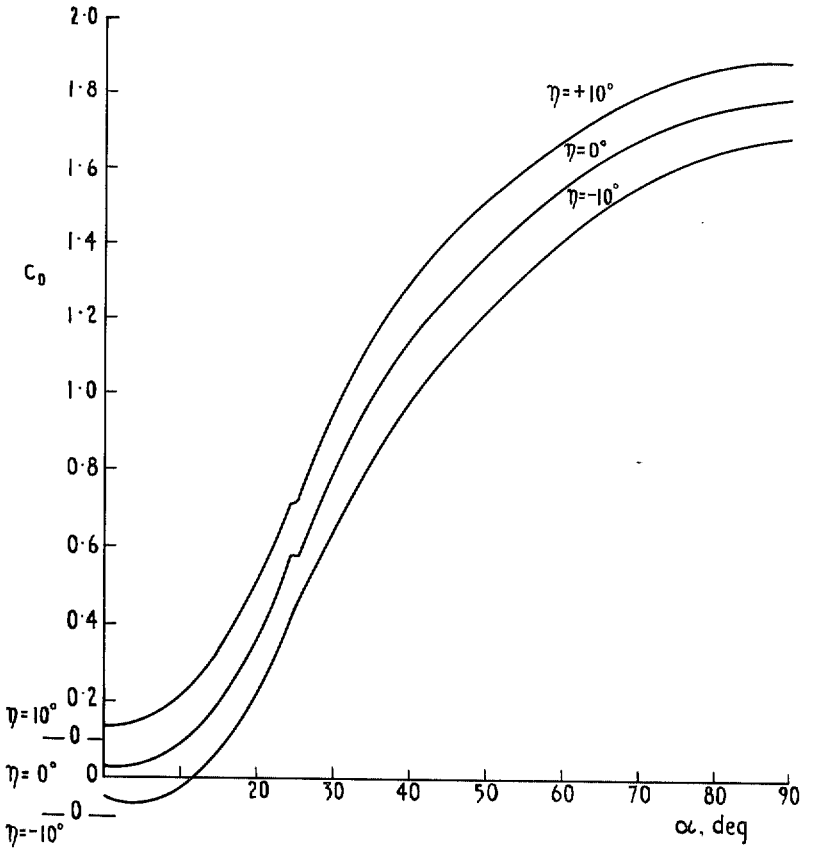

FIG. 47. Drag characteristics assumed for the slender-wing aircraft.

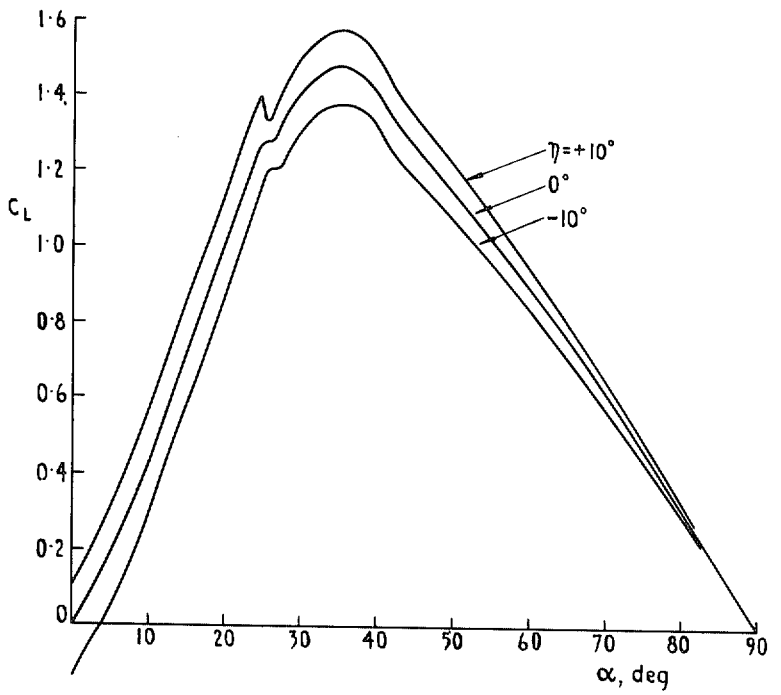

FIG. 48. Lift characteristics assumed for the slender-wing tailless aircraft.

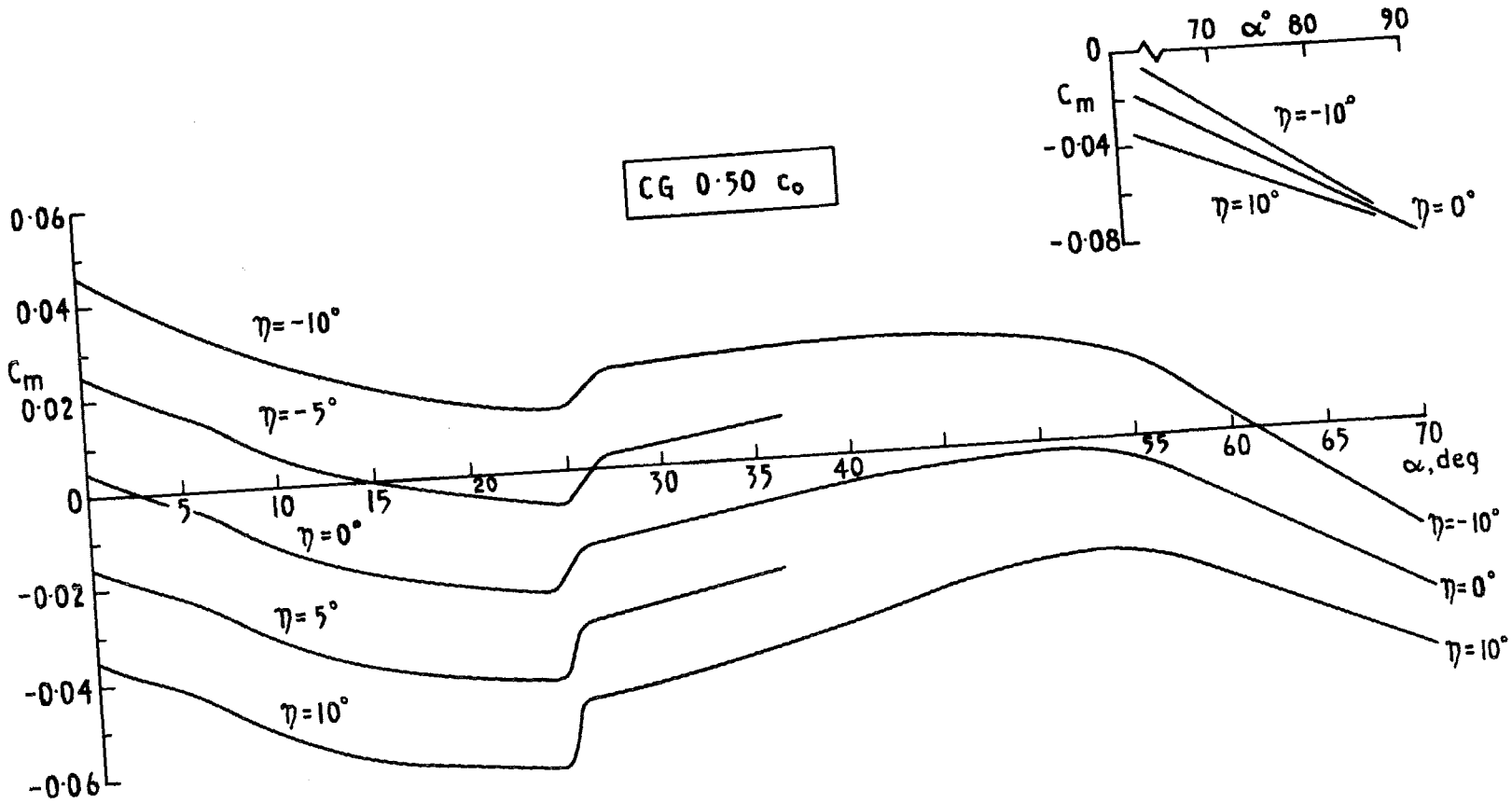

FIG. 49. Pitching moment characteristics assumed for the slender-wing aircraft.

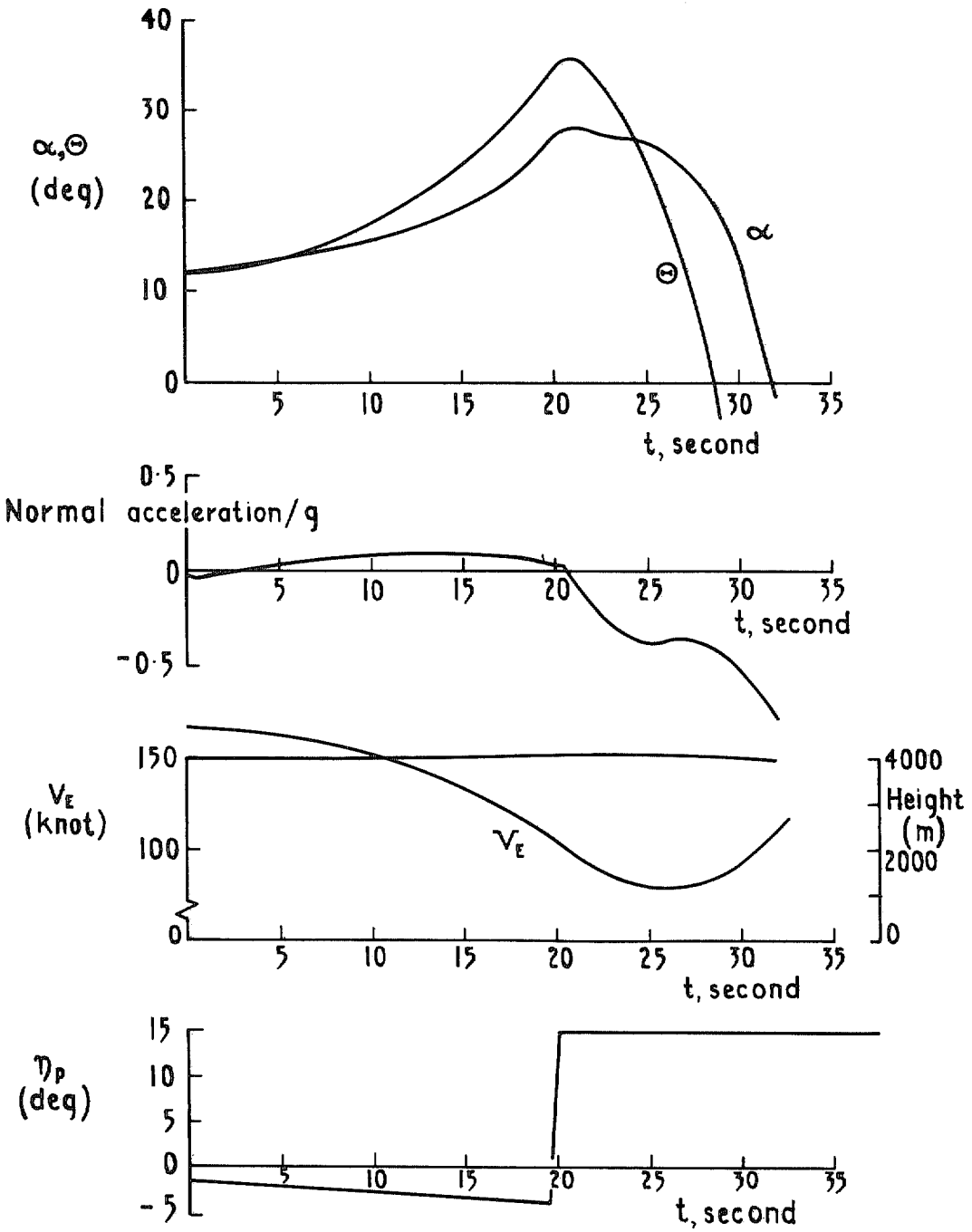

FIG. 50. Longitudinal motion with a marginal recovery ($\alpha_r = 26°$, CG $0{\cdot}52c_0$, no thrust moment).

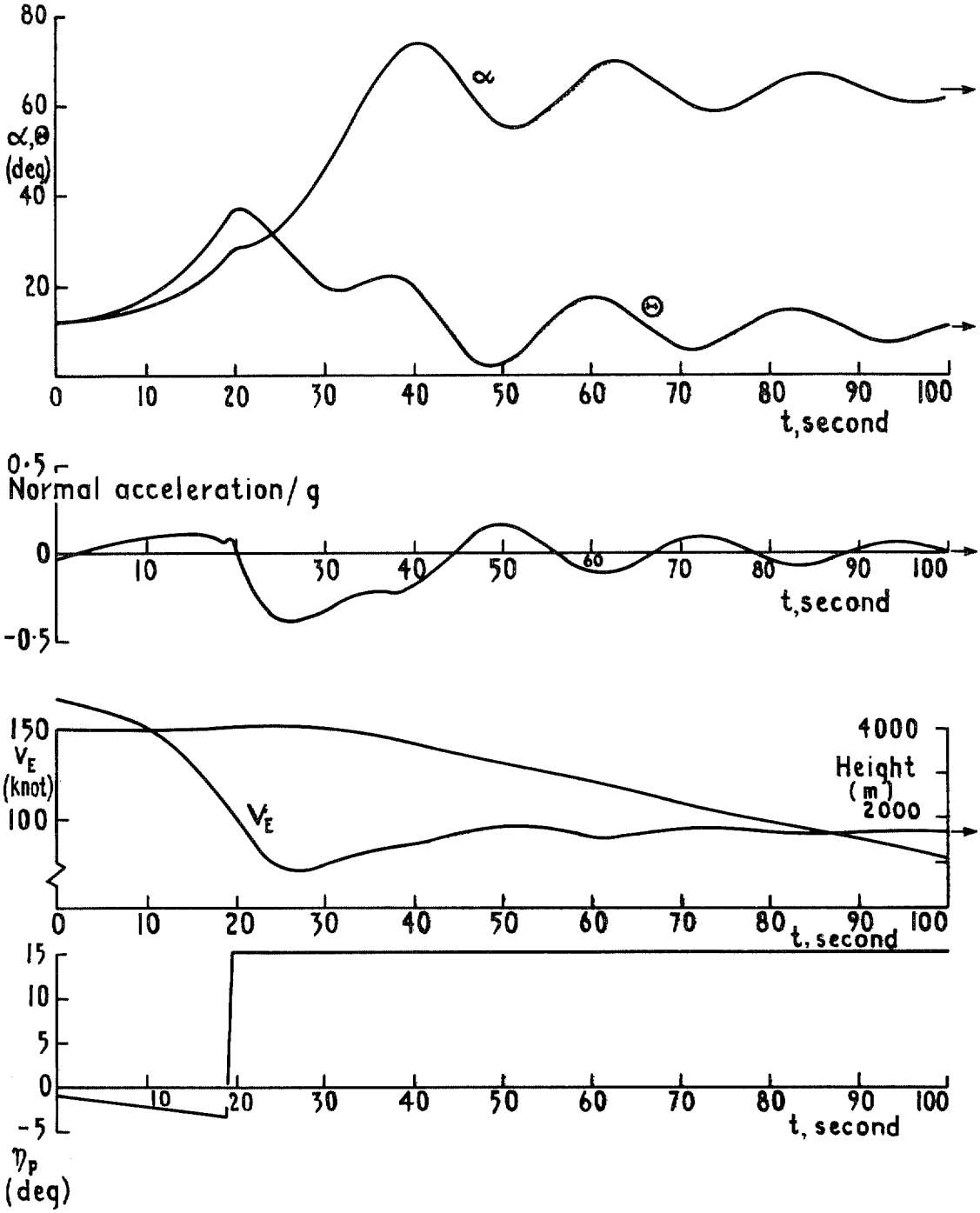

FIG. 51. Longitudinal motion resulting in a convergence to the stable high angle-of-attack steady state. ($\alpha_r = 26°$, CG $0{\cdot}52c_0$, with thrust moment).

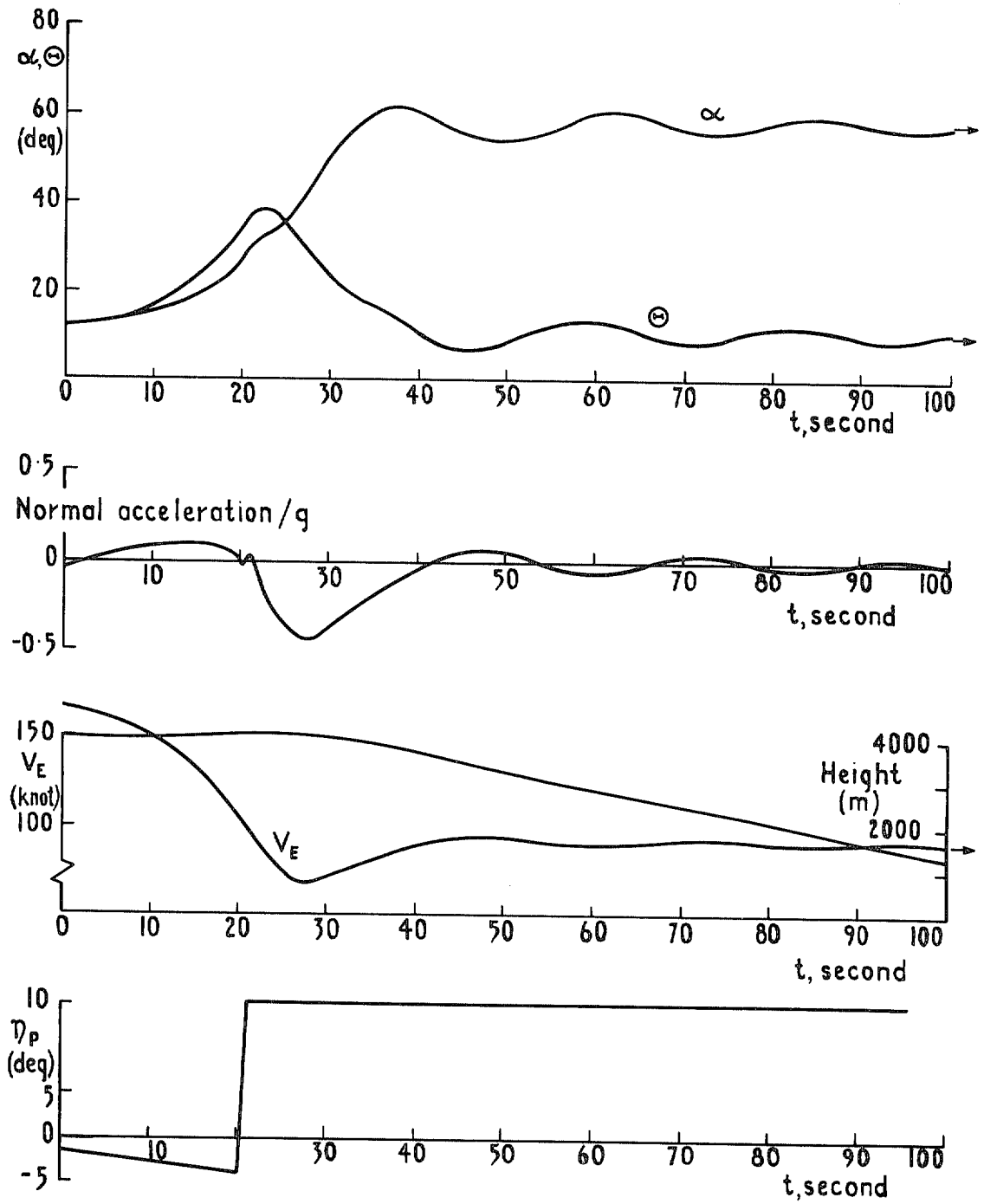

FIG. 52. Longitudinal motion resulting in convergence to the stable high angle-of-attack steady state. ($\alpha_r = 28°$, CG $0{\cdot}52c_0$, no thrust moment).

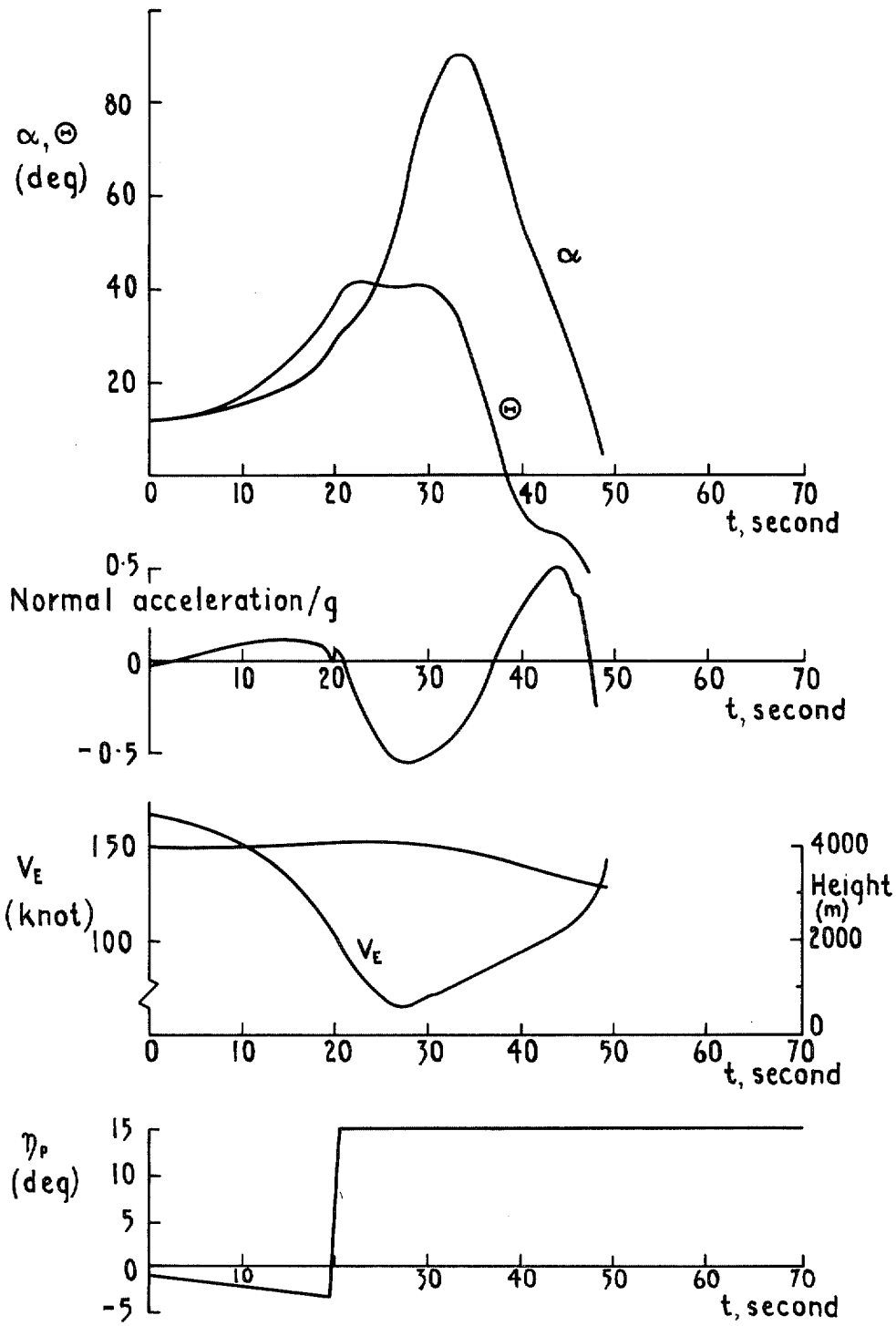

FIG. 53. Longitudinal motion resulting in a 'bounce' recovery ($\alpha_r = 28°$, CG $0{\cdot}52c_0$, with thrust moment).

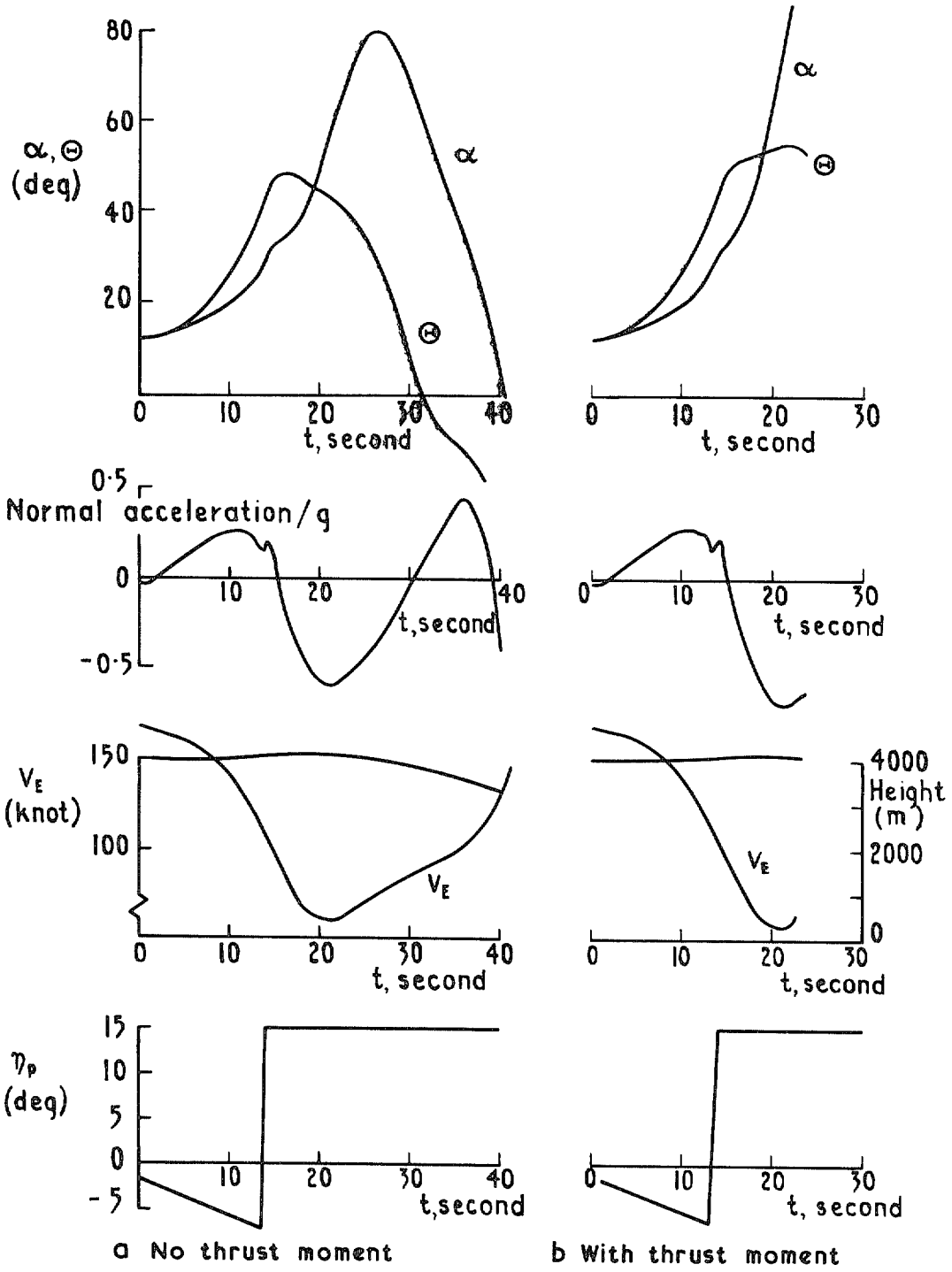

FIG. 54a and b. Effect of rate of application of up-elevator on motions with and without thrust moment ($\alpha_r = 28°$, CG $0{\cdot}52c_0$, *cf.* Fig. 52 and 53).

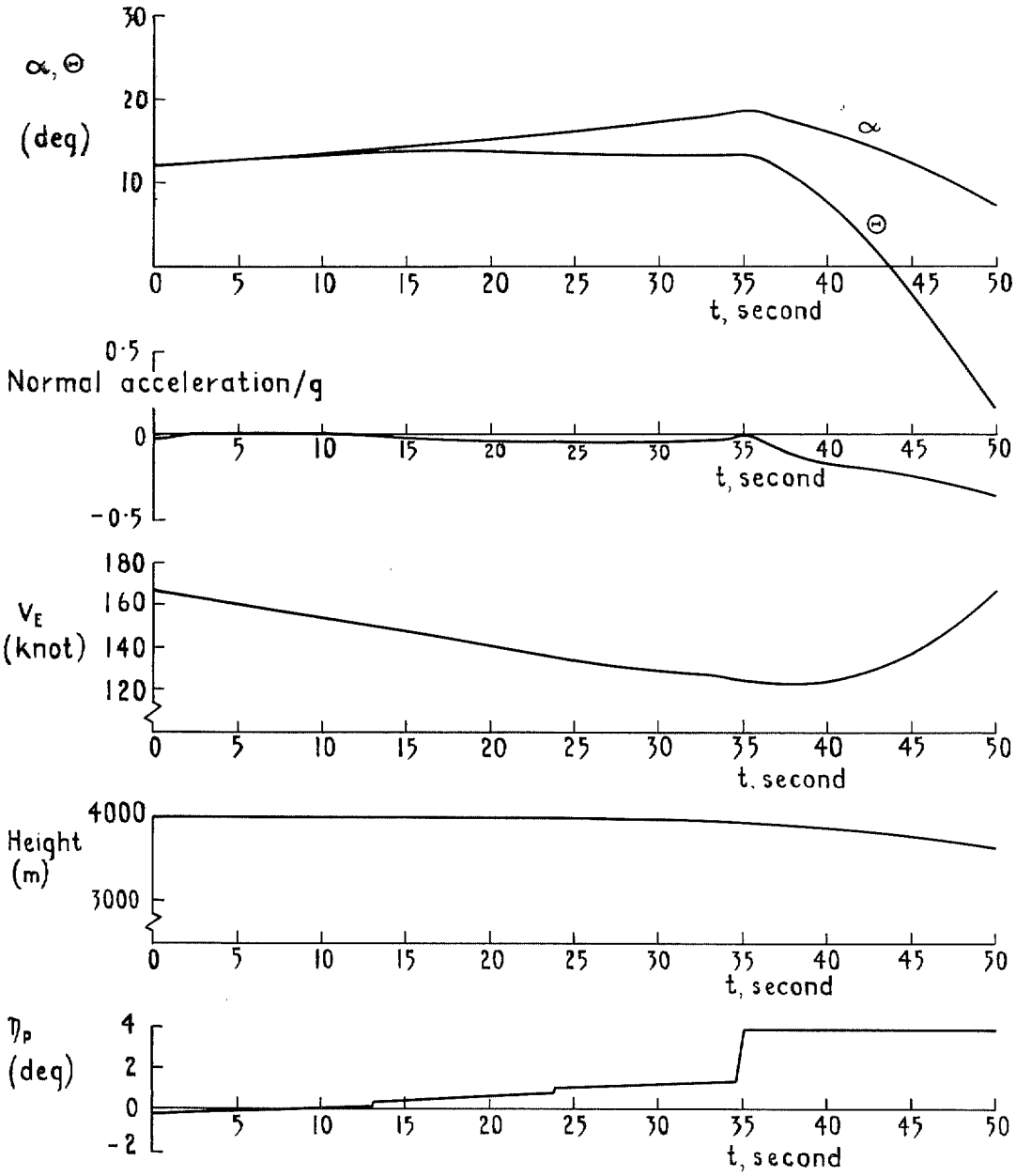

FIG. 55. Recovery from a motion involving a low and almost constant deceleration and slight rotation (slender wing aircraft, CG $0{\cdot}525c_0$).

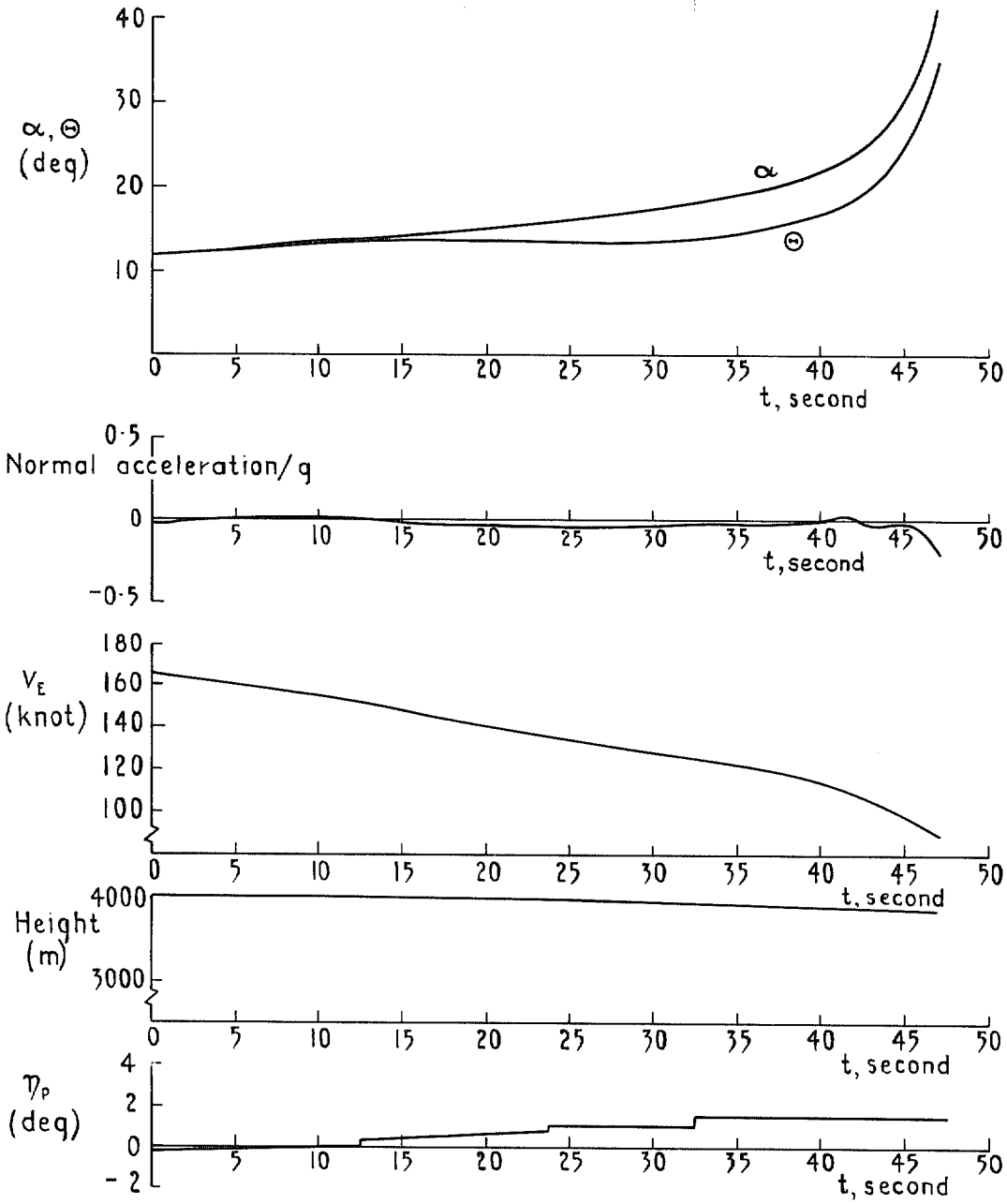

FIG. 56. Excursion to large angles of attack from a motion involving a low and almost constant deceleration and slight rotation (slender-wing aircraft, CG $0{\cdot}525c_0$)

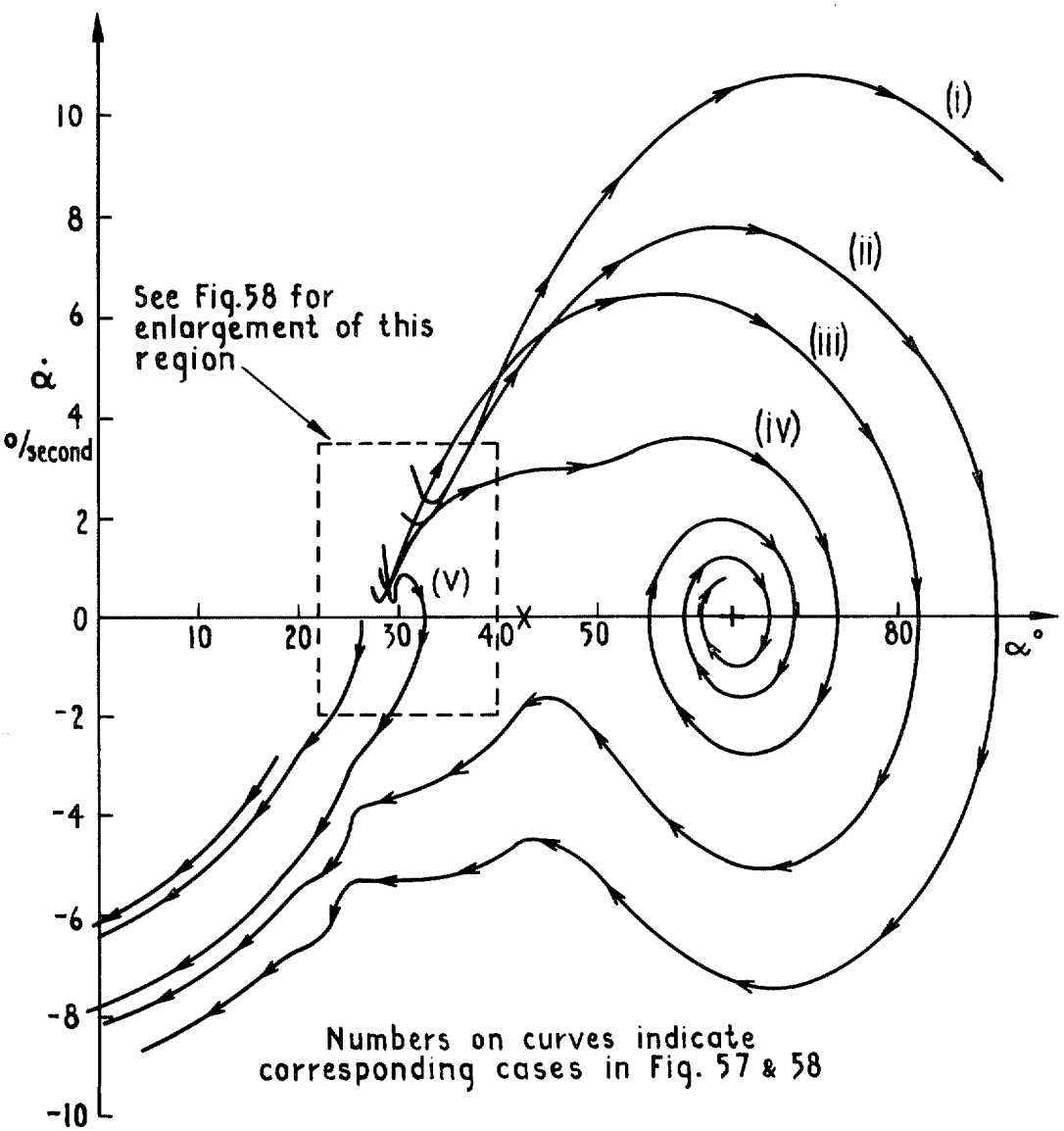

FIG. 57. Longitudinal motion of a slender-wing aircraft with fixed down-elevator during attempted recovery phase (CG $0{\cdot}52c_0$, with thrust moment, *cf.* Fig. 58).

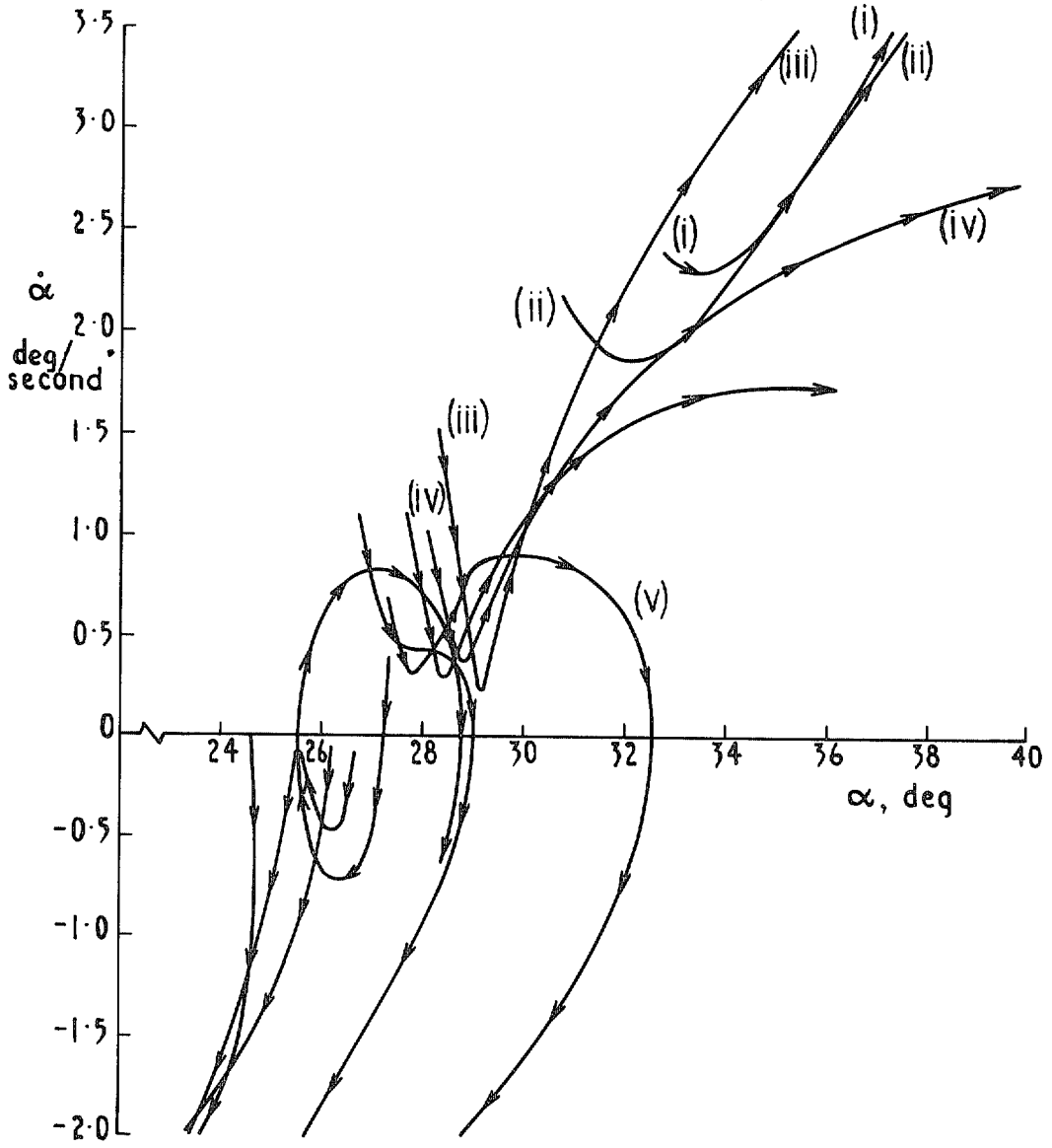

FIG. 58. The nature of the curves adjacent to the boundary region (CG $0{\cdot}52c_0$, with thrust moment, *cf.* Fig. 57).

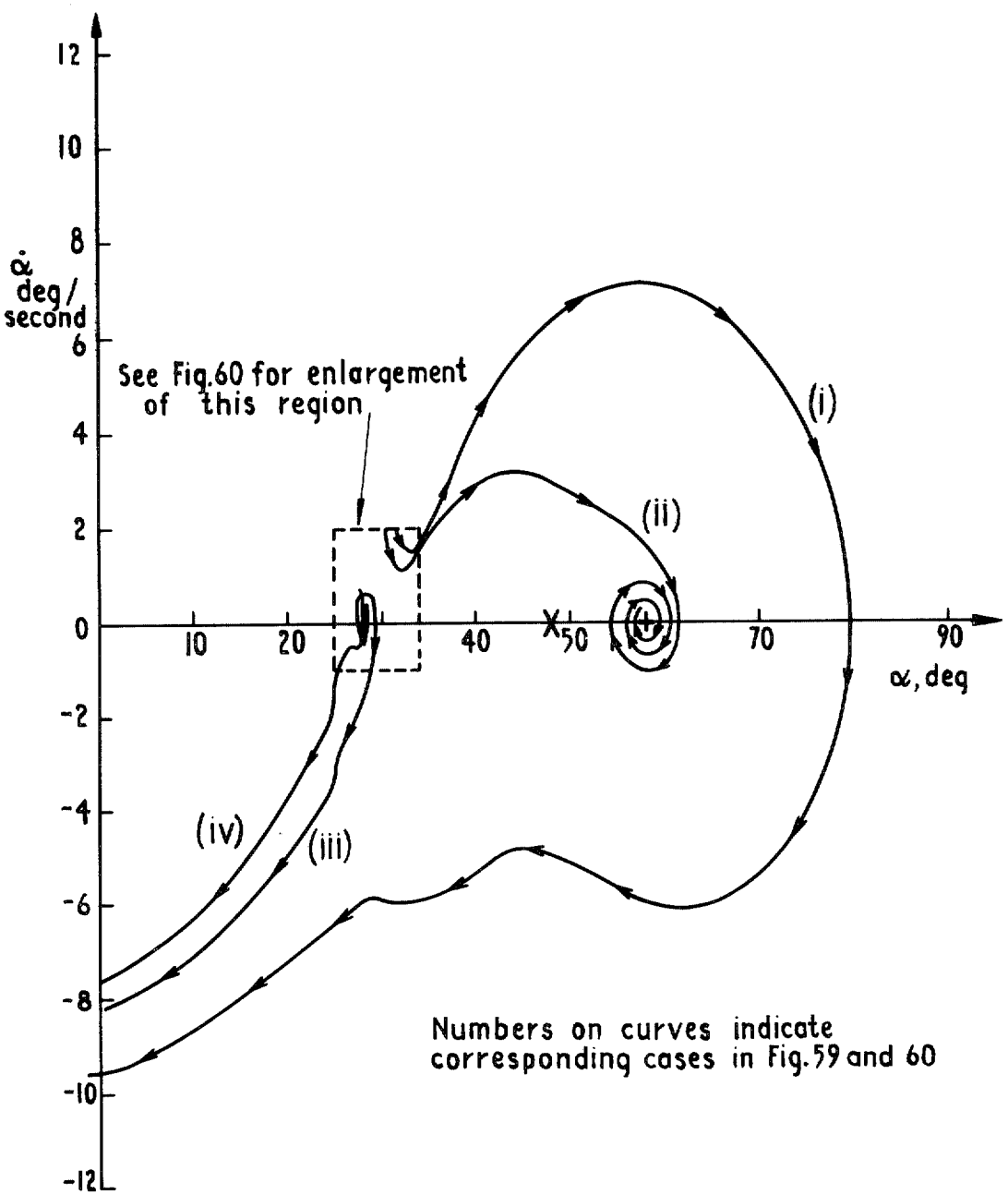

FIG. 59. Longitudinal motion of a slender-wing aircraft with fixed down-elevator during attempted recovery phase (CG 0·52c_0, zero thrust moment).

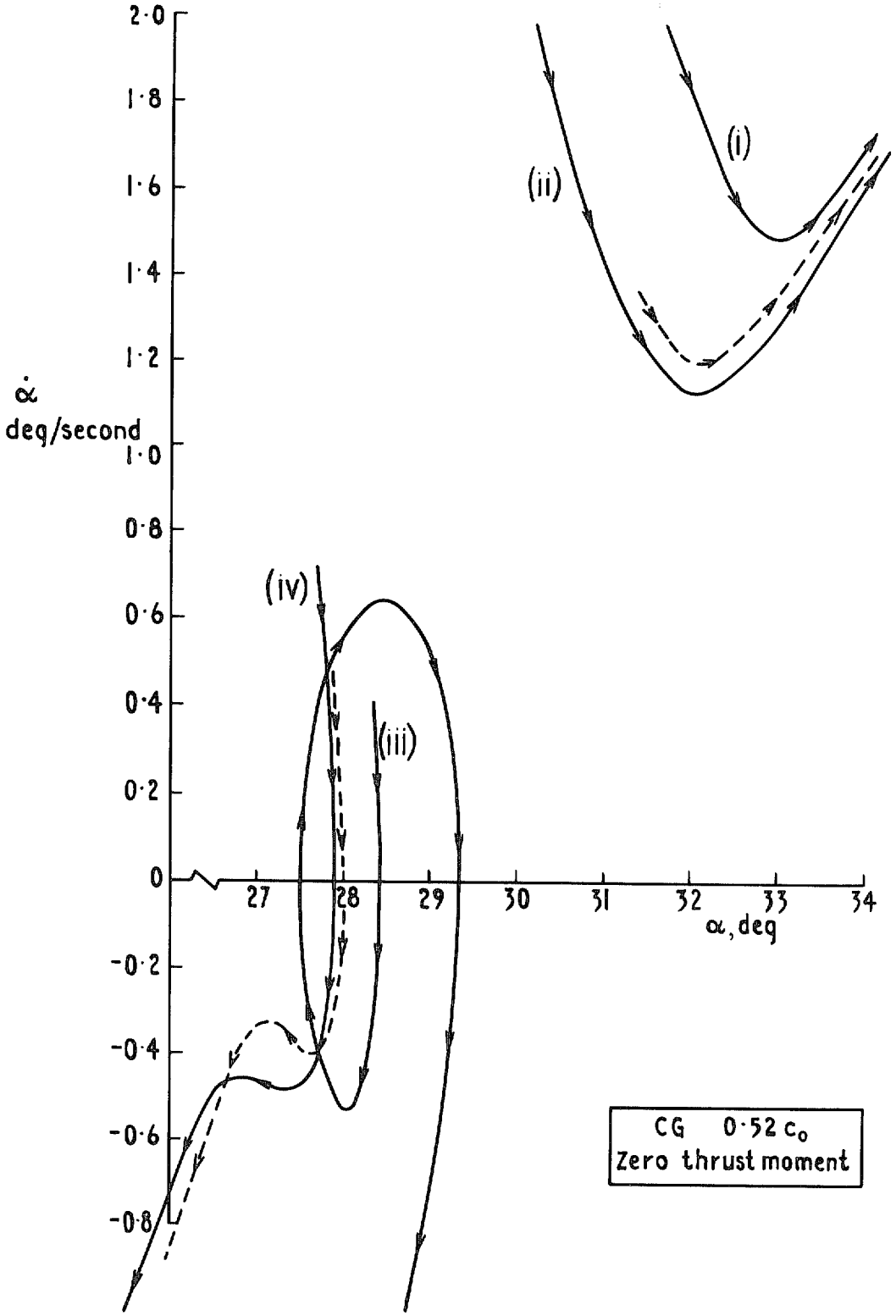

FIG. 60. The nature of the curves adjacent to the boundary region (*cf.* Fig. 58).

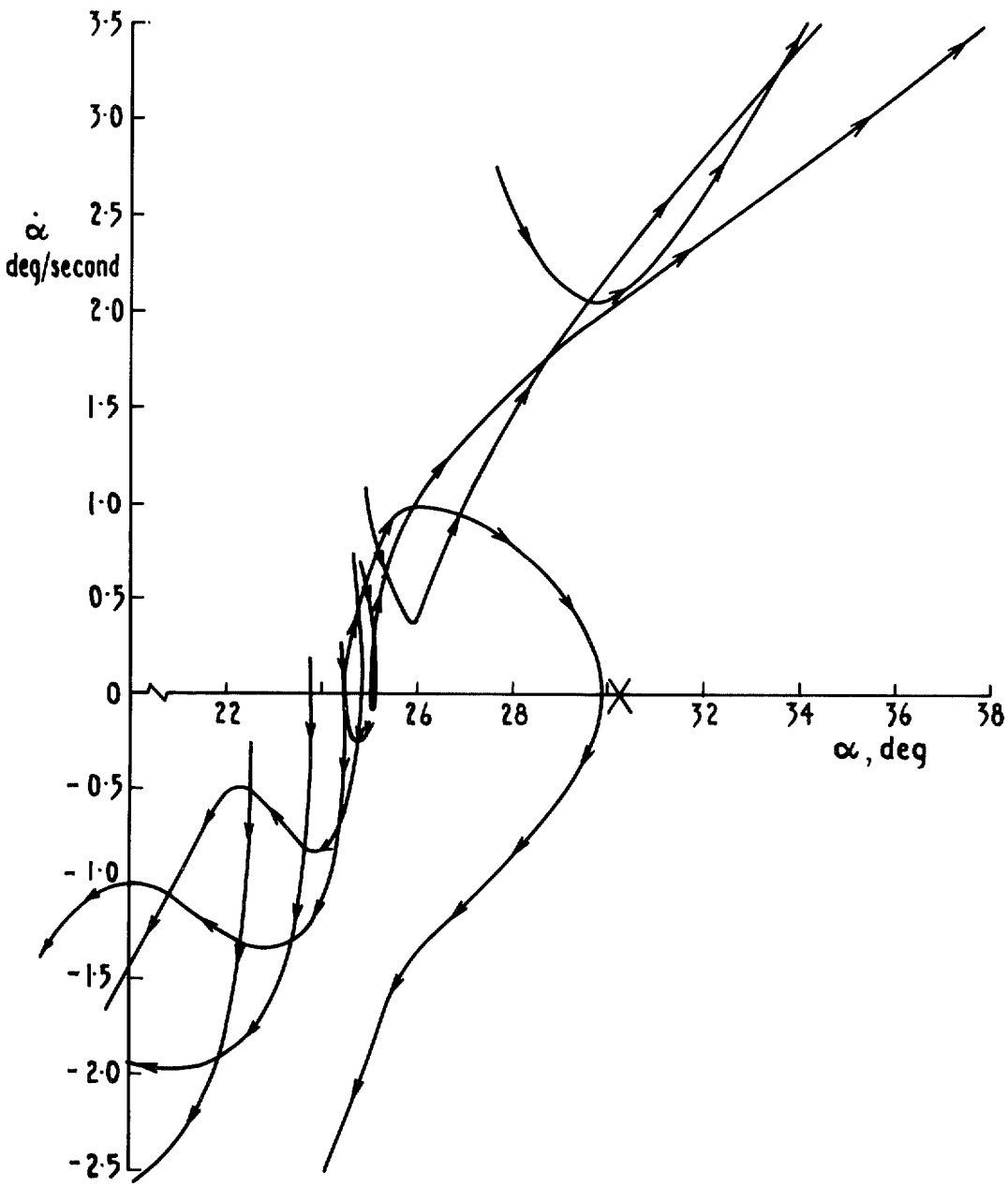

FIG. 61. The nature of the curves adjacent to the boundary region (CG $0{\cdot}53c_0$, with thrust moment).

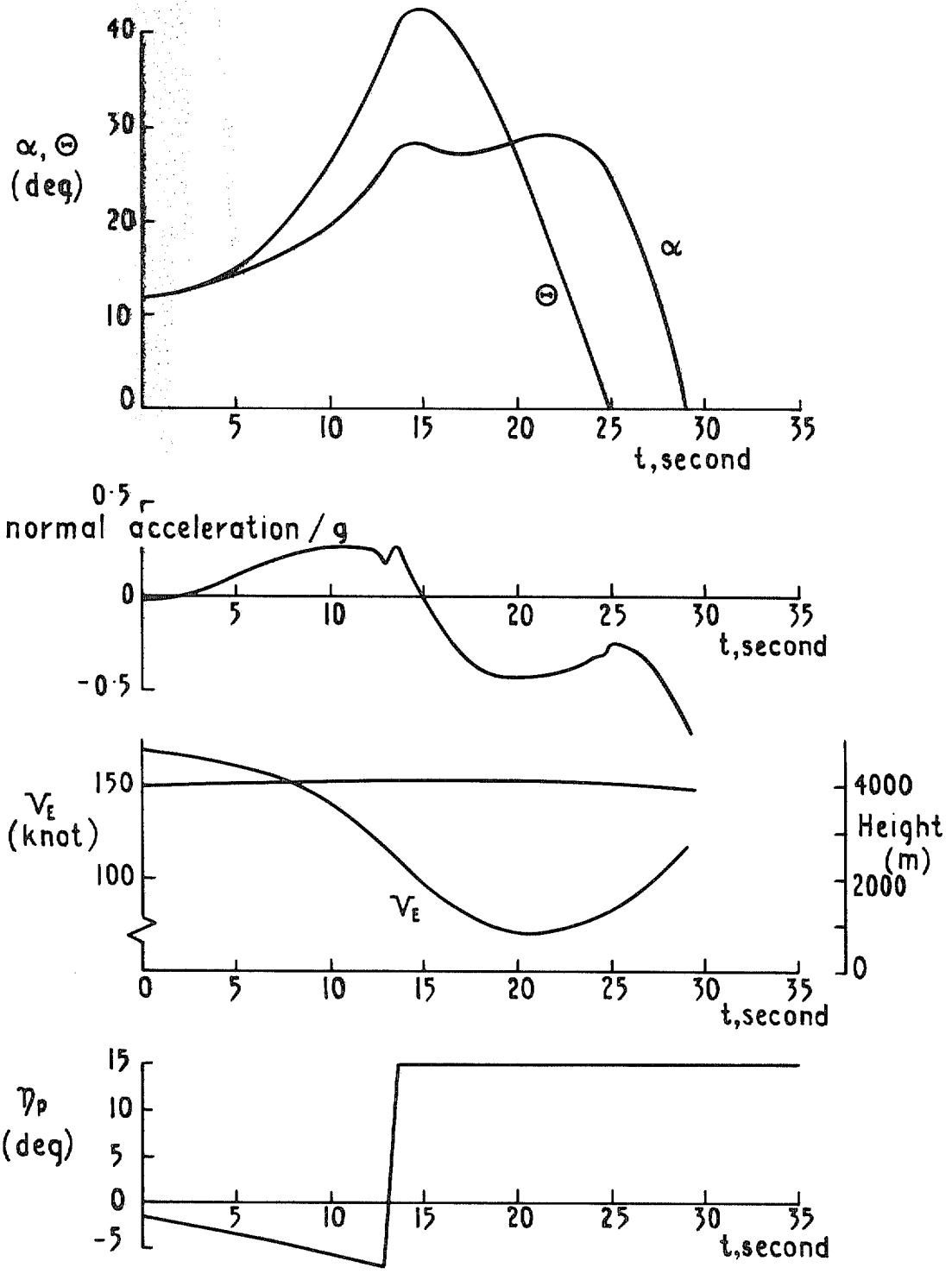

FIG. 62. A very slow recovery following a rapid approach to a recovery angle-of-attack of 26° (CG $0{\cdot}52c_0$, no thrust moment).

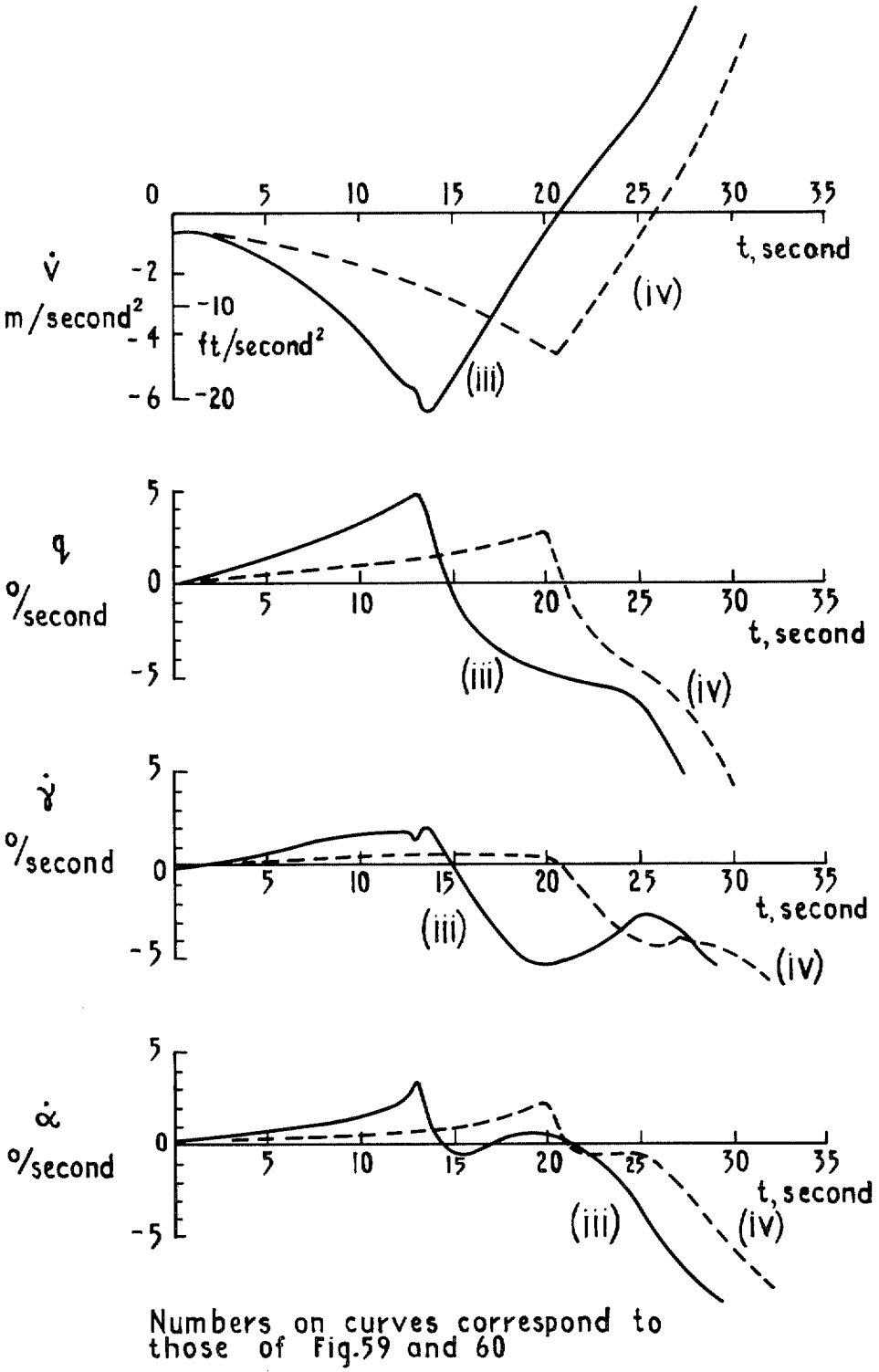

FIG. 63. Details of the motion for the two marginal normal recoveries of Fig. 60 ($\alpha_r = 26°$).

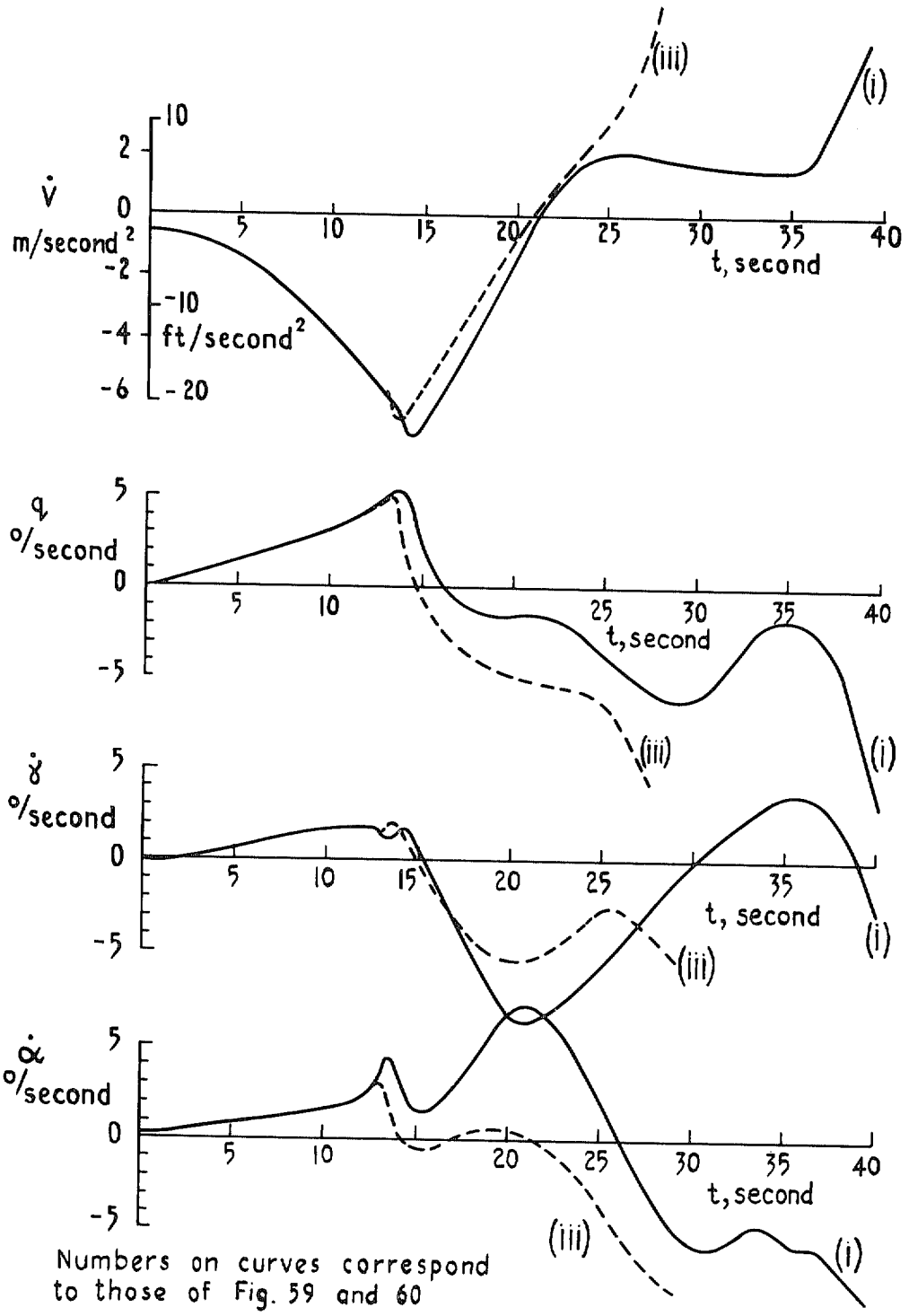

FIG. 64. Details of the motion during attempted recovery from slightly different high angle-of-attack conditions (α_r = 26° and 28°).

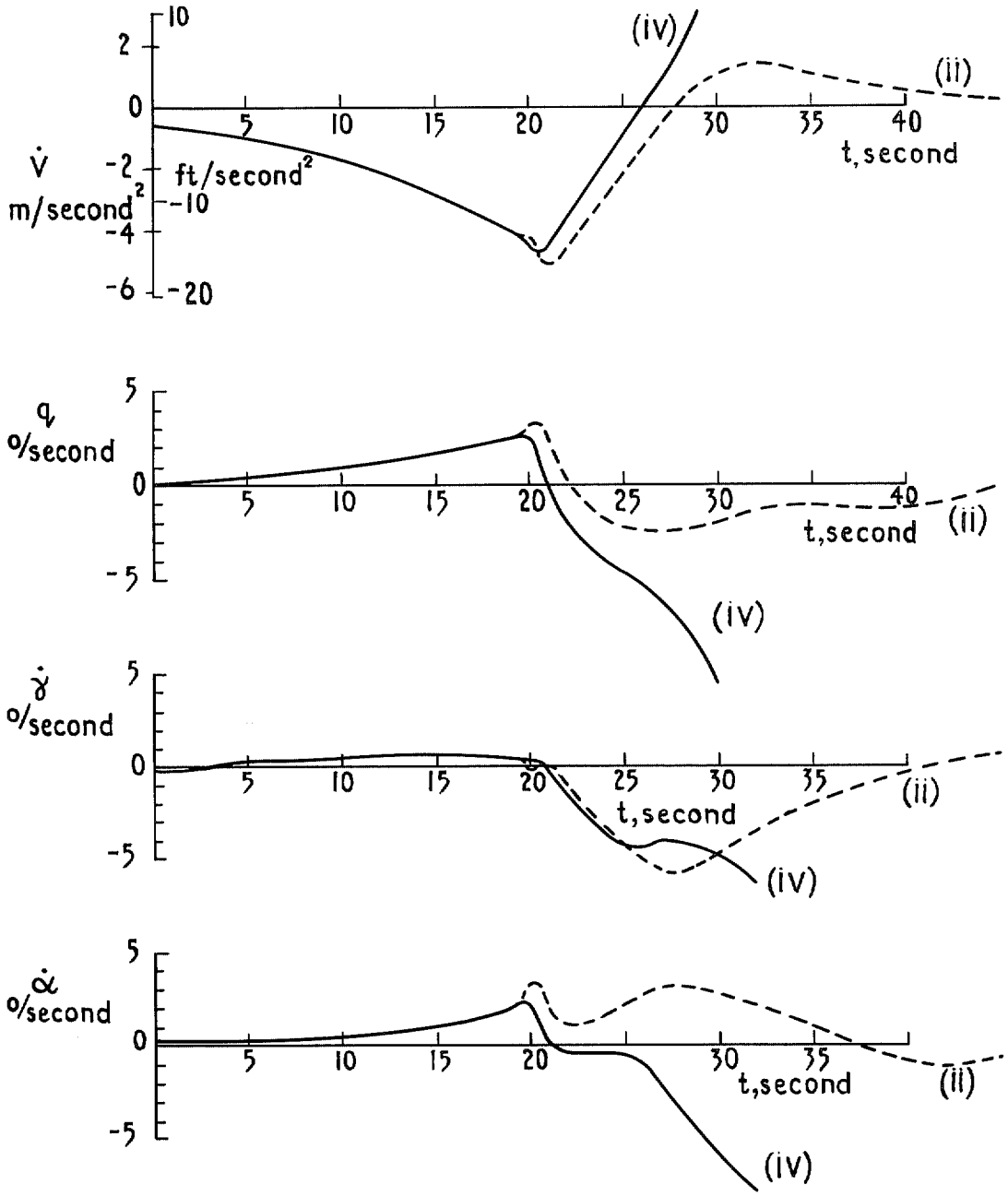

Numbers on curves correspond to those of Figs. 59 and 60.

FIG. 65. Details of the motion during attempted recovery from slightly different high angle-of-attack conditions (α_r = 26° and 28°).

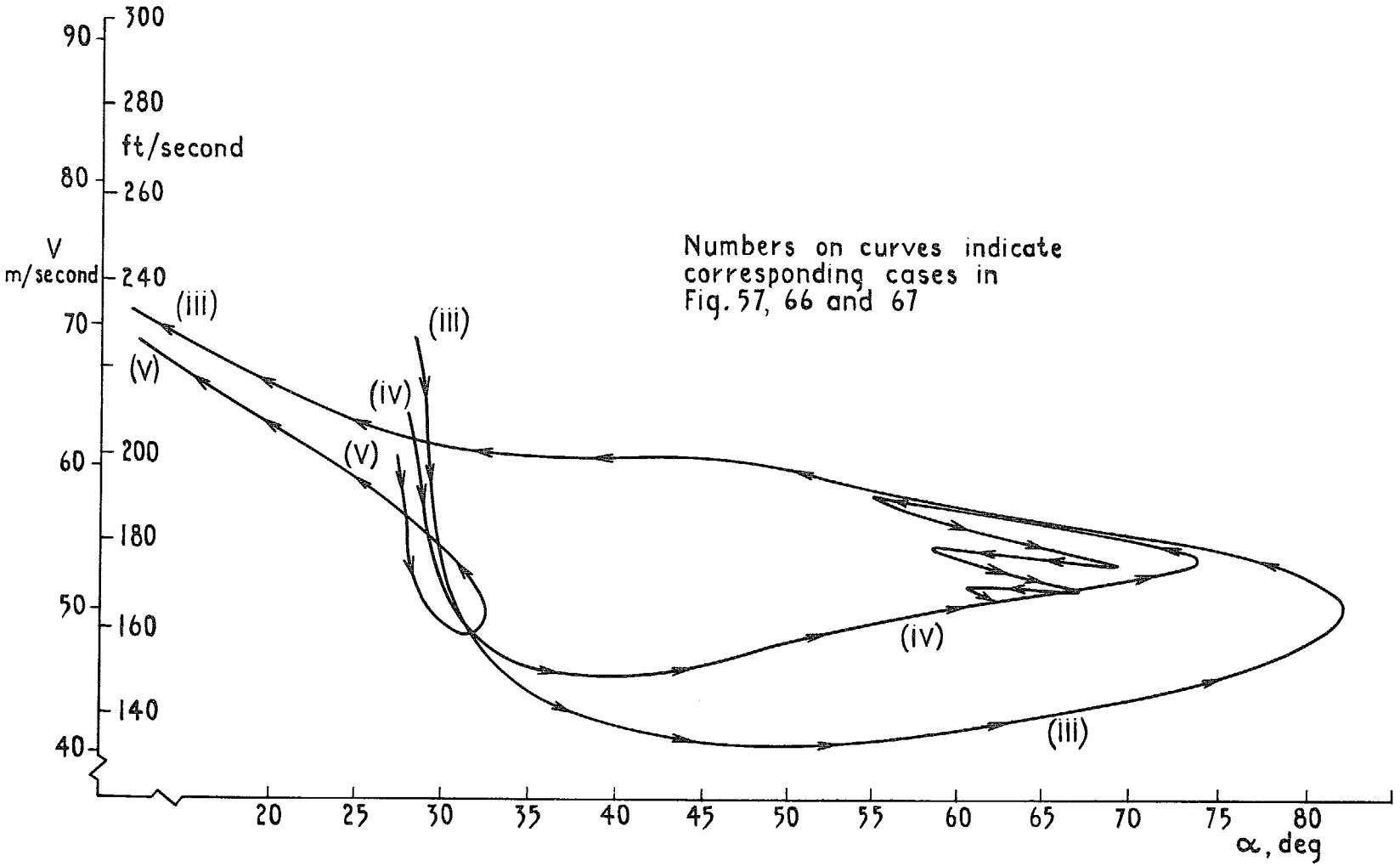

FIG. 66. Speed variation during attempted recoveries.

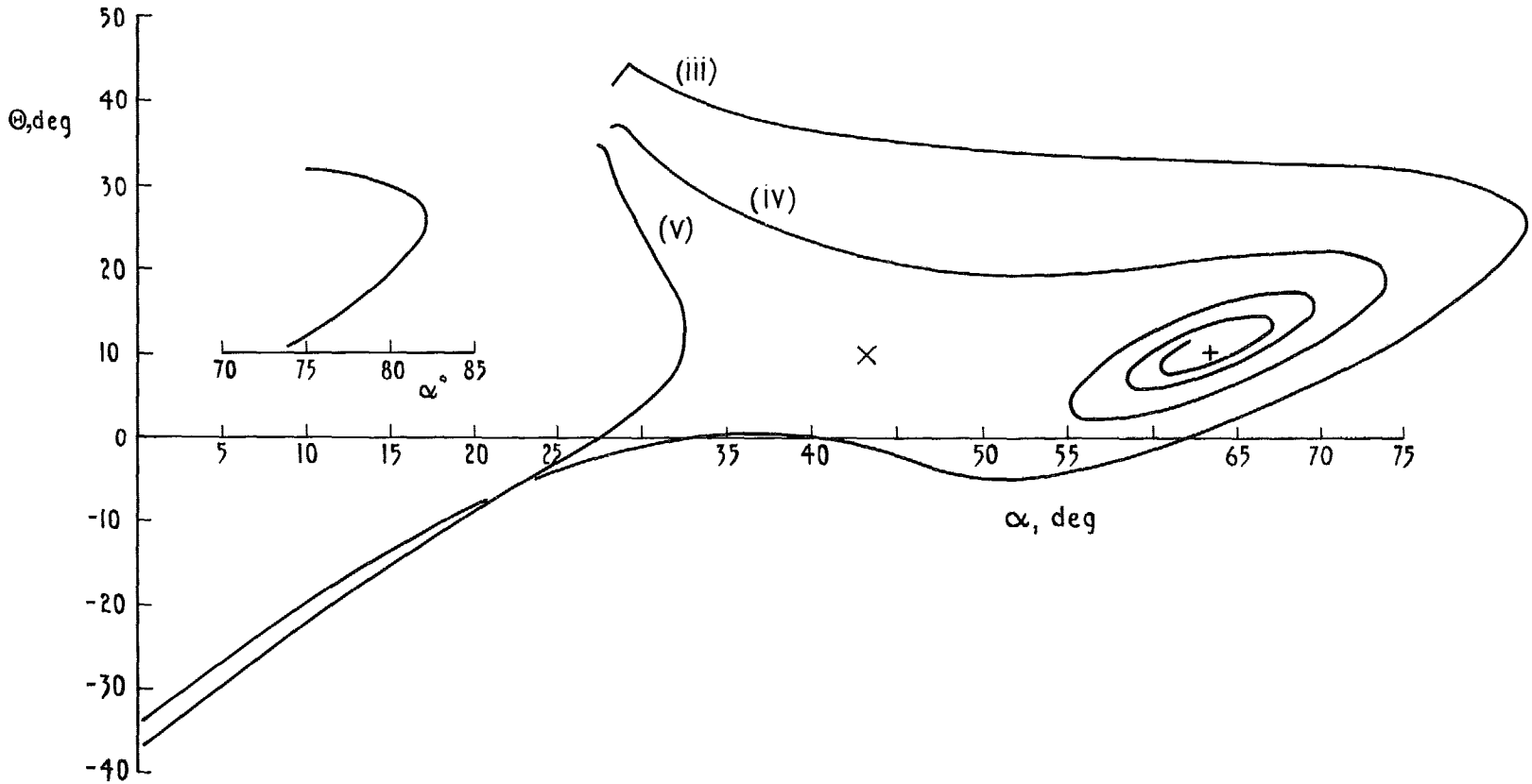

FIG. 67. The variation of the attitude angle (Θ) with the angle-of-attack (α) in the motions to which the curves of Fig. 57 refer.

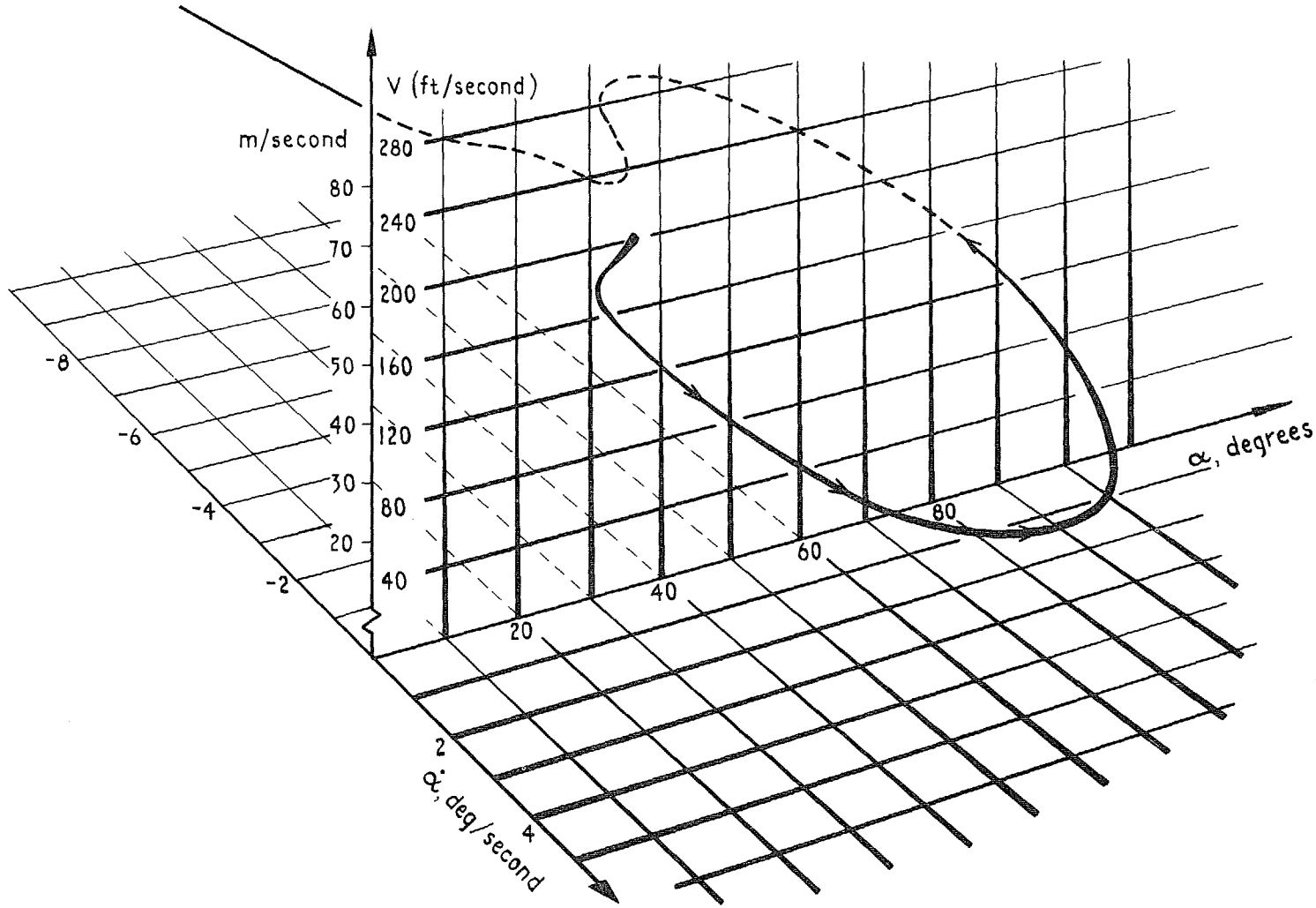

FIG. 68. The 'bounce' recovery, curve (iii) of Fig. 57.

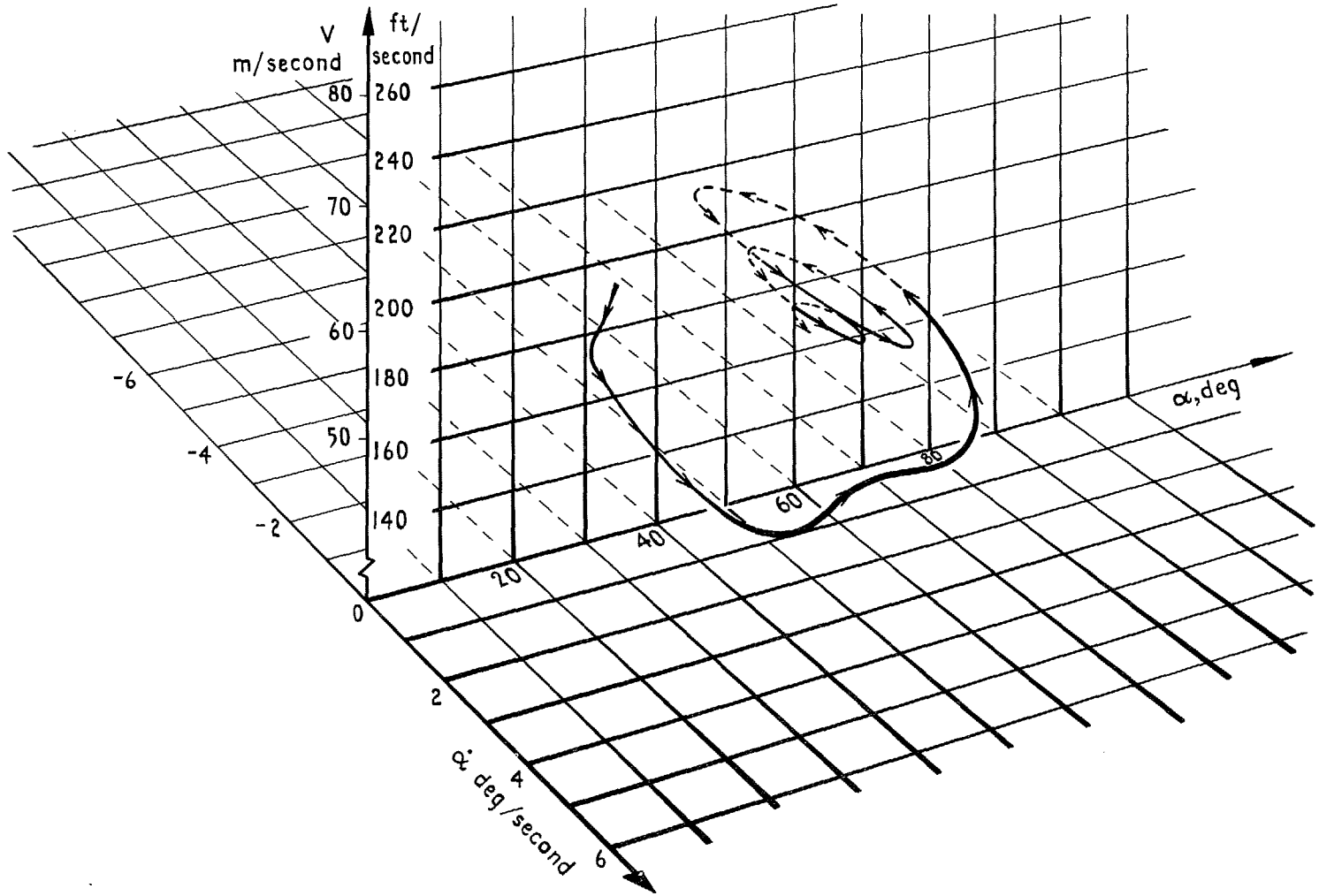

FIG. 69. The 'superstall' motion corresponding to curve (iv) of Fig. 57.

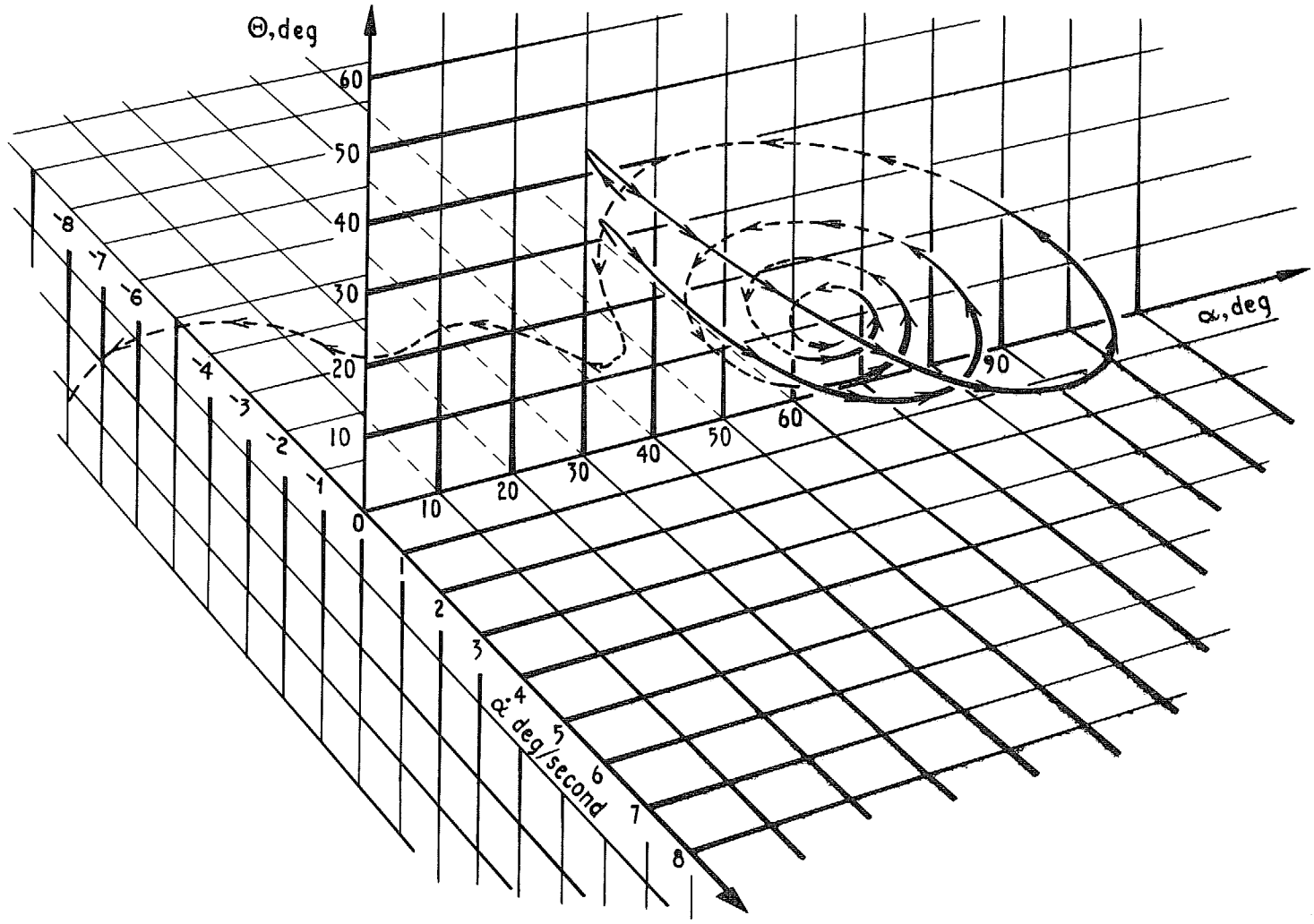

FIG. 70. The 'bounce' and 'superstall' motion showing separation of trajectories in the α, $\dot{\alpha}$, Θ space.

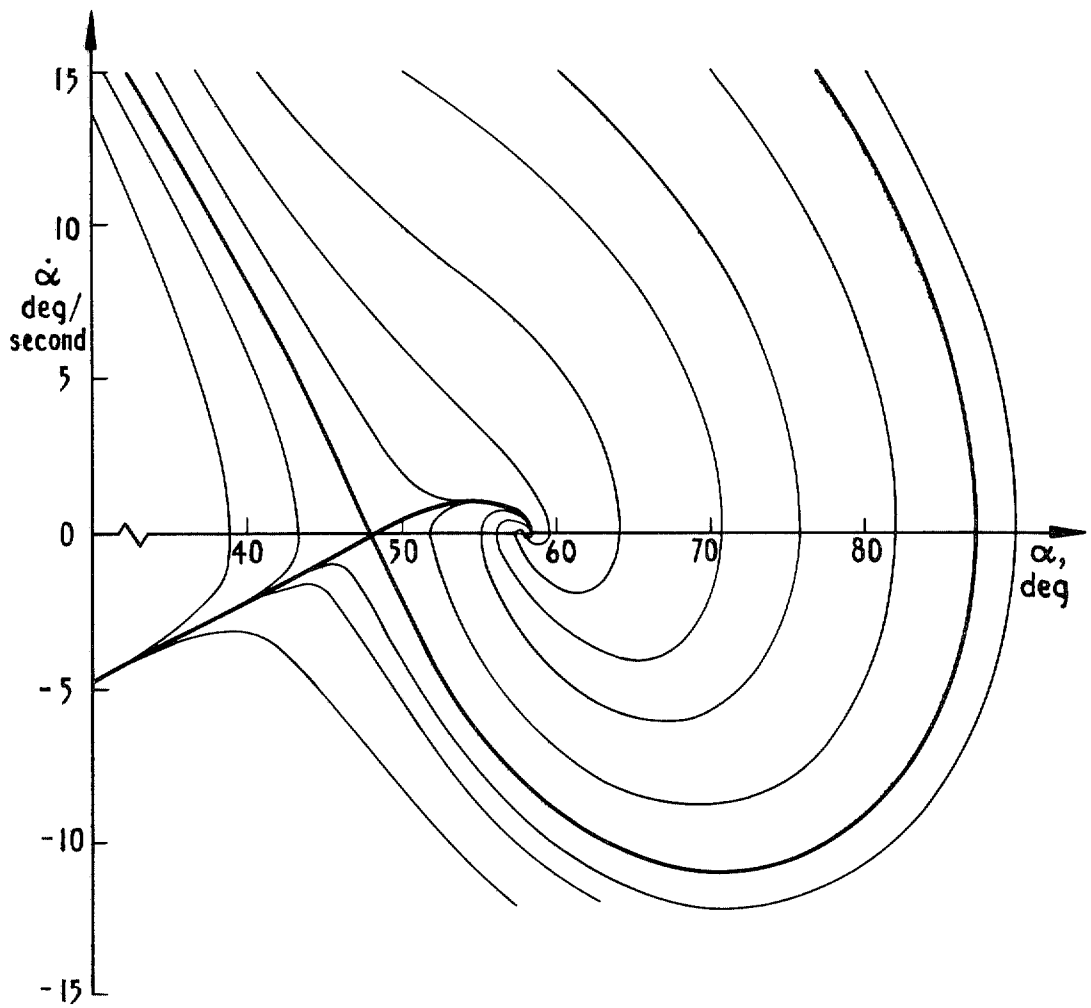

FIG. 71. Single degree-of-freedom motion at the initial speed of the three degree-of-freedom motion (*cf.* Fig. 72 and 73) (CG $0{\cdot}52c_0$, increased damping and zero thrust moment).

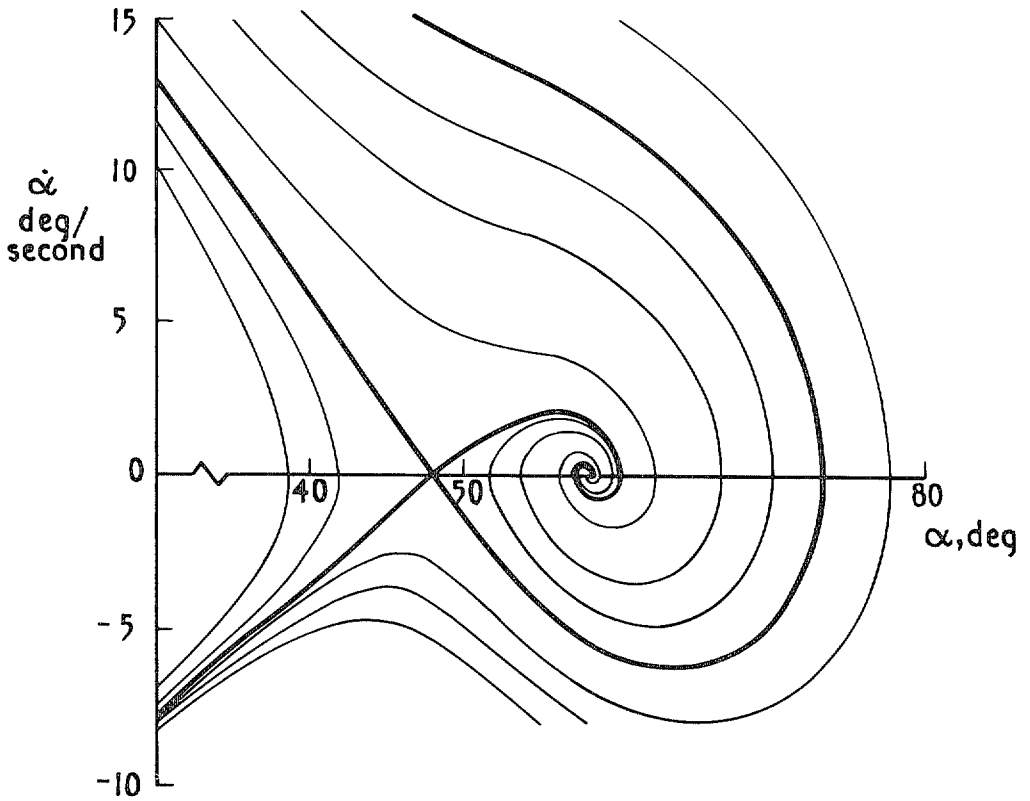

FIG. 72. Single degree-of-freedom motion at the initial speed of the three degree-of-freedom motion (*cf.* Fig. 71 and 73) (CG $0{\cdot}52c_0$, basic damping and zero thrust moment).

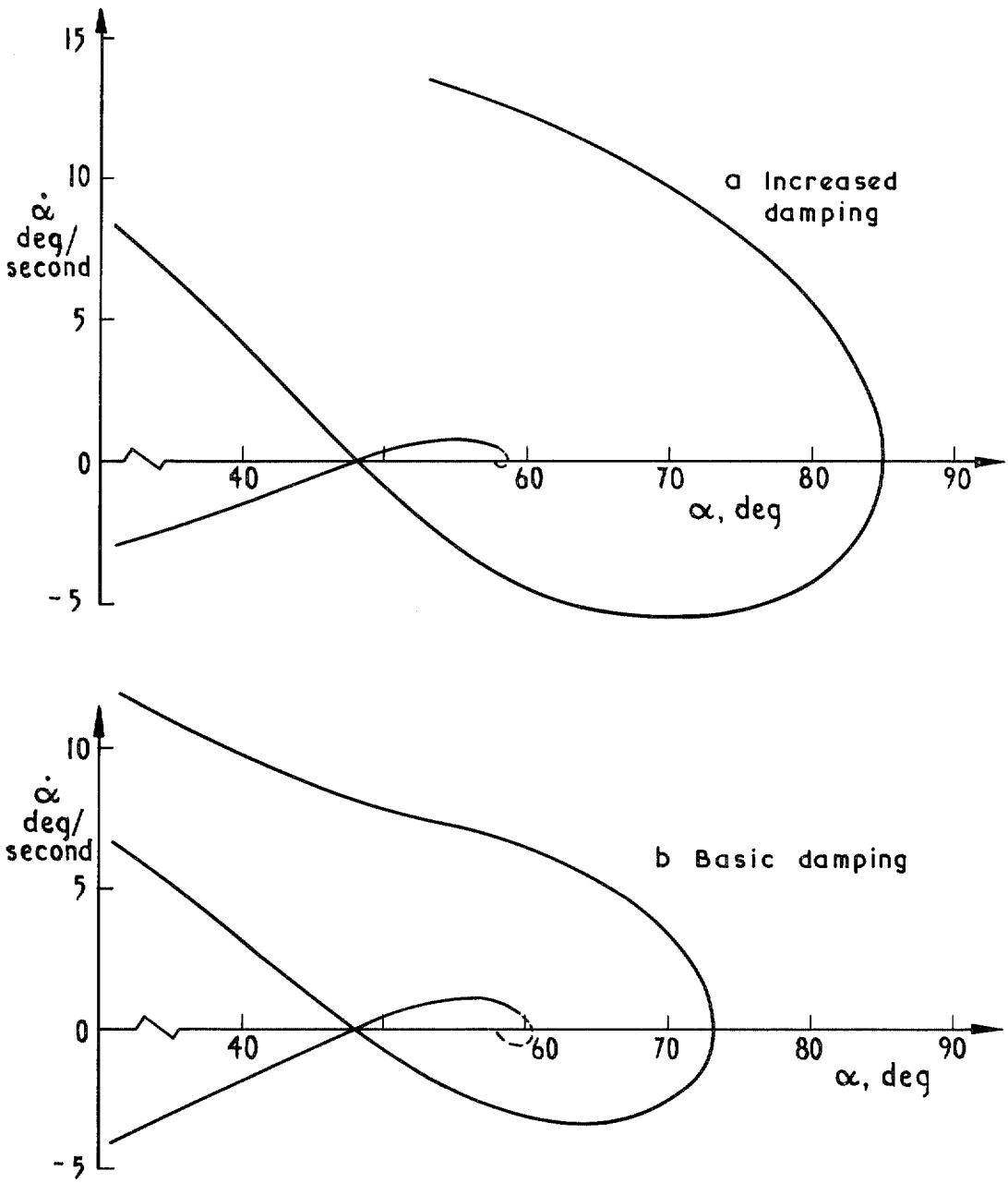

FIG. 73a and b. Effect of reducing aircraft speed on the single degree-of-freedom motion (CG $0{\cdot}52c_0$, zero thrust moment).

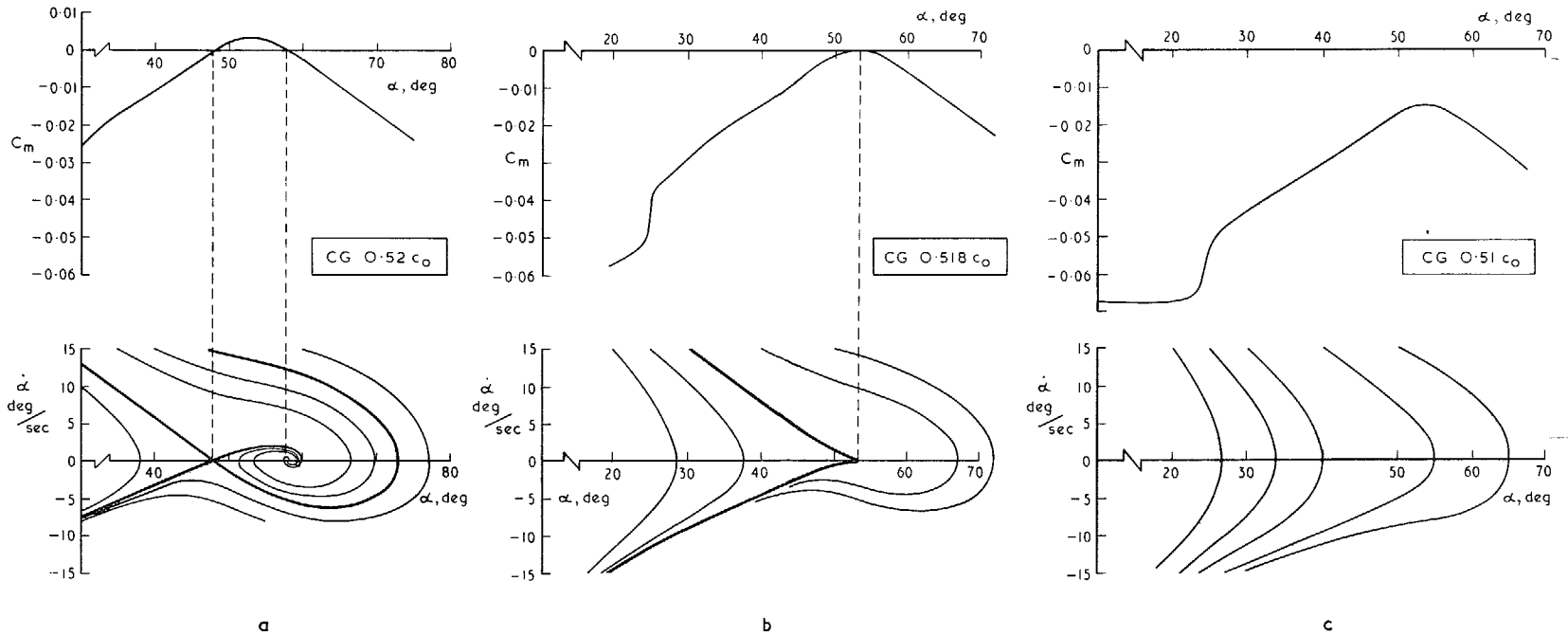

FIG. 74a–c. The effect of changing the centre of gravity on the motion with freedom to pitch only.

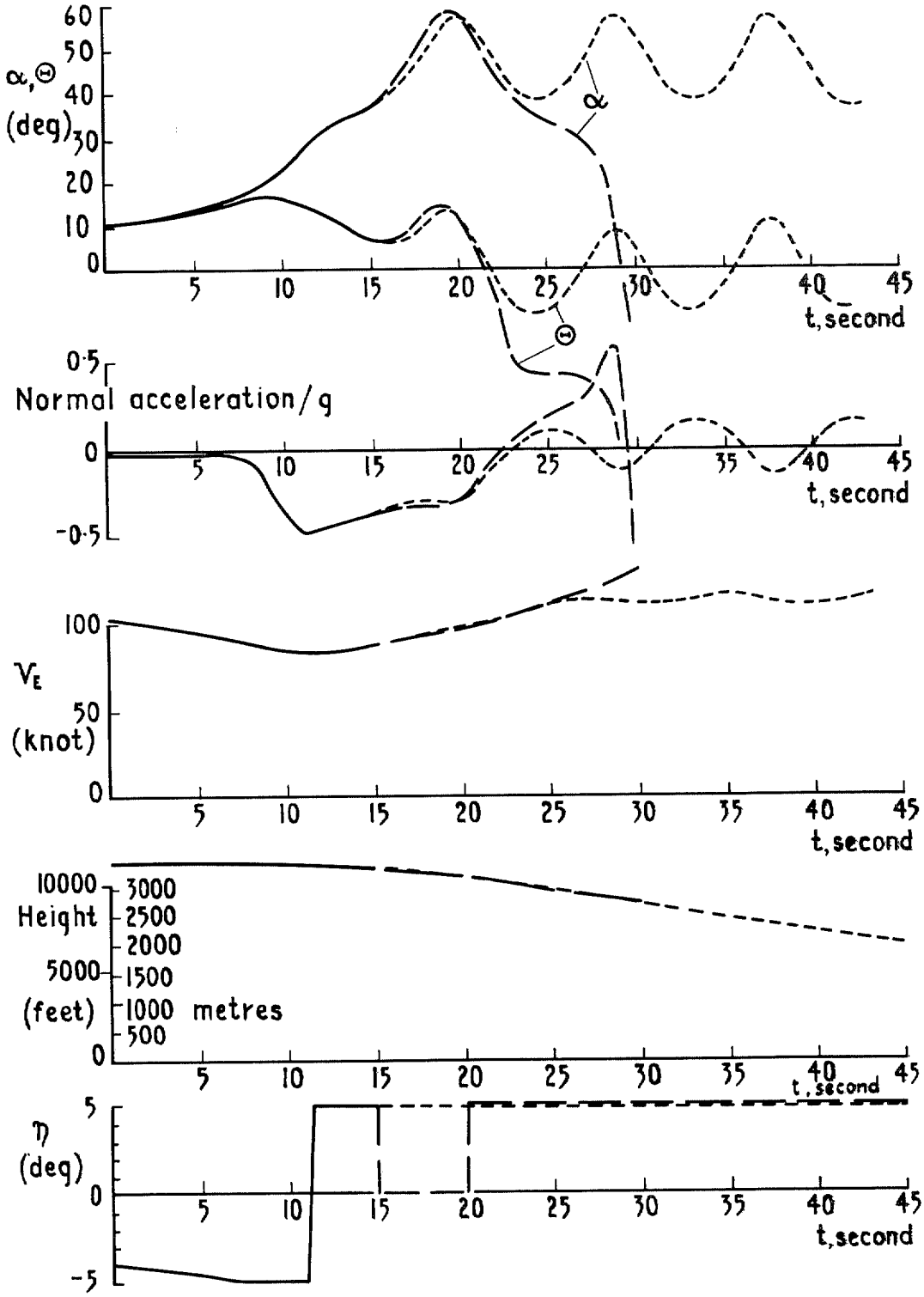

FIG. 75. Conversion of a 'superstalled' motion into a 'bounce' recovery.

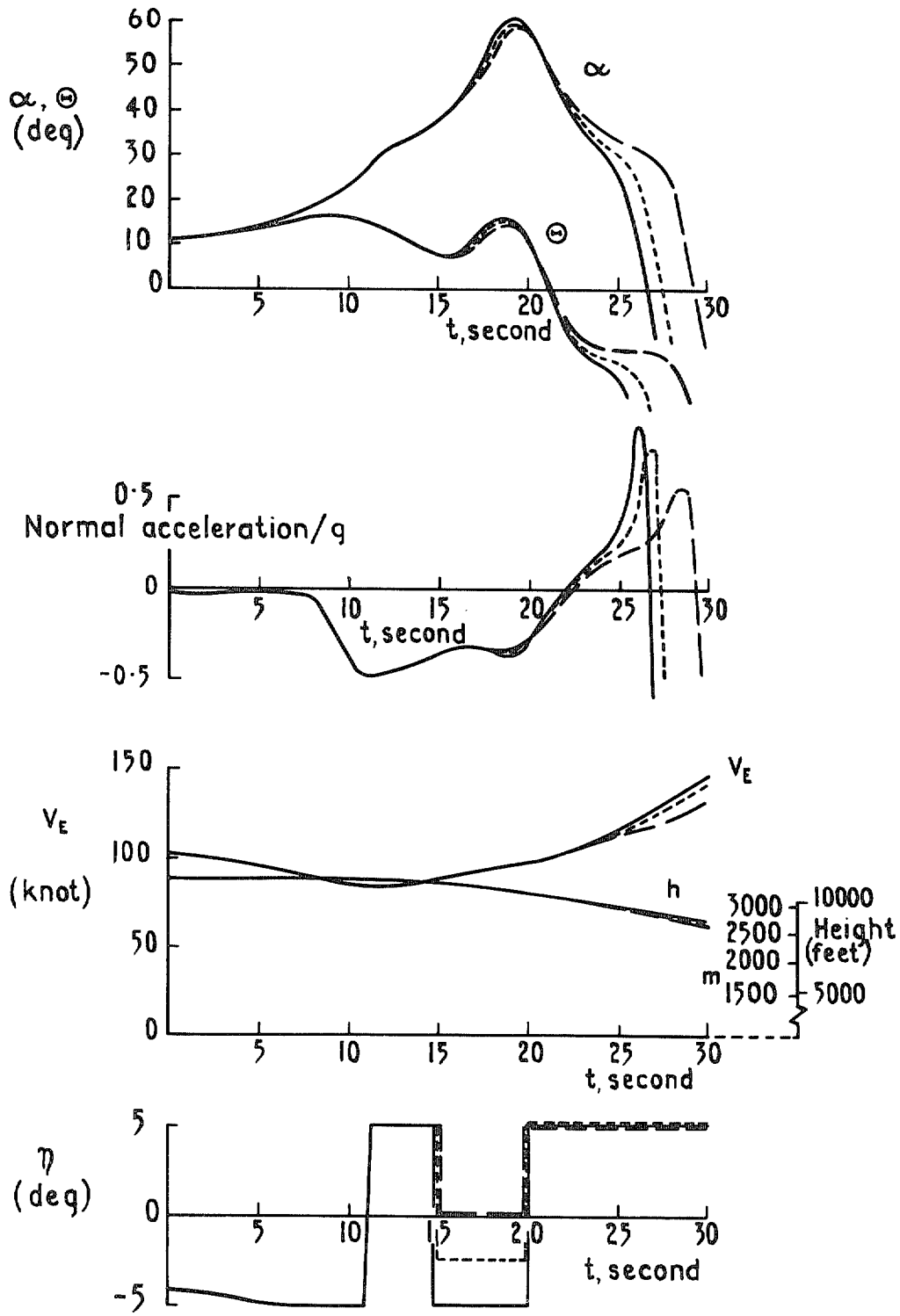

FIG. 76. Effect of varying control inputs on the conversion of a 'superstalled' motion into 'bounce' recoveries (*cf.* Fig. 75).

Printed in England for Her Majesty's Stationery Office by J. W. Arrowsmith Ltd., Bristol BS3 2NT
Dd. 505374 K5 10/74

HER MAJESTY'S STATIONERY OFFICE

Government Bookshops

49 High Holborn, London WC1V 6HB
13a Castle Street, Edinburgh EH2 3AR
41 The Hayes, Cardiff CF1 1JW
Brazennose Street, Manchester M60 8AS
Southey House, Wine Street, Bristol BS1 2BQ
258 Broad Street, Birmingham B1 2HE
80 Chichester Street, Belfast BT1 4JY

Government publications are also available through booksellers

ISBN 0 11 470846 0*